THE REACTION OF HYDROGEN ATOMS WITH SIMPLE ORGANIC MOLECULES IN A FAST-FLOW SYSTEM

by

Robert C. Galloway, B.Sc.

Thesis presented for the Degree of Doctor of Philosophy
of the
University of Edinburgh

Kirkcaldy. August, 1974.

ACKNOWLEDGEMENTS

I wish to thank Dr. J. H. Knox for his help, advice, tolerance and particularly his encouragement during the final stages of this work.

I am indebted to Professor Kemball for the provision of laboratory and library facilities at the University of Edinburgh and also to the Carnegie Trust for the Universities of Scotland for a Scholarship during most of the period of this work.

"A peace above all earthly dignities,
A still and quiet conscience."

'King Henry VIII'

- William Shakespeare.

TABLE OF CONTENTS

CHAPTER I

INTRODUCTION

1.1 The Reaction of Hydrogen Atoms with Olefins

The reactions of olefins with hydrogen atoms have been of continuing interest for many years. This interest results from the importance of these reactions in complex reactive systems. Thus radiation chemists, photochemists and thermal kineticists have inferred the importance of these reactions in a wide variety of experimental systems which range from radiation induced polymerisation to flame or shock tube studies. However despite much experimental work on this topic and a wealth of experimental data on the relative rates of reaction of H atoms with olefins, there were until recently, few determinations of absolute rate constants. Several recent determinations have been achieved using fast discharge-flow systems (BAR69, COW70, DAB70, DAL67) and this was the technique adopted in this study.

The addition of a hydrogen atom to an olefin yields a vibrationally excited alkyl free radical with about 40kcal. $mole^{-1}$ energy. This radical can,

(1) redissociate

(2) be deactivated by collision

(3) dissociate into different products

$$H + A \underset{D}{\rightleftharpoons} R^{*} \xrightarrow{S} R$$

$$R^{*} \xrightarrow{D} CH_3 + A'$$

D = dissociation

S = stabilization

The rate of stabilization can be assumed and so the rate of addition can be found by standard gas kinetic techniques.

The H atom addition to simple olefins is particularly interesting since it is possible to correlate the results

with theories of unimolecular reaction, in particular with the Marcus-Rice theory.

1.2 Unimolecular Reactions

A unimolecular reaction is one in which the activated complex is formed from a single reactant molecule. They are of the first order under certain circumstances, but they become of the second order at low pressures. The development of the theory of unimolecular reactions has been a somewhat involved one, and even today some important features of the treatment are not completely understood.

Lindemann's Theory

The first successful collision theory was proposed in 1922 by Lindemann (LJN22) to replace the unsatisfactory radiation hypothesis of Perrin. In this Lindemann showed how activation of molecules by bimolecular (second-order) collisions could in certain circumstances lead to first-order kinetics for the unimolecular reaction of the molecules thus activated. The essential feature of Lindemann's mechanism was that he postulated that there is a time lag before an activated molecule can react once it has received sufficient energy to do so. During this time the activated molecule may suffer further bimolecular collisions which may de-activate it. The simplest form of this mechanism may be written,

$$A + M \xrightarrow{ka} A^* + M \quad \text{activation}$$

$$A^* + M \xrightarrow{kd} A + M \quad \text{de-activation}$$

$$A^* \xrightarrow{kr} \text{products} \quad \text{unimolecular reaction}$$

A^* is a molecule of reactant with sufficient energy (correctly distributed if necessary) to undergo spontaneous unimolecular reaction to form products. M is any molecule that can transfer energy to A by collision. In the simplest theory, all A molecules are treated alike and it is assumed that their specific rate of reaction, k_r, is independent of the degree of activation. If the energy possessed by A^* is very large compared to the average energy it may be treated as a 'very reactive' intermediate in the steady state sense.

$$\frac{dCA^*}{dt} = ka\ CA\ CM - kd\ CA^*\ CM - kr\ CA^*$$

$$= 0$$

$$\therefore\ CA^* = \frac{ka\ CA\ CM}{kd\ CM + kr}$$

The rate of formation of products,

$$\frac{dC\ \text{products}}{dt} = r = kr\ CA^*$$

$$= \frac{ka\ kr\ CA\ CM}{kd\ CM + kr} \qquad (1)$$

This rate expression will approximate to a simple rate law under certain conditions. At high pressures of gas, the concentration CM becomes large and so

$$k_d\ CM \gg k_r$$

i.e. the majority of A molecules that are activated by collision are de-activated similarly before they can undergo reaction.

The rate of formation of produces (1) becomes

$$r = \frac{(ka)}{(kd)} \times krCA$$

This is a simple first order rate law and the first-

order rate constant at infinite pressure defined by

$$r^{\infty} = {}_1k^{\infty}\, C_A$$

is given by,

$${}_1k^{\infty} = \frac{(ka)}{(kd)}\, kr \qquad (2)$$

At sufficiently low pressures C_m may become small enough that

$$k_d\, CM \ll k_r$$

In this case every A molecule that is activated undergoes reaction, the time between collisions being so long that the chance of a de-activating collision occurring before A* has time to undergo reaction is negligibly small. Under these conditions,

$$r = k_a\, C_A\, CM$$

the activation step is rate determining, and the reaction is second order overall.

Although the simple Lindemann theory can explain many of the important general characteristics of unimolecular reactions it fails when more detailed quantitative aspects of these reactions are investigated. The most serious discrepancy occurs when the actual manner in which the reaction rate changes from first to second order is considered. The first order constant, ${}_1k$ is given by Lindemann's theory (equation (1)) as

$${}_1k = \frac{ka\ kr\ CM}{kd\ CM + kr}$$

$$\therefore\ 1/{}_1k = \frac{kd}{ka\ kr} + (1/ka) \times 1/CM \qquad (3)$$

Thus a plot of $({}_1k)^{-1}$ versus the reciprocal of pressure should be linear. In fact the experimental plots are

distinctly curved and the fall-off in rate in practice is much slower than expected from the simple equation (3).

The Hinshelwood Modification

The rate constant k_a, according to the simple collision theory, is calculated from the product of the collision number and the chance that the two colliding molecules have relative translational energy greater than E_0. (E_0 = critical energy). Hinshelwood (HIN27) developed an idea of Lindemann's that a more realistic model would be obtained by assuming that the required energy could be drawn in part from the internal degrees of freedom (mainly vibrational) of the reactant molecule. The chance of a molecule containing energy greater than E_0 clearly increases with the number of degrees of freedom which contribute, and the rate of energization is thus increased. Hinshelwood showed that the chance of a molecule possessing total energy greater than E_0 in s classical degrees of freedom is much higher than $\exp(-E_0/kT)$, and is in fact approximately

$$\frac{(EO/kT)^{S-1}}{(S-1)!} \quad EXP(-EO/kT)$$

The rate constant k_a in the modified Hinshelwood-Lindemann (H-L) theory is therefore given by (4) which even for moderate values of s leads to much bigger values of k_a than does the simple collision theory.

$$ka = \frac{Z}{(S-1)!} \frac{(Eo)^{S-1}}{(kT)} \quad EXP(-Eo/kt) \qquad (4)$$

(Z = collision number)

This has the effect of reducing dramatically the calculated transition pressure (3). However the anomaly

still remains that the experimental plots are strongly curved.

To account for this observation a more detailed theory than the simple Lindemann mechanism which considers only two classifications of reactant molecules, i.e. normal and activated, must be used. Some allowance that the rate of unmolecular reaction, k_r depends on the degree of activation of A* must be introduced. Equation (2) gives

$$ {}_1k^{\infty} = \frac{(ka)}{(kd)} \quad kr $$

$$ = Kc\ kr $$

(where K_c is the equilibrium constant of activation of A)

$$ \text{i.e. } {}_1k^{\infty} = k_r\ f \qquad (5) $$

where f is the equilibrium fraction of A molecules that are activated.

The high pressure first-order rate constant may be calculated from this, modified to allow for this dependance on degree of activation thus

$$ {}_1k^{\infty} = \sum k_r\ f $$

where f is now the equilibrium fraction of A in a specified activation state, and k_r is the rate constant for reaction of that state and the sum is taken over all activated states of A, i.e. states for which $k_r \neq 0$. Similarly from (3) the general first-order constant is,

$$ {}_1k = \sum \frac{kr\ f}{1 + kr/kd\ CM} \qquad (6) $$

In expressions (5) and (6), f is readily calculated statistically since it is an equilibrium property. The

rate of deactivation, k_d, is usually taken to be equal to the collision frequency Z_{AM}, that is it is assumed that deactivation occurs on every collision of activated molecules. The problem then reduces to one of calculating k_r as a function of the state of activation, and later theories, outlined below, attempt this calculation.

The Kassel Theory

The theories due to Rice and Ramsperger (RIC27), and Kassel (KAS28,32) were developed virtually simultaneously and are very similar in their approach. They followed the pioneering work of Hinshelwood and Lindemann and were the first satisfactory unimolecular theories which allowed for the dependance of both f and k_r on energy.

Both use the basic Hinshelwood-Lindemann mechanism of collisional energization and de-energization, but consider more realistically that the rate of conversion of energized molecule to products is a function of its energy content. The differences between the Rice-Ramsperger and the Kassel treatments are twofold. Firstly, Rice and Ramsperger used classical statistical mechanics throughout, whereas Kassel also developed a quantum treatment which is very much more realistic and accurate. Secondly, different assumptions were made about the part of the molecule into which the critical energy E_0 has to be concentrated. In the calculations of Rice and Ramsperger this was taken to be one squared term in the energy expression, Kassel assumed that the energy had to be concentrated into one oscillator (i.e. two squared terms) which seems more realistic. The

two theories give very similar results in practice although the Kassel version has been used the more widely.

The molecule is regarded as a system of n_k loosely coupled degenerate simple harmonic oscillators of vibrational frequency ν. The loose coupling of the oscillators allows free flow of energy between them to occur with a frequency ν, without introducing significant anharmonicity. Reaction is assumed to occur when at least an energy E_c out of the total energy of the oscillators, E , by chance finds its way into one particular oscillator. If $E<E_c$ the chance of this happening is zero, but if $E \geqslant E_c$, there is a definite probability of this accumulation occurring. The theory is a statistical one in that all detailed arrangements of energy between the oscillators are considered equally likely provided the total energy is constant.

It can be shown that,

$$\text{probability of reaction} = \frac{(E - E_c)^{n_k - 1}}{E}$$

This reaction probability as a function of energy E is plotted in figure 1.1 for several values of n_k.

Figure 1.1.

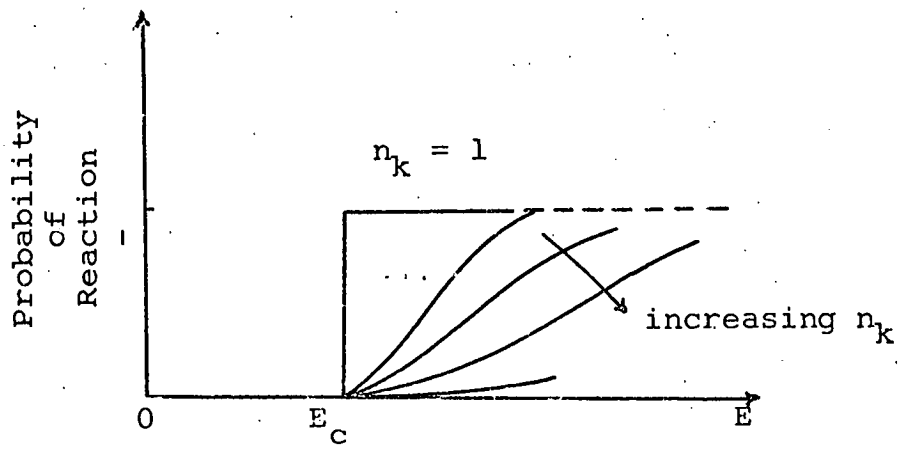

In the case of $n_k = 1$ it corresponds to the simple step function assumed in the Lindemann-Hinshelwood treatment. For $n_k > 1$, the distinction between activated and non-activated molecules becomes less clear-cut. For very complex molecules (large n_k) the reaction probability increases slowly with energy and remains quite small even for energies appreciably above the critical energy. Since energy is reshuffled ν times per second the specific reaction rate k_r is equal to ν times the probability that a reshuffle causes reaction, i.e.

$$k_r = \nu \left(\frac{E - Ec}{E}\right)^{n_{k-1}}$$

This rate constant is a function of total energy, E, only and does not depend on the distribution of the energy ove r the oscillators or on such factors as the vibrational phases of the oscillators. This is a consequence of the statistical assumption outlined above that total energy is the only relevant parameter in determining the relative probability of formation of the various detailed arrangements.

In the general pressure case equation (5) becomes

$$1^k = \int_{Ec}^{\infty} \frac{kr\ f(e)dE}{1 + kr/kd\ CM}$$

Thisleads to,

$$1^k = \nu \frac{e^{-b}}{(nk-1)!} \int_0^{\infty} \frac{x^{nk-1}\ e^{-x}\ dx}{1 + \frac{\nu}{Zam\ Cm}\left(\frac{x}{b + x}\right)^{nk-1}} \qquad (7)$$

where $Zam = k_d$ (assuming deactivation on every collision)

$x = (E-Ec)/kT$

$b = Ec/kT$

This integral can be evaluated numerically and a plot of log

($_1$k) versus log (pressure) constructed. The formula gives good agreement with most experimental data provided n_k is treated as an adjustable parameter and chosen to give the best fit. If this is done the value for n_k obtained is generally about one half the possible maximum value, which is the number of normal modes in the molecule.

RRKM(Marcus-Rice) Theory

This theory was developed essentially by Marcus (MAR52) from an earlier paper by Marcus and Rice (MAR51) and is known by the names of these authors or very often by the initials RRKM since its basic model is the Rice-Ramsperger-Kassel (RRK) model discussed previously.

The RRKM theory of unimolecular reactions employs two new principles. Firstly, the energization rate constant k_a is evaluated by a quantum-statistical-mechanical treatment instead of the classical treatment used in the RRK theory. The de-energization rate constant k_d is considered as in other theories to be independent of energy, and is often equated to the collision number Z or to λZ where λ is a collisional deactivation efficiency. The second feature of the RRKM theory is the application of Transition State Theory to the calculation of k_r. For this purpose the overall reaction is written in terms of two steps

$$A^* \longrightarrow A^\dagger \longrightarrow \text{products}$$

in which a careful distinction is made between the energized molecule A* and the activated molecule $A^\dagger$ (sometimes called the activated complex). The rate at which molecules pass

through the critical configuration (activated complex) is a function of energy in the reaction coordinate, Rotational and vibrational modes of motion of the molecule are classed as either adiabatic or active; the former remain in the same quantum state throughout the reaction, the latter exchange energy freely. The rate constant k_r then has the form

$$k_r = \frac{1}{h} \frac{Z_1^+}{Z_1^*} \frac{\sum P(E^+)}{N^*(E)}$$

The terms Z_1^+ and Z_1^* are the products of the partition functions for adiabatic degrees of freedom of the activated complex and the molecule, respectively and their ratio is usually near unity. $\sum P(E^+)$ is the total sum of the degeneracies of all possible energy eigenstates of the active degrees of freedom of the activated complex up to a total energy E^+:$N^*(E)$ is the number of eigenstates per unit energy of the active degrees of freedom for the molecule at energy E;h is Planck's constant; E_o is the minimum energy necessary for reaction; and $E^+ = E - Eo$.

For thermal unimolecular reactions

$$f = \frac{N^*(E)\, e^{-E/kT}}{Qa}$$

where Q_a is the ordinary molecular partition function for all the active modes of A. This gives

$$_1k = \frac{Z_1^+}{h\ Qa\ Z_1^*} \int_{E=Eo}^{\infty} \frac{\left\{\sum P(E^+)\right\} e^{-E/kT}\, dE}{1 + kr/kd\ CM}$$

where $CM \longrightarrow \infty$

In the high pressure limit this reduces to

$$_1k = \frac{kT}{h} \frac{Q+}{Qa}\ e^{-Eo/kT}$$

Where $Q^{\dagger}$ is the partition function of the active modes of the activated complex.

Expressions have been developed for $P(E^{\dagger})$ and $N^*(E)$ (MAR51) and Whitten and Rabinovitch (WHI63) have developed more accurate approximations, which they have checked by employing high speed computational techniques which allowed the quantum-statistical summation to be done with relative ease.

The RRKM theory has the advantage, relative to any dynamic theory, of great simplicity. In principle a knowledge of the thermochemistry and a vibrational analysis of A together with use of the above equations gives a method of calculating unimolecular rate constants based solely on molecular structure, and with no adjustable parameters. In practice, however, there are two semi-empirical aspects which must be considered. (a) the structure and the frequencies assigned to the vibrational modes of the transition complex; (b) the degree of anharmonicity in the vibrations of the molecule at high energies.

The first aspect, although conceptually very important, is not critical for the practical numerical evaluation of k_r. It has been shown that as long as the entropy of activation requirements are roughly satisfied (SET62, WIE62, RAB61) the magnitude of the specific rate constant will not be particularly sensitive to details in structure or vibrational frequencies of the activated complex.

Little information is available about anharmonicity constants, particularly for bending modes, even at low

levels of vibrational excitation. However, plausible limits have been calculated which indicate these effects to be small (SCH62), especially for larger molecules where the average degree of excitation of any one mode is relatively low. So it is assumed that internal molecular motions may be described as weakly coupled harmonic vibrations, with sufficient coupling to ensure rapid relaxation of energy among the vibrational modes but not enough to effect the density of states calculated on the assumption of harmonic modes.

Slater's theory

In contrast to the RRKM theory this is a dynamic theory in which the rate of decomposition of activated molecules is calculated using classical mechanics, without the 'statistical' assumption (SLA59). The model of a reactant molecule that is used in this theory is one consisting of a number of simple harmonic normal mode oscillators of various frequencies. These normal modes are taken to be strictly harmonic so that no energy transfer can occur between them. Thus it is assumed that the amount of energy in each normal mode stays fixed between collisions and can only change when collision occurs. Decomposition is assumed to occur when the phases of the vibrations are such that one particular coordinate (q) of the molecule exceeds some critical value (q_c). This coordinate may be the distance between the atoms, a bond angle or any linear combination of any number of these coordinates. This coordinate must be chosen with reference to the motion of the atoms that is believed to

accompany the reaction and so in most cases some uncertainty exists in making this choice. Since after an activating collision has occurred no energy flow between the normal modes is possible in this theory, not only must the activated molecule possess an energy at least equal to E_c but this energy must be correctly distributed at the instant of activation if this molecule is to undergo subsequent reaction. This activation requirement is more stringent than that of the RRK theory and so rates of activation in the Slater sense must be slower. Also the rate of reaction k_r is no longer simply a function of total energy only, but it depends on the way the energy is distributed over the normal modes. The critical coordinate will be a linear combination of a number, say n_s, of simple harmonic normal modes, of different frequencies, and therefore, constantly varying relative phases.

The results of this theory when made the subject of certain approximations are rather similar to the RRKM theory, but with certain important differences. Firstly, the number of normal modes n_s is the number that may contribute to altering the coordinate q, i.e. it includes all the normal modes of the molecule except those which for symmetry reasons cannot affect q. Secondly, the formula for k_r as a function of total energy becomes,

$$\bar{k}_r = \bar{\nu} \left(\frac{E-E_c}{E}\right)^{ns-1}$$

only after it has been averaged over all distributions of the internal energy. The frequency $\bar{\nu}$, is given by

$$\bar{\nu}^2 = \frac{\sum_1^{ns} \alpha_i^2 \nu_i^2}{\sum_1^{ns} \alpha_i^2}$$

It is a weighted root mean square of all the normal mode frequencies ν_i, the weighting (amplitude) factors α_i representing the magnitude of the contribution of each normal mode coordinate Q_i to the displacement q (i.e. $q = \sum_1^{ns} \alpha_i Q_i$). $\bar{\nu}$ must therefore lie between the greatest and the least vibration frequencies of the molecule.

The general formula for $_1K$ approximates to the RRK expression (equation (6)) but with the substitution,

$$n_k = \tfrac{1}{2}(n_s + 1) \qquad (8)$$

Since n_s is usually not very different from the total number of modes, while a value of n_k of about half this maximum often gives the best fit to experimental data, it can be seen from (8) that the predictions of the two theories about the shape of the fall-off curves do not differ greatly in many cases. This is illustrated in figure 1.2

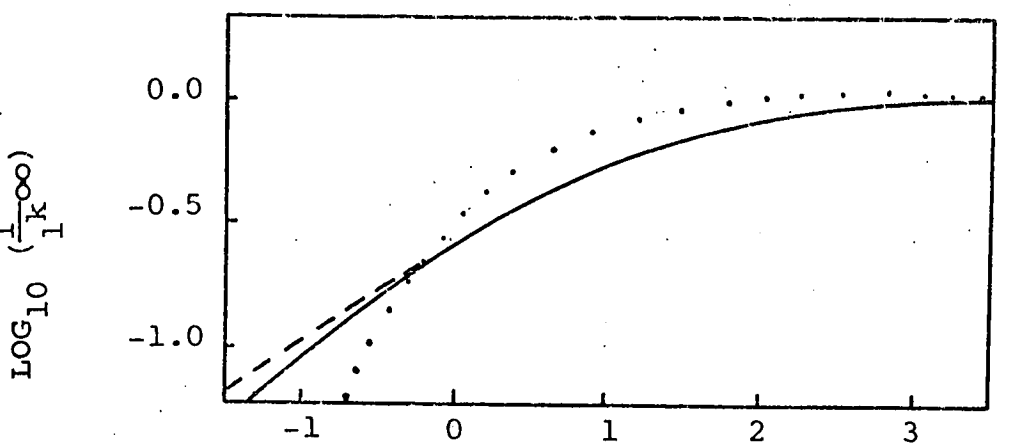

Fig. 1.2

A comparison of the fall-off curves predicted for the isomerization of cyclopropane at 500'c

..... Hinshelwood-Lindemann theory

_____ Slater theory (PRI53)

- - - - - Kassel theory

All the experimental evidence is that energy flow does occur freely between the normal modes of real molecules, because at the high energy levels associated with chemical reactions the molecular vibrations are considerably anharmonic. The parabolic potential curve is a valid approximation for the low vibrational levels only as illustrated in figure 1.3.

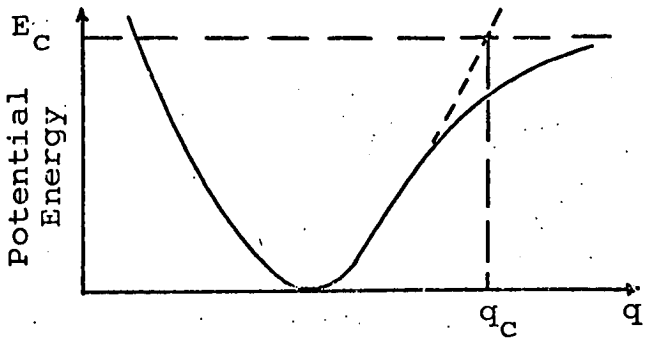

Fig. 1.3

(a comparison of the potential energy curves for a simple harmonic oscillator and a typical molecular vibrational mode. S.H.O. - - - ; molecule ———)

Hence rates of decomposition in Slater's theory must be too low since they do not allow for this redistribution of energy between the normal modes. On the other hand the view that reaction occurs when a coordinate reaches a particular value, e.g. a bond length reaches a critical extension, is a more reasonable picture of a chemical reaction than the RRK criterion that a certain amount of energy must be accumulated in a particular oscillator. A molecule could well have more energy than Ec in this mode and yet its configuration might not be such that it could be said to be undergoing reaction. In an attempt to reconcile these two viewpoints Gill and Laidler have proposed a hybrid of the two theories.

Gill and Laidler's theory

The mechanism envisaged is summarized as

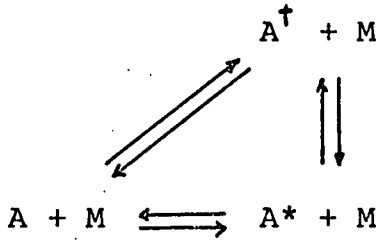

PRODUCTS

Where $A^{\dagger}$ is a reactant molecule that is activated in the RRKM sense and A* is one that is activated in the more stringent Slater sense. Only the latter is assumed to be able to react to give products but an RRKM molecule may become an A* molecule by internal energy transfer (without collision). Free flow of energy is assumed in accordance with experiment but the criterion for reaction is the Slater one of coordinate extension. At high pressures this mechanism leads to the same results as Slater's theory, but at low pressures the results of the RRKM theory are obtained. This is because at low pressures an $A^{\dagger}$ molecule always has time to reorganize its energy distribution to form A* and hence to react before it is deactivated by collision. At high pressures this is not so and only A* molecules formed directly by collision are likely to produce products. Since the differences between the predictions of the Slater and RRKM theories are not easily detected experimentally both can be fitted to many results within experimental error. It follows that this combined theory can also give good agreement with experiment.

1.3 Unimolecular Decomposition Reactions of Simple Alkanes and Alkyl Radicals

Molecules undergo thermal unimolecular reactions as a result of energization by molecular collisions. Collisions between molecules at a given temperature produce energized molecules with an equilibrium distribution of energy (the Maxwell-Boltzmann distribution) which enables the fraction of molecules energized into a particular energy range to be calculated.

Methods of energization other than by molecular collisions may produce a non-equilibrium situation in which molecules can acquire energies far in excess of the average thermal energy. This excess energy may be lost by molecular collisions or may result in further chemical reaction if a suitable reaction path is available. One such method of activation is by absorption of radiation. However, most of these photoprocesses are poorly understood and it has been virtually impossible to apply a theoretical treatment to the initial decomposition process in these systems.

When the energization occurs by virtue of the energy changes in a chemical reaction producing the molecules, the process is known as chemical activation. Among the best known of chemically activated systems are the reactions between atoms (principally H atoms) and olefins to produce vibrationally excited radicals, e.g.

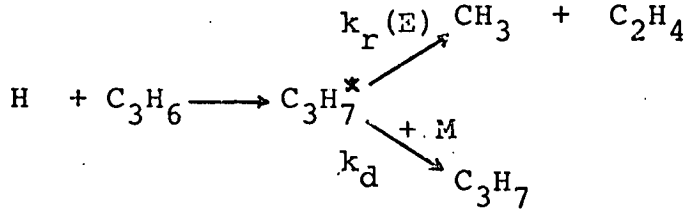

The competition between decomposition of the vibrationally excited species (rate constant $k_r(E)$) and collisional stabilization (rate constant k_d) is reflected in the experimentally determined ratio (D/S) of decomposition to stabilization products obtained. For each system studied, the overall mechanism must be established to enable this ratio to be determined from the experimental product analysis. If it assumed that deactivation occurs on every collision, the rate constant k_d can be equated with the standard collision frequency Z which can be calculated from the collision theory expression,

$$Z = (\sigma d^2\ NA/R)(8\pi NAk/\mu)^{\frac{1}{2}}(1/T)^{\frac{1}{2}} \qquad (9)$$

where

Z will be in $Torr^{-1}s^{-1}$
σd = Collision diameter in cm
μ = reduced molar mass in $gmole^{-1}$
T = Temperature in ^oK
NA = 6.0225×10^{23} $Mole^{-1}$
R = 6.2362×10^{4} $cm^3\ Torr\ K^{-1}\ MOL^{-1}$
k = 1.3805×10^{-16} erg K^{-1}

It is then possible to derive an experimental value of k_r (E) which will in fact be an average value for the range of energized molecules involved.

The average rate constant ⟨kr⟩

For a nonthermally activated unimolecular reaction if the steady state is considered in which an excited species A* is formed (A* is an alkane or an alkyl radical) the situation is represented by

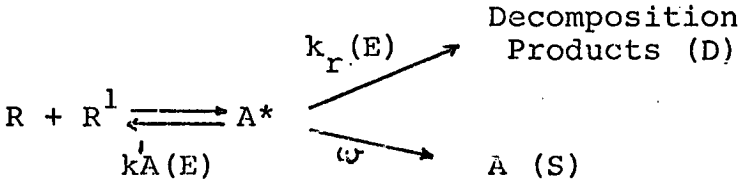

According to this scheme, energized molecules A* at energy E can reform reactants with a rate constant k_r^1 (E), form decomposition products with a rate constant $k_r(E)$ or be de-energized to stable species A. For the strong collision assumption the first order rate constant for de-energization is equal to the collision frequency, $\omega = Zp$ where p is the total pressure and Z is given by (9). If the fractional flux of species which are energized per unit time into the range between E and $E + \delta E$ is $f(E)\delta E$, then the fraction of A* decomposing by path D compared with those stabilized by path S is,

$$k_r(E)/(k_r(E) + \omega)$$

If the back reaction reforming reactants can be ignored, the fraction of species in the energy range E to $E + \delta E$ decomposing to products is therefore

$$\left\{(k_r(E)/(kr(E) + \omega)\right\} f(E)\delta E$$

The total number of species decomposing per unit time (D) at all energies above the critical energy E_o, is therefore given by (10)

$$D = \int_{E_o}^{\infty} \frac{kr(E)}{kr(E) + \omega} f(E)dE \qquad (10)$$

The total rate of stabilization(s) is given by a similar expression with $k_r(E)$ in the numerator replaced by ω. In a strictly monoenergetic system, the experimental ratio D/S is equal to $k_r(E)/\omega$. Where there is a distribution of energies, an average rate constant $\langle k_r \rangle$ for all energies above E_o is defined by

$$\frac{\langle kr \rangle}{\omega} = \frac{D}{S} = \frac{\text{No. of molecules decomposing per unit time}}{\text{No. of molecules being stabilized per unit time}}$$

Hence utilizing (10) and the equivalent expression for stabilization the result is obtained for $\langle k_r \rangle$

$$\langle k_r \rangle = \omega \frac{\int_{\varepsilon_0}^{\infty} \{ kr(E)/(kr(E) + \omega) \} f(E)dE}{\int_{\varepsilon_0}^{\infty} \{ \omega/(k_r(E) + \omega) \} f(E)dE}$$

At high pressures $\omega \gg k_r(E)$ and so

$$\langle k_r \rangle_\infty = \omega \frac{\int_{\varepsilon_0}^{\infty} (kr(E)/\omega) \; f(E)dE}{\int_{\varepsilon_0}^{\infty} f(E)dE} = \omega \langle k_r(E)/\omega \rangle = \langle k_r(E) \rangle$$

Similarly at low pressures $\omega \ll k_r(E)$ and so

$$\langle k_r \rangle_0 = \omega \frac{\int_{\varepsilon_0}^{\infty} f(E)dE}{\int_{\varepsilon_0}^{\infty} (\omega/k_r(E)) \; f(E)dE} = \omega \langle \omega/k_r(E) \rangle^{-1} = \langle 1/k_r(E) \rangle^{-1}$$

Calculations have been presented by Rabinovitch and Setser (RAB64) for model molecules which resemble the simple alkanes (C_1,C_2,C_3 and C_4) and the corresponding alkyl radicals. The models are not identical with real molecules since the principal purpose was to vary energetic, structural and frequency parameters in order to display their effects on the reaction rate and its characteristics. From their calculations they were able to predict;

(a) the variation of S/D with temperature and pressure

(b) the value of $\langle k_r \rangle_\infty$ and $\langle k_r \rangle_0$ for each reaction.

Table (1.1) shows a selection of their results which is relevant to the systems studied in this work.

Table 1.1

Data on Activated Molecules and Radicals

Source of Activated Species	Activated Species	Decomposition Products	$\langle kr \rangle_\infty$	$\langle kr \rangle_o$	S/D at 1 torr and 298°K
H + CH_3	CH_4*	H + CH_3	1.2×10^{10}	6.3×10^{9}	0.02(EST)
CH_3 + CH_3	C_2H_6*	CH_3 + CH_3	3.7×10^{7}	4.2×10^{6}	0.96
H + C_2H_5	C_2H_6*	CH_3 + CH_3	3.2×10^{9}	2.8×10^{9}	0.006(EST)
CH_3+C_2H_5	C_3H_8*	CH_3 + C_2H_5	2.3×10^{5}	1.04×10^{4}	90
H+1SO-C_3H_7	C_3H_8*	CH_3 + C_2H_5	2.72×10^{7}	1.85×10^{7}	0.89
H+n-C_3H_7	C_3H_8*	CH_3 + C_2H_5	1.59×10^{8}	1.26×10^{8}	0.115
C_2H_5 + C_2H_5	nC_4H_{10}*	C_2H_5 + C_2H_5	4.69×10^{4}	1.16×10^{3}	442
H+C_2H_4	C_2H_5*	H + C_2H_4	4.2×10^{7}	1.27×10^{7}	0.85
H+C_3H_6	n-C_3H_7*	CH_3 + C_2H_4	7.81×10^{7}	5.70×10^{7}	0.321
H+C_3H_6	n-C_3H_7*	H + C_3H_6	6.04×10^{5}	2.54×10^{5}	64.9
H+C_3H_6	1SO-C_3H_7*	H + C_3H_6	3.24×10^{5}	4.26×10^{4}	65.2
H+1-Butene	Sec C_4H_9*	CH_3 + C_3H_6	2.6×10^{7}	1.7×10^{7}	1.5

1.4 Rate Constants for the Reactions of Hydrogen Atoms With Olefins

The H atom addition to olefins has been the subject of extensive experimental and theoretical studies. Most of the work which has been done to specifically characterize these reactions in the gas phase has been carried out at room temperature and early studies were directed towards obtaining rate constants of these reactions relative to that of some common reaction. The most important contributions in this area have been due to Cvetanović and coworkers and in table 1.2 the mean values of the relative addition rates obtained by this group are compared with those of other systematic studies. The measurements lack consistency with the exception of Cvetanović's photochemical studies.

Table 1.2

Relative Rates for H + Olefins at 25°

Olefins	Allen Melville (ALL53) and Robb	Yang (YAN62)	Cvetanović (CVE69)
ethylene	1.0	1.0	1.0
propene	0.32 (1.6)	1.3	1.53
1-butene			1.58
isobutene	0.76	13.3	3.85
cis-2-butene	1.06	0.49	0.72
trans-2-butene	0.83	0.52	0.90

Several absolute determinations on reaction systems of this type have also been reported (table 1.3). In general, the correlations between the relative and absolute determinations have not been altogether satisfactory.

Table 1.3

Absolute Rate Constants for H + Olefins (room temperature)

	Rate Constant $l.mole^{-1} sec.^{-1} \times 10^{-8}$	Pressure Torr	Reference
H + ethylene	2.17	1.2(He)	TEN72
	1.02 ± 0.06	2(Ar)	KN069
	1.02 ± 0.06	2.4(He)	WES69
	2.28 ± 0.24	5(He)	BAR70
	1.98 ± 0.06	5(He)	KUR70
	1.2	8(Ar)	HAL70
	5.1 ± 1.8	10(He)	DOD69
	2.52 ± 0.06	10(He)	KUR70
	7.2 ± 0.6	500(He)	"
	5.45 ± 0.54	700-1500(He)	EYR70
H + propene	3.98 ± 0.36	1.9(He)	COW71
	4.56 ± 0.24	2(Ar)	DAB71
	7.30 ± 0.06	5(He)	KUR71
	7.83 ± 2.4	6.7(He)	DOD69
	10.30 ± 0.06	500(He)	KUR71
H + 1-butene	8.32 ± 0.48	2(He)	DAB71
	6.81 ± 0.48	2.9(He)	COW71
	9.0 ± 2.7	6.7(He)	DOD69
H + isobutene	19.3 ± 12.0	2(Ar)	KNO69
	22.9 ± 3.6	8-50(He)	BRA67
H + cis-2-butene	4.8 ± 0.4	2(He)	DAB71
	3.9 ± 0.3	3.2(He)	COW71
H + trans-2-butene	4.3 ± 0.2	1.8	"
	5.4 ± 0.4	2(He)	DAB71
	6.0 ± 1.0	5.5-50(He)	BRA67

Arrhenius Parameters, resulting from temperature studies on some of the above systems are shown in table 1.4

Table 1.4

Reaction	Arrhenius Parameters $Ax10^{-10}$ $l.mole^{-1}sec^{-1}$	E $kcal.mole^{-1}$	Reference
H + ethylene	5.6	3.4	YAN62
	1.86	1.6	DOD69
	2.68	3.3	KNO69
	0.078	0.73	TEN72
H + propene	4.45	3.0	YAN62
	0.95	2.0	DAL67
	0.61	1.2	KUR71
H + isobutene	4.45	1.6	YAN62
	3.36	1.36	KNO69

CHAPTER 2

EXPERIMENTAL METHODS

2.1 Flow Systems

The flow of compressible fluids is a highly complex phenomenon and if the fluid is also undergoing chemical reaction the situation becomes impossibly complex to deal with exactly unless drastic simplification is possible. Considering the flow of gas in a cylindrical pipe the types of flow observed fall into four main categories - molecular, viscous, turbulent, and supersonic. The conditions for each regime are defined in table 2.1.

Table 2.1 - Flow Types

Type of Flow	Theoretical requirement	Definition	Value of parameter under standard conditions*	Experiment Conditions
molecular	$\lambda > d$	$\lambda = 1/2\frac{1}{2}\pi N d^2$	$\lambda = 5.7 \times 10^{-6}$ m	$\lambda \ll d$
viscous	Re < 2000	$Re = \bar{u}\rho d/\eta$	Re=60	Re $\ll$ 2000
turbulent	Re > 2000	"		
supersonic	u > Usound	$Usound = \left(\frac{\gamma KT}{m}\right)^{\frac{1}{2}}$	U=10m sec^{-1} Usound=324ms^{-1}	U $\ll$ Usound

Hence the flow type is viscous under these standard conditions

$\pi\sigma^2$= collision cross section, m = molecular mass, T = temperature, γ = heat capacity ratio, K = Boltzmann's constant, $\bar{u}$ = mean linear velocity, ρ = density, λ = mean free path, η = viscosity, d = vessel dimension, N = number of atoms per cm^3, Re = Reynold's number, * standard conditions - Argon at 2 torr pressure, 300^{o}K, with U = 10 m.sec^{-1} and d = 3 cm.

In molecular flow the gas moves as individual molecules rather than as a continuous fluid. This occurs if the mean

free path of the gas molecules between collisions is greater than the dimensions of the apparatus. If air is taken as an example, the flow is molecular if the pressure $P < 500/d$ microns, where one micron is 10^{-3} torr and d is the diameter of the pipe in cm. Molecular beam flow systems operate in this region where λ may be many metres. If the mean free path is lessthan d then the flow is not molecular but may be viscous (streamlined) provided that the Reynold's number (Re) falls below a critical value. (see table 2.1 over). For long cylindrical tubes the flow ceases to be viscous and becomes turbulent if the Reynold's number exceeds about 2×10^3. Finally, flow in the supersonic region occurs when the flow velocity exceeds the velocity of sound. Under the conditions used in our experiments the flow was viscous.

If the flow is viscous the flow rate through the pipe is given by Poiseuille's equation, and although the velocity distribution across the pipe is parabolic, the average residence time of the reacting gas within a tubular reactor can be taken approximately as being the volume of the reactor divided by the total flow rate - that is by assuming plug flow. The condition for this to hold is that the diffusion time across the tube is much less than the passage time along it, i.e.

$$t_{diff} = r^2/2D \ll L/U = t_{flow}$$

r = radius of pipe, D = diffusion coefficient, L = length of pipe, U = flow velocity

With standard conditions as defined above and L = 0.1m, and D = 0.13 $m^2 sec^{-1}$

$$t_{diff} = 9.9 \times 10^{-4} sec \text{ amd } t_{flow} = 10^{-2} sec$$

Under these conditions, time is related to distance along the reactor in a fairly simple fashion and the system is reasonably well suited to kinetic measurements.

When the Reynolds' number exceeds the value given above the flow becomes turbulent and the situation is considerably changed. The flow pattern is no longer streamlined and becomes very sensitive to the exact shape of the pipe through which the gas flows. In particular any rapid changes in diameter of the pipe may have a marked influence on the flow pattern. For reactors which consist of a wide tube with narrow inlet and outlet tubes at opposite ends, the large change in diameter between the inlet tube and the main reactor can cause the onset of non-viscous flow at Reynolds' numbers, within the reactor itself, much lower than 2×10^3. The result may be 'channelling' of the gas flow through the reactor, in which a narrow fast moving stream of gas passes through the reactor from inlet to outlet without expanding to fill the whole volume of the vessel, most of which is occupied with almost stationary gas. It appears that some of the early work conducted in conventional kinetic flow systems suffers from this defect and in consequence the results so obtained must be treated with some reserve. It is therefore essential that the fluid dynamic characteristics of the flow be

determined so that the relation between flow rate and the effective average residence time can be found. We believe that the equipment used in this study effectively eliminated channelling.

This is equally true in the fourth region where flow velocities exceed the velocity of sound. The gas flow is made supersonic by passing an inert gas through a suitably shaped convergent - divergent nozzle. The reactants are then injected into the flowing gas stream in the supersonic region. Owing to considerable experimental difficulties, applications of this technique are limited to a few simple and very fast reactions.

By operating a flow tube reaction system at relatively low pressures of the order of a few torr the gas density is sufficiently low that quite high flow velocities of the order of $10 msec^{-1}$ can be achieved at low Reynolds' numbers. The simplicity of viscous flow is obtained yet fast reactions may be studied with a time resolution of 10^{-3} sec or better.

Atoms may be generated in the flowing gas by passage through an electric discharge and provided the pressure is low and the walls of the tube are suitably deactivated, the recombination of the atoms may be sufficiently slow that appreciable atom concentrations (e.g. 1% of the total gas) exist for considerable distances, e.g. a metre or more, downstream of the discharge. Nitrogen, hydrogen and oxygen atoms are easily obtained in this way by discharging the diatomic gases, provided small quantities of certain impurities are present in the gas. The action of these

impurities is poorly understood but there is considerable empirical evidence that their only effect is to increase the efficiency of dissociation without appreciable contamination of the product. Reactions of the atoms produced in this way may be studied by adding reactants to the flow downstream of the discharge. The progress of the reaction along the tube can be followed by the techniques described later, for the detection of H atoms and products.

2.2 Production of Hydrogen Atoms

A stable and efficient source of hydrogen atoms is required in a flow system. Stability is important since runs may last for several hours, and fluctuations in the atom supply would destroy any meaningfulness of the results. High efficiency is also desirable, particularly at high flowrates, since the residence time of a molecule in the dissociation region is short, and the chance that it should be dissociated in this time should be as high as possible.

Jennings (JEN61) has reviewed the production of atoms in general. From the methods listed therein only the following satisfy the above criteria; (1) electrical discharges (2) thermal dissociation. All other methods fail on one or both counts. Thus photolysis produces too low a concentration of atoms while shock tube methods give high but transient concentrations.

(1) Electrical Discharges. These produce high concentrations of atoms at pressures up to 15 torr, with the disadvantage that work at higher pressures is not possible, due to failure of the discharge.

Three main types have been used to produce atoms.

(a) The low frequency electrode discharge or Wood's tube.

(b) The radio frequency or electrodeless discharge, operating at a frequency of a few mHz.

(c) The microwave discharge which operates at a frequency of2500 - 3000 mHz.

The earliest system was due to Wood (WOO21), and consisted of a U-tube, one to two metres long, with a stream of gas passing through the arms and being withdrawn from the middle, pressures in the tube being between 0.5 and 5.0 torr. The gas was dissociated by a discharge between aluminium electrodes situated at the ends of the arms, to which an AC voltage of 2KV at 50Hz was applied. This achieved about 50% dissociation of the gas (POO37) but had the disadvantage that the electrodes were in contact with the atom stream, allowing the atoms formed to attack the electrode surface, and causing the risk of contamination of the atom stream (LIN56).

The problem of this attack on the electrodes can be obviated by use of the radiofrequency 'electrodeless' discharge which also has the advantage that no special discharge tube is required. The electrode assembly outside the tube may consist either of two electrodes wrapped round the tube (capacitative coupling) or of a coil of copper wire wound round the tube (inductive coupling). (The former is to be preferred, however, since it gives a discharge over a wider pressure range (HOR69)). The power is supplied by a radiofrequency generator operating between 1 and 30 MHz

with a power output of up to 200 Watts. This type of discharge can operate efficiently at lower pressures than a Wood's tube and has an upper pressure limit of about 10 torr. Care must be taken in this system and the Wood's tube that stray fields are not generated in the discharges, since these may affect instruments in the vicinity.

Microwave discharges, operating at 2500 - 3000 MHz with power outputs of several hundred Watts are the most recent developments in discharges. The discharge is generated inside a quartz tube passing through a tunable resonance cavity coupled to a waveguide leading from a microwave source. This arrangement is suitable for use at pressures of up to 15 or 20 torr.

Both radiofrequency and microwave discharges have been used to produce the following atoms from their parent molecules in the presence of an inert gas: hydrogen, oxygen, nitrogen and the halogens.

Table 2.2 summarises the yields so obtained.

Table 2.2

Gas	% Dissoc. of Parent Molecule	Power (Watts)	Frequency (MHz)	Pressure (torr)	Reference
Hydrogen	90	100	3000	0.5	SHA59
	not quoted	50	2927	3-48	GRE59
	¼-1	350	18	2	CLY63
	½-5	350	18	0.8-4	"
	20	150	18	2-4	DAL67
	10-50	-	33	1-20	DOD69
Oxygen	-	70	2-6	0.05-2	LIN56
	½-5	350	18	-	CLY63
Nitrogen	½-2	350	20	1.26-6.32	"
	¼-1		18		
Halogens					
Cl_2	8-18	-	-	0.2-0.7	ROD33
up to	100	100	2450	-	OGR61
I_2/Br_2	80-100	-	450	-	GAR58

(2) Thermal Dissociation. This has been used by LeRoy (LER53) to produce H atoms, the source being a tungsten filament, electrically heated to about 1700°K, placed in a stream of hydrogen. Concentrations of H of about 0.1% of the original H_2 are produced : this may be compared with the dissociation caused by discharges as given by table 2.2 above. Recently hydrogen atom concentrations of 'good' intensity have been produced by thermal dissociation in a tungsten tube heated electrically to 3000°K(MAR66). However it would be difficult to cool the atom stream sufficiently

to prevent thermal decomposition of the reactants added to the atoms at a later stage.

From the point of view of percentage dissociation table 2.2 indicates that microwave discharges are superior to r.f. discharge units but as to pressure range, according to Jennings (JEN61) r.f. discharges work better at lower pressures. His evidence seems to be based solely on the work of Greaves and Linnett (GRE59) who found that a microwave discharge could be sustained in hydrogen only over the pressure range 3-48 torr. Since it was intended to work at pressures less than 3 torr an r.f. discharge was chosen as a source of hydrogen atoms.

It is interesting to note that Ogryzlo's high yields (OGR61) were achieved only after he had coated the inside of his discharge tube with an oxyacid. This procedure was not adopted by the other workers although it was noted in some cases (GRE59), that 'wet' gases gave higher dissociations under comparable power and pressure conditions. This seems to be due to some catalytic process occurring in thedischarge rather than to the possible poisoning of the walls of the system by the impurity, as has been suggested by Wood (WOO22). Poisoning of the walls is desirable, and it is known that water deposited on the walls is a good agent for preventing atom recombination (POO37), but the characteristics of the impurity effect suggest that some homogeneous mechanism increases the yield of atoms, rather than that the heterogeneous recombination of the atoms is decreased. It has been shown (DAL67) that if the impurity

is removed by cold trapping, the atom production rate drops immediately; were the effect due to poisoning, it would be expected that the removal of the impurity would cause a slower change in rate, since the absorbed impurity would take some time to desorb. In order to purposely poison the walls for atom recombination, it is the practice either to coat the walls with boric acid or to treat them witha mixture of dichloro-dimethyl-silane and trichloro-methyl-silane; even in these cases, traces of water vapour appear to help in inhibiting surface recombinations.

2.3 Detection of Hydrogen Atoms

Apart from the conventional methods of following chemical reactions by product analysis, pressure change etc., (MEL64), a variety of techniques has been used to determine H atom concentrations in reaction systems. Their usefulness is dependent on the extent to which they are quantitative and specific, and they are mainly used for discharge-flow experiments.

Wrede-Harteck gauges (WRE29) give absolute atom concentrations although they cannot distinguish between different atomic species. These gauges depend upon the steady-state pressure difference which is established when the atoms and molecules being studied effuse through a small orifice on to a catalyst which recombines atoms and only molecules effuse back into the main stream. Such gauges are normally limited to low total pressures by their response time, which is determined by the volume of the gauge

and the need to keep the dimensions of the orifice or slit small compared to the mean free path (GRE59).

Catalytic probes, which depend on the heat released when atoms recombine on an efficient catalyst, provide a convenient non-specific method for measuring atom concentrations. Relative concentrations can be determined simply by mounting the catalyst on the tip of a fine thermocouple and measuring the e.m.f. produced (LIN56). Absolute concentrations are best measured with the isothermal calorimetric probe developed by Tollefson and LeRoy (TOL48), in which the detector is a platinum spiral forming one arm of a Wheatstone Bridge. The spiral is maintained at constant temperature (resistance) by varying the current through the bridge so that it remains balanced. In this way constant heat losses are maintained and the rate of atom recombination on the detector can be determined from the difference in electrical powers dissipated in the spiral, knowing the heat of recombination. Careful design is important as the efficiency with which hydrogen atoms recombine on a platinum surface is low at room temperature although it increases with temperature (WOO61). A further advantage of working at elevated temperatures is a reduction in the rate of surface poisoning (FOX59). Errors due to the incomplete release of the heat of recombination on the surface and to change in thermal conductivity of the gas with its degree of dissociation appear to be small, although diffusion effects can introduce serious errors if gas flow is not rapid enough (SCH62).

The electron spin resonance spectrum of the hydrogen atom provides a very sensitive method of detecting hydrogen atoms, the spectrum consisting of a widely spaced doublet (BER52). Normally the spectrum is displayed in a differential form which is obtained by applying a small sinusoidal modulation to the magnetic field as it is swept through the resonance, the microwave output being passed through a phase sensitive detector locked to the modulation signal. The greatest sensitivity is obtained under conditions where the modulation amplitude corresponds roughly to line width; this introduces a certain amount of distortion. The dependence of the line width on the spin-spin relaxation time and hence on the number of collisions with other particles, particularly with other hydrogen atoms, introduces a further complication (BAR62). The use of oxygen gas to calibrate an e.s.r. spectrometer for concentration measurements is discussed by Kronberg and Strandberg (KRO59) and by Westenberg and de Hass (WES64). They show that the integrated absorption in a line is proportional to the number of hydrogen atoms present and is unaffected by modulation distortion (HAL60) and variation of the spin-spin relaxation time. The technique has been developed so that it is now extremely sensitive, allows essentially unambiguous identification with little interference, has considerable generality and possesses the advantage of any spectroscopic method of not perturbing the system.

In an attempt to eliminate the complications of the diffusion problem inherent in the catalytic probe type of

detector Michael and Weston (MIC66) developed Lyman-α absorption photometry as a means of detecting H atoms. The method uses a hydrogen-neon lamp emitting Lyman-α radiation at 1216Å and a nitric oxide filled ion chamber which serves as a detector. A photometric calibration curve was obtained by using titration with NO_2 as an absolute measure of H concentration. The technique has been used in conjunction with flash photolysis (BRA67) and a pulse radiolysis method for the production of ground state hydrogen atoms (EYR70).

Hydrogen atom concentrations can be determined directly in discharge flow experiments with a mass spectrometer by using a molecular beam inlet system arranged so that particles can pass directly into the ionizing region of the spectometer without colliding with any surfaces (FON53). Hydrogen atoms can be measured provided the electron energy used and the composition of the gases are not such that any other species (e.g. H_2) makes an overwhelming contribution to masspeak 1. Phillips and Schiff (PHI62), using a fast-flow reactor coupled to a mass spectrometer, were able to identify H atoms simply by sampling through a pinhole punched in a pyrex thimble. However, their results indicate that only a rough guide to H atom concentration was obtained. A sophisticated mass spectrometric method of investigating reactions involving hydrogen atoms, using gas diffusion in a flow, has been developed by Dodonov and co-workers (DOD66). Their main attention was directed to the solution of problems connected with specific difficulties in the mass spectrometry

of radicals, namely the disappearance of radicals in the inlet system and differentiation of their mass spectra from the molecular backgrcund. The first difficulty was overcome by admitting the gas as a modulated molecular beam, and the second by obtaining mass spectra of a single or a few lines, using various ionization techniques. Determination of the atomic hydrogen concentration in the reactor was made spectrometrically from the mass 1 peak, with a correction factor to allow for the contribution to mass 1 from the dissociation of molecular hydrogen.

The Bendix 'Time of Flight' mass spectrometer has been coupled to a fast-flow system and used for measuring H atom concentrations(ARR65). Samples from the gas stream were obtained through a pinhole in a teflon wall at the end of the reaction tube. This technique has the advantage that reactants and products as well as H atoms can be measured directly with the spectrometer.

A variety of methods for the detection and estimation of hydrogen atoms depend on their high chemical reactivity. The introduction of metal oxides into reactions (MEL49) has been used frequently for their estimation and hydrogen atoms have also been determined by introducing para-hydrogen into the reaction system (MEL49) and following the rate of reaction,

$$H + p\text{-}H_2 \longrightarrow o\text{-}H_2 + H$$

A disadvantage of the method is that conversion is also catalysed by paramagnetic substances such as other radicals that may be present in the reaction system.

Due to the lack of specificity in the thermal methods and the Wrede gauge, the search for more specific means of determining H atom concentrations has led to the development of the gas titration technique. Hydrogen can be estimated by titration with NO_2 (CLY62), the reactions involved being,

$$H + NO_2 = OH + NO \quad (1)$$

$$H + NO = HNO^* \quad (2)$$

$$HNO^* = HNO + h\nu \quad (3)$$

$$H + HNO = H_2 + NO \quad (4)$$

$$OH + OH = H_2O + O \quad (5)$$

$$O + NO_2 = O_2 + NO \quad (6)$$

$$O + NO = NO_2^* \quad (7)$$

$$NO_2^* = NO_2 + h\nu \quad (8)$$

Reactions (3) and (8) produce the so-called air afterglow. If the injected NO_2 is just sufficient to react with all of the H by (1) and all of the O produced, by (6), then no air afterglow will appear; but if the added NO_2 is not sufficient for this, then the air afterglow will appear. At the end-point, when the glow is just extinguished, the concentration of added NO_2 will be 1.5 times the H concentration. This technique depends on the absence of other means of removing OH, such as

$$OH + H_2 = H_2O + H \quad (9)$$

$$OH + O = O_2 + H \quad (10)$$

since this will distort the mechanism as given in the simple scheme above. Kaufman (DEL62) found that OH was destroyed by (10), and estimated that (9) was also important; the

rate constant of (10) was estimated as being about 0.2 of that of

$$O + NO_2 = O_2 + NO \qquad (6)$$

In the titration system, which differed from Kaufman's in that excess of NO_2 was present, the effect of (10) is probably small. Kaufman also estimated an activation energy of 6.5 Kcal.mole^{-1} for (9); this differs from the 10Kcal.mole^{-1} estimated by Fenimore, Avramenko, Lorentzo and Jones (FEN58). Baldwin has also shown that the lower activation for (9) is unlikely. Thus, it appears that the higher activation energy is the more probable, and reaction (9) will be important only in the presence of a large excess of hydrogen.

Although titration methods are useful in many studies, they tend to be unreliable when applied to any but the simples systems, since, for the method to be useful, the other reactants present must not interfere with the titration mechanism. Thus, in the study of the reactions of H with olefins, titrations with NO_2 cannot be used, due to the interactions of alkyl radicals with titrants, resulting in the irreversible removal of the titrant molecules. The titrations may only be used in the absence of the olefins, to determine the initial atom concentrations, and so cannot be used to observe the decay of the H atom concentration during the reaction with olefin: for this, some other method, such as the catalytic probe or the isothermal calorimeter, must be used.

2.4 Methods of Analysing Reactants and Products

For stable species that can exist for some hours under normal laboratory conditions the technique 'par excellence' is gas-chromatography and to a lesser extent mass-spectrometry.

Gas-chromatography

The impact of gas-chromatographic analysis on experimental gas kinetics over the last 15 years or so has been considerable, and it has virtually superseded all other means of quantitative analysis previously used. Not only has it made possible studies of reactions which could not be attempted before, but it has shown that much of the data obtained by older less reliable methods such as total pressure measurement in closed systems, or low temperature distillation, etc. were inaccurate.

In its most usual form a gas-chromatographic unit for use in gas kinetic situations has the outline shown,

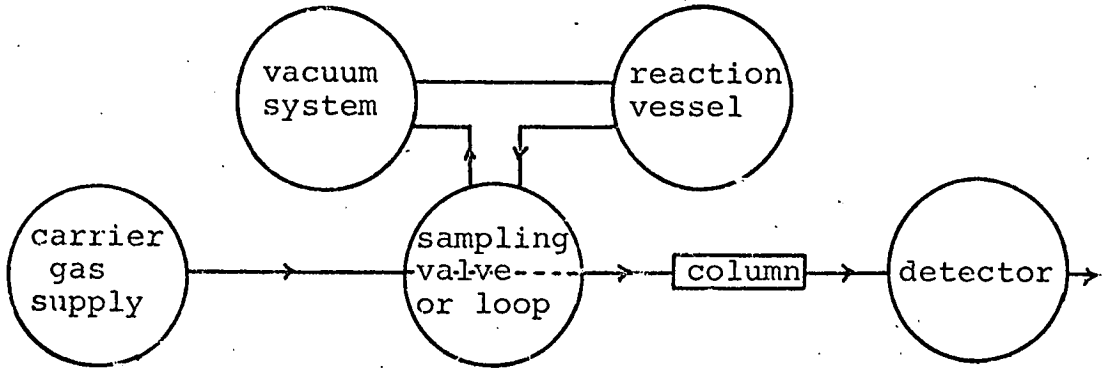

Small discrete gas samples to be analysed are taken from the reaction mixture by a sampling valve or loop and injected into the flow of the inert carrier gas which passes into the chromatographic column. The mixture is separated into its constituents and their concentrations are separately measured

by the detector as they emerge from the column. Very high separating efficiencies from 10^3 to 10^4 plates are relatively easily obtained. Analysis time can be as low as a few seconds in favourable cases and quite difficult separations may take only a few minutes. Very sensitive detectors can measure accurately (to better than 1%) the composition of samples of 10^{-10} moles. The method is general, virtually all volatilizable compounds can be analysed, and compounds differing only very slightly, e.g. isomeric forms, are readily distinguished and so their interconversion and other reactions can be studied. However, it is inapplicable to reactive intermediates such as atoms and free radicals and so it must be used in conjunction with some other method (see section on detection of H atoms) if a complete study of a reaction involving such species is desired.

Mass-spectrometry

For the chemical analysis of reaction mixtures of stable species mass-spectrometry has largely been superseded by gas-chromatography. This is due to the complex nature of mass-spectra, which arises since nearly every possible fragment ion is formed to some extent from each molecule present in the sample mixture, compared to the simple nature of chromatograms where each component yields only a single peak. However a number of features make mass-spectrometry very suitable for the study of unstable reactive intermediate reaction products such as ions, atoms and radicals. The low pressure existing in a typical mass spectrometer allows

the species to travel in virtually collision-free paths during analysis so that the loss due to reactive collisions with other gas-phase species or with the walls of the instrument are minimized. Also the time of flight through an instrument is very short, typically 10^{-5}sec or less, so that species with very short dissociative lifetimes can be studied. Ions produced in external reaction systems such as flames, explosions electric discharges, shock tubes, photolyses, and radiolyses can be introduced by collision-free molecular beam sampling systems into the mass spectrometer for analysis and measurement. Free radicals can be similarly introduced and their presence detected by making use of the fact that the appearance potential for the radical ion obtained directly from the radical is lower than that of the same ion when obtained from a molecule. The difference is equal to or greater than the energy required to produce the radical from the molecule by dissociation. For example, Barker, Keil, Michael and Osborne (BAR70) used a 'time of flight' mass spectrometer to investigate the addition of H atoms to ethylene. As well as being able to determine the concentration of hydrogen atoms their technique established that the major products were methane, ethane and methyl radicals with only minute traces of C_3 and C_4 compounds.

Several studies of the H-ethylene reaction have been reported recently and table 2.3 lists these together with the techniques used to monitor reactants and products and the results obtained.

Table 2.3

$$H + C_2H_4 \xrightarrow{k_1} C_2H_5$$

H Atom Detection	Products Detection	k_1 ($l.mole^{-1}sec^{-1}$)	Reference
catalytic probe	gas chromatography	1.02×10^8 (2 torr)	KNO69
electron spin resonance	-	1.02 " (2.4 torr)	WES69
Lyman-photometry	-	2.1 " (4 torr)	BAR70
time of flight mass spectrometry	-	2.4 " (4 torr)	"
Lyman-photometry	-	2.0 " (10 torr)	KUR70
-	gas chromatography	1.2 " (8 torr)	HAL70
mass spectrometry	mass spectrometry	5.1 " (10 torr)	DOD69
Lyman-photometry	-	5.4 " (700 torr)	EYR70

CHAPTER 3

APPARATUS AND EXPERIMENTAL PROCEDURE

3. Apparatus and Experimental Procedure

The flow system consisted of a long, wide-bore tube, through which a mixture of 2-5% hydrogen in argon could be passed, at a pressure in the region 0.6-3.6 torr. Before the gases entered the tube, they passed through a radio-frequency electrodeless discharge, which dissociated approximately 20% of the hydrogen. At a short distance after the discharge, an inlet was provided for the introduction of gaseous titrants into the system.

After titration, the reaction was studied by analysing the reaction mixture at various distances down the tube, for both hydrogen and hydrocarbon products. Product samples were withdrawn for analysis by a probe which could be moved axially along the flow tube; the atom concentration was measured by a catalytic probe assembly, which was also axially movable.

The complete apparatus can be considered as four separate sections. These are:

(1) the gas-handling system;

(2) the flow tube and discharge;

(3) the sampling and gas chromatography analysis system;

(4) the catalytic probe.

3.1 The Gas-handling System (Figure 3.1)

(For clarity figure 3.1, is a simplified drawing of this part of the apparatus.)

This was designed for storage, and to deliver the correct flowrates, of the four different types of gases involved, namely (a) hydrocarbon, (b) nitrogen dioxide,

(c) argon, and (d) hydrogen.

(a) Hydrocarbon system

The main storage was in a 10L bulb with 3l and 2l bulbs as subsidiaries (not illustrated). The hydrocarbon flowed from the 10L bulb via a glass capillary resistance through the jet inlet system and then into the flow tube.

(b) Nitrogen Dioxide system

The gas was contained in a 2l bulb, connected to a 2l storage bulb with cold finger, and linked also to a spiral gauge for pressure measurement (both not shown). The NO_2 flowed from the 2l bulb via a capillary resistance through the jet inlet into the flow tube in a similar fashion to the hydrocarbon.

(c) and (d) Argon and Hydrogen system.

A 2l bulb was used as a ballast volume to preserve a constant flowrate. The gas, from a cylinder, passed via a capillary to the 2l bulb. The outlet was through a second capillary after which the hydrogen and argon mixed prior to their passing through the discharge tube.

The volumes of the globes mentioned above were found by evacuating them and expanding air into them from a globe of known volume; measurement of the pressure change in the two linked globes allowed a simple Boyle's Law calculation to find the unknown volume. The pressures in the globes used for hydrogen argon and hydrocarbon were measured by manometers containing mercury. Since NO_2 attacks mercury, the pressure in the NO_2 globe was measured with a calibrated spiral gauge.

The flowrates of the gases were calculated in two ways. The hydrocarbon, NO_2 and H_2 gas flows were non-turbulent

and Poiseuille's equation, for laminar flow through the outlet capillaries, was applied, namely,

$$F = \frac{(P_1^2 - P_0^2)\pi r^4}{16\eta LRT} \qquad (1)$$

where F = flowrate in moles sec^{-1}

P_1 = inlet pressure

P_0 = outlet pressure

L and R are the length and radius of the capillary

η = viscosity of the gas

Since $PV = nRT$

$$\frac{dn}{dt}(=F) = \frac{dp}{dt}\frac{V}{RT}$$

Substituting for F in (1) gives

$$\frac{dP}{dt} = \frac{P^2\pi r^4}{16\eta LV} \qquad (P_o \approx 0)$$

Integration gives

$$\frac{1}{Pt} - \frac{1}{Pi} = \frac{\pi r^4}{16\eta LV} t$$

P_t = pressure at time t

P_i = initial pressure

Thus a plot of $\frac{1}{P}$ Vs t yields a straight line of gradient $\frac{\pi r^4}{16\eta LV}$.

V the volume of the bulb is known so that $\frac{\pi r^4}{16\eta LRT}$ (=c) can be found.

From (1) $F_t = c_t P^2$ and F can be found simply by measurement of the bulb pressure at that temperature (t).

The measurement of the NO_2 flowrate is complicated by the fact that at most pressures NO_2 is in equilibrium with

a significant porportion of N_2O_4. To find the flowrate of NO_2, it is necessary to know the equilibrium constant for,

$$2\ NO_2 \rightleftharpoons N_2O_4$$

It is assumed that at flowrate pressures the gas is completely dissociated into NO_2 and that the gas in the globe is always in a state of equilibrium, since the flow is small. Factors to take account of this were calculated from the data of Verhoek and Daniels (VER31) who studied the variation of the equilibrium with total pressure. The calculation is given in appendix 1.

The argon flowrate could not be calculated in this way since the gas flow was turbulent at the pressures required and this invalidates Poisseuille's equation. A calibration curve was constructed instead. As the argon escaped from the outlet capillary the decay of bulb pressure with time was noted over a large pressure range. A graph of pressure versus time was plotted and then with the aid of a computer a polynomial fit applied to the curve so that pressure (P) could be expressed as a function of time (t). This enabled $\frac{dP}{dt}$ to be calculated and since $\frac{dP}{dt} = \frac{dn}{dt} RT$ then $\frac{dn}{dt}$ (= flowrate) could be found. A calibration curve of flowrate versus pressure was then plotted (Figure 3.4).

3.2 The Flow Tube and Discharge (Figures 3.2)

The flow system consisted of a 28 mm diameter pyrex tube, 70 cm in length. This was surrounded by a vapour jacket of somewhat larger tubing, through which water or the vapour of boiling liquids could be passed to regulate the temperature

of the system. This jacket was fitted with B14 cone and socket joints, on which the boiler and condenser for vapour could be fitted when required. At the inlet end of the main tube a B34 socket was fitted, and 15cm. from the downstream end was a T-junction, which led, via a B34 cone and socket connection, and thence to the pump. The extreme downstream end of the tube was used to admit the probes for determining atom concentrations and sampling the reaction mixture.

The pump used to produce the fast flow was an Edwards 1SC 900 single stage rotary pump, which had a pumping speed of 900 litres per minute. This pump was connected to the outlet of the large cold trap by a metal coupling and four feet of heavy-duty rubber radiator hosepipe, of 2 inches diameter.

The discharge system was situated underneath the flow tube and was connected to it by a right angle bend in 14 mm diameter tubing leading to the B34 cone which fitted the socket at the upstream end of the flow tube. Also incorporated in this B34 cone and passing axially down the flow tube was the titrant inlet. This was made up of 5 mm diameter pyrex tubing terminating in a jet inlet system (figures 3.3) consisting of 37 glass capillaries of 1 mm diameter arranged radially. This arrangement ensured that good mixing of the reactant gases was obtained.

The discharge itself was produced inside a 14 mm diameter quartz tube. Two coils of copper tubing, 7 mm in diameter and 10 cm. apart, were wrapped round the tube and connected to the terminals of a radiofrequency transmitter (Wolfendale

Electronics Ltd., Bournemouth) which was operated at a frequency of 18 Hz., with a power output of 100-150 watts at 5 kV. The discharge tube and coils were enclosed in an outer glass tube and cold water was passed through the coil and around the tube. This kept the gas inside the tube and the coils at cold water temperature.

It was found, by NO_2 titration, that about 20% dissociation of the H_2 in a 5% H_2/Ar mixture could be obtained without difficulty. The walls of the system were coated with a mixture of dichlorodimethyl-silane, and trichloro-methyl-silane, which effectively poisoned the walls towards H atom recombination.

Pressure measurement in the flow tube was by means of a vacuostat attached near the outlet.

3.3 The Sampling and Gas Chromatography Analysis System (Figure 3.5)

The probe for removing samples from the system was made of 5 mm diameter pyrex tubing, which entered the flow tube via a coupling at the extreme downstream end of the tube. The probe could be moved axially along the tube, so that samples could be taken at any position. At the end, the probe widened to a diameter of 7 mm and contained a small roll of platinum foil; this was capped with silver gauze and the function of both metals was to recombine H atoms present at the moment of sampling. After exiting from the system, the probe was connected to the rest of the sample system by a 3 ft. length of 5 mm diameter nylon tubing. This flexible junction allowed the probe to be moved along the flow tube.

Samples for analysis were withdrawn through the probe and nylon tube into an evacuated 150 ml. capacity Töpler pump. A sample collected over a period of 5 minutes under average conditions of pressure (1.5 torr) and concentration was sufficient for analysis and this was pumped to the chromatography injector system. Two different types of column were used for different separations.

(a) Five feet of 'Porapak Q' 80/100 mesh, was used for the separation of hydrocarbons and olefins up to C_3. The running temperature was 40°C maintained by a glass sleeve surrounded by heating wire and suitably insulated with asbestos string.

(b) 15 feet of acetonyl acetone (hexane-2,5-dione) on 60/80 mesh celite (3%) kept at 0°C with a one foot column of 20% dinonyl phthalate on 60/80 mesh celite at either end gave good separations of all the alkanes and alkenes between C_2 and C_4.

The columns used were in the shape of U-tubes, and consisted of 4 mm internal diameter pyrex tubes. Column (b) was made up of three such U-tubes, each five feet in length, with short capillary connections between them. To cut down dead space within the chromatography system, all connections between the injector and the column and between the column and the detector were of 0.3 mm bore capillary. For the same reason, and also to prevent absorption of products in tap grease, Hone instrument valves (Hone instruments Limited, London) were used instead of stopcocks in the chromatography system.

Hydrogen was used as a carrier gas in both these columns, the flowrate in both cases being about 40 ml. $min.^{-1}$ After leaving the columns the gas joined a second stream, also flowing at 40 ml. $min.^{-1}$ and passed into a flame ionisation detector, where it was burned in a stream of air flowing at 800 ml. $min.^{-1}$.

The potential between the electrodes of the detector was maintained at 270 V by means of three 90V radio batteries arranged in series. Output from the detector was amplified by a Vibron electrometer and resistance unit, and was fed into a 1mV. pen recorder, via a resistance network, so that full deflection of the Vibron would give 1mV. input to the recorder.

The area of each peak was measured with a Perkin-Elmer integrator coupled to the recorder. From these peaks the relative amounts of each compound present in any given sample could be determined. The analytical procedure depended on finding the relative amounts of all of the components of the mixture, and, knowing that they had all come from a measured amount of starting material, the concentration of each component could be calculated.

3.4 The catalytic Probe - Measurement of H Concentration.

The measurement of (H) can be achieved by NO_2 titration, as long as no interfering radicals are present (page 41). This method cannot be used during an experiment with hydrocarbon, and so the catalytic probe was selected as a suitable means of measuring the atom concentration during these reactions.

The arrangement used was a small piece of gold foil, about 2 mm square mounted on one junction of a platinum/ platinum-rhodium thermocouple. The other junction of the thermocouple was situated about 2 mm away and was coated with clean glass, so that no re-combination of atoms would occur on it. When this whole assembly was placed in the flow tube, the temperature difference was that due to the recombination of H atoms on the gold, independent of the temperature at which the reaction was taking place. The leads of the thermocouple were encased in 5 mm diameter pyrex tube, and passed out of the system by the same exit as the sample probe. The leads were then connected directly to a 1mV. Kent pen recorder, so that the e.m.f. of the thermocouple could be read directly.

Since this gave only relative atom concentrations, the probe was calibrated at the start of each run by comparing the e.m.f. of the thermocouple with the result of an NO_2 titration, which gave the absolute value of (H). The NO_2 titration involved the addition of a gradually increasing amount of NO_2 to the atom steam at a measured flowrate. At the equivalence point the air afterglow is extinguished and $(NO_2) = 1.5(H)$ (page 42). The absolute value of (H) then allowed the response of the probe to be calibrated.

3.5 Reagents.

The gases used in these experiments were supplied from two sources. Hydrogen, argon and air were supplied by the British Oxygen Co.; NO_2, ethylene, propene, and 1-butene by Matheson Gases Inc.

Hydrogen and argon were supplied in cylinders of 200 cubic feet capacity. The only purification required was to remove oxygen with columns of manganous oxide supported on celite. The MnO was made in situ by reduction of MnO_2 at 200°C with hydrogen.

All of the other reagents were used without purification, since in all cases they were at least 99.9% pure. It was found that the lecture bottle size of cylinder was the most useful and economical method of obtaining these gases.

3.6 Problems in the Use of the Apparatus.

There are several difficulties associated with the use of flow systems, the neglect of which can lead to erroneous results. The main sources of possible error are:

(1) pressure drop along the length of the system;

(2) insufficient mixing of the reactants;

(3) unreliability of the catalytic probe.

As has been mentioned earlier (page 50), the flowrate and concentration estimations will be affected by the pressure drop in the system, going from end to end.

From Poisseuille's Equation,

$$F_m = \frac{(P_2^2 - P_1^2)\,\pi r^4}{16\,LMRT}$$

$$(F_m = \frac{dn}{dt} = \text{molar flowrate})$$

Now since $PV = nRT$

$$\text{then } \frac{dv}{dt} = \frac{dn}{dt}\frac{RT}{P}$$

So the volume flowrate,

$$F_v = \frac{(P_2^2 - P_1^2)\pi r^4}{16 L \eta P_{av.}} \qquad (P_{av} = \text{'average' pressure})$$

and the linear flowrate $F_1 = \frac{(P_2^2 - P_1^2) r^2}{16 L \eta P_{av}}$ (dividing by πr^2)

assuming $P_2 \doteq P_1$

$$F_1 = \frac{2P_{av.} \Delta P r^2}{16 L \eta P_{av}} = \frac{\Delta P r^2}{8 L \eta}$$

So $$\Delta P = 8F_1 L \eta / r^2$$

With $r^2 = 1.96 cm.^2$, $L = 20.0 cm.$, $F_1 = 2000 cm.sec.^{-1}$ and $\eta = 2.22 \times 10^{-4}$ poise.

$P = 0.02$ torr approximately.

Since the total pressure is about 2 torr, this will constitute about a 1% error, which is not likely to be important. This disposes of Kaufman's objection to flow systems (KAU61).

The mixing of the reactants after injection of the titrants is very important since, if this is not complete, the calculated concentrations might be considerably in error. Titration experiments showed a flat flame front about 2 mm from the end of the inlet capillary system. This indicates that mixing is very rapid and uniform and is complete within a few mm (10^{-4} sec.). This is a considerable improvement over other inlet systems, where the first few milliseconds of reaction have to be ignored because of the rather nebulous atom and radical 'soup' produced by incomplete mixing.

The catalytic probe technique has been criticized on three accounts:

(1) the metal catalyst may become poisoned

(2) the action of the probe can cause high estimations of atom concentration

(c) the readings may be distorted by diffusion effects.

Various metals were examined as a catalyst for the probe and gold proved to be the most successful. However, over the length of time it took to complete a run it was found that some diminution of the probe response did occur. The problem was overcome by adopting the following procedure, prior to each run. The catalyst was first heated to redness with a small flame. This made the catalyst extremely active. The activity was then reduced by exposing the foil to NO_2 for a few seconds, which removed the most active sites by partial poisoning.

Reproducible readings were then obtained, for both increasing and decreasing distances from the inlet.

There is also the possibility (STE31) that, when atoms combine on the catalyst, a local pressure gradient is created, which could pump atoms on to the surface and cause overestimations, but if the atom flow is small compared with the total flow, as in these experiments, the pressure drop will be small compared to the total pressure, and so this effect will be small.

Kondratiev (KON 61) criticized LeRoy's use of the isothermal calorimeter by showing that the apparent rate of decay of (H) as measured by this method is not a true measure of the

rate constant, due to diffusion effects. However, it has been established that in a flow system similar to ours (DAL67) the diffusion effect is in fact small, and the rate of decay of (H) will give the true rate constant.

3.7 Experimental Procedure.

Prior to a series of experiments the following procedure was carried out. The flow tube was washed with detergent followed by distilled water and it was then cleaned with 4% aqueous HF solution. Another rinse with distilled water was followed by acetone to dry the tube. The coating material was then applied by washing the tube with a 25ml. portion of 25ml. dichloro-dimethyl silane and 25ml. trichloro-methyl silane in 500ml. of carbon tetrachloride. After drying with compressed air, the flow tube was ready for use and was fixed in position on the apparatus. This procedure was repeated whenever the flow tube showed signs of high catalytic activity towards atom recombination, which happened on average after about 15 runs.

An experimental run was started by setting up suitable flowrates of argon and hydrogen through the discharge, and switching the generator on. The system was then left running for 20 minutes so that conditions would stabilise; this time was not critical, since the catalytic probe showed that the H atom concentration stabilised within 10 minutes. The flowrate of argon was read from the calibration graph, after reading the argon bulb pressure, and the hydrogen flowrate calculated, assuming Poisseuille's equation applied and knowing the

hydrogen bulb pressure. The flowrate of H was determined by NO_2 titration, giving $(H)_o$, the concentration of H at time T =0.

The NO_2 flow was turned off and the hydrocarbon admitted to react with the H atoms. Samples were then taken at various distances along the tube, and collected and analysed as described previously. At this point flows were stopped for a short period while the sample probe was replaced by the catalytic probe. Pumping was then resumed and a further 20 minutes allowed for stabilization; it was verified by NO_2 titration that this stopping and restarting had no effect on H atom production. (H) was now measured, both with and without added hydrocarbon, as a function of distance after injection. The plots of H-decay in the absence of titrant showed little decrease in (H) on going down the tube, indicating that gas phase recombination of H was not important.

From the knowledge of flowrates and amounts of gases passing through the flow tube, concentrations were calculated for each constituent in the reaction mixture. Changes in concentration were determinable and so reaction-time plots could be produced, since reaction time may be found by dividing the distance after injection by the total flowrate.

Calculation of run parameters

The experimental results and calculations for a typical run were:

NOTES

Pressure in the hydrogen bulb = 229.4 torr (a)

So hydrogen molecule flowrate = $4.02\times10^{-10}\times(229.4)^2$

$= 2.115\times10^{-5}$ mole sec^{-1}

Pressure in argon bulb = 468.9 torr

So argon flowrate (from calibration graph) = 90.0×10^{-5} mole sec^{-1} (b)

Pressure in NO_2 bulb at end point = 214.3 torr.

So NO_2 flowrate = $2.34\times10^{-10}\times(214.3)^2\times c$ (c)

$= 1.605\times10^{-5}$ mole sec^{-1}

(where c is the correction factor for $NO_2 \rightleftharpoons N_2O_4$ equilibrium see appendix 1)

So hydrogen atom flowrate = $2/3\times(1.605\times10^{-5})$ mole sec^{-1}

$= 1.07\times10^{-5}$ mole sec^{-1}

Pressure in ethylene bulb = 93.2 torr (d)

So ethylene flowrate = $3.12\times10^{-11}\times(93.2)^2$

$= 2.710\times10^{-7}$ mole sec^{-1}

Total gas flow = $(90.000 + 2.115 + 1.070 + 0.027)\times10^{-5}$ mole sec^{-1} = 93.212×10^{-5} mole sec^{-1}

Pressure in flow tube (from vacuostat) = 1.60 torr

Temperature in flow tube = 289°K

$$PV = nRT$$

$$\text{so } n/V = P/RT$$

i.e. concentration (mole l^{-1}) = $5.55\times10^{-5}\times P(\text{torr})$ (e)

Thus the concentration at 1.60 torr = 8.89×10^{-5} mole l^{-1}

Linear flowrates $\left(\frac{dl}{dt}\right) = \frac{RT}{\pi r^2} \times \frac{\text{molar flowrate}}{P} \left(\frac{dn}{dt}\right)$ (f)

$$= 2.92\times10^{4} \times \frac{\frac{dn}{dt}}{P(\text{torr})} \text{ (mole } sec^{-1})$$

$= 17.02$ m sec^{-1}

NOTES

(a) For H_2 flowrate at 289^oK

$$F_{H_2} = C_{H_2} xP^2 \quad \text{(See Page 50)}$$

$$C_{H_2}^{289} = 4.02x10^{-10} \text{ mole sec}^{-1}(\text{torr})^{-2}$$

(b) See Figure 3.4

(c) For NO_2 flowrate at 289^oK

$$F_{NO_2} = C_{NO_2} xP^2 xc \quad \text{(See page 50 and Appendix 1 for c)}$$

$$C_{NO_2}^{289} = 2.34x10^{-10} \text{ molesec}^{-1}(\text{torr})^{-2}$$

c = 1.53 at a bulb pressure of 213.4 torr

(d) For ethylene flowrate at 289^oK

$$F_{eth} = C_{eth} xP^2 \quad \text{(as above)}$$

$$C_{eth}^{289} = 3.12x10^{-11} \text{ molesec}^{-1}(\text{torr})^{-2}$$

(e) concentration $(\text{molel}^{-1}) = P(\text{torr}) x \frac{1}{RT}$

with R= 62.361 ltorr $^oK^{-1}\text{mole}^{-1}$ and T = 289^oK

This gives concentration$(\text{molel}^{-1}) = 5.55x10^{-5} xP(\text{torr})$

(f) PV = nRT

Therefore dV/dt(volume flowrate) = $RTx \frac{dn/dt}{P}$ (dn/dt = molar flowrate)

Hence dL/dt(linear flowrate) = $\frac{RT}{\pi r^2} x \frac{dn/dt}{P}$

with dn/dt, P,R,T, as already described and r = 1.4 cm.

The concentration of each of the gases were calculated as follows by proportion.

	flowrate(mole sec^{-1})	concentration(mole l^{-1})
argon	90.000×10^{-5}	8.581×10^{-5}
H_2	2.115 "	0.202 "
H	1.070 "	0.102 "
ethylene	0.027 "	0.0025 "
total	93.212 "	8.89×10^{-5}

So from these initial calculations, carried out for every run, the run parameters of flowrate (and hence the time-scale of the reaction) and initial reactant concentration were found. From the calculated (H) it was possible to calibrate the probe to allow the determination of (H) at any time during the subsequent reaction.

From the determination of hydrocarbon concentration at zero time, it is known how many carbon atoms are present in the system; this must remain constant although the various hydrocarbon concentrations change. This latter determination and the measured areas of the peaks obtained by chromatographic separation of the samples, allowed the absolute concentrations of all hydrocarbon constituents to be found.

For the example above, involving the reation of H with ethylene, the initial ethylene concentration is 2.50×10^{-8} mole l^{-1} and so the total carbon atom concentration is 5.00×10^{-8} mole l^{-1}. The areas of the C_1-C_2 peaks, the only products, in integrator units;

methane = 94

ethylene = 319

ethane = 23

Since the size of the peak is dependent on the number of carbon atoms, in the molecule, and also on the type of molecule being detected, it is necessary to multiply each of the measured areas above by a sensitivity factor. Sternberg (STE62) gives the sensitivity of each carbon atom in an alkane as unity. Thus the number of carbon atoms in an alkane is directly proportional to the area of the chromatographic peak. For olefins there is a small correction to be made, since the sensitivity of an olefinic carbon atom is 0.95. So for ethylene above the peak area must be divided by this to give a true representation of the actual number of carbon atoms present in the ethylene peak. Similarly, the average sensitivity of a carbon atom in propene is 0.967 and in a run involving propene the corresponding correction must be made. Applying the sensitivity factor for ethylene in the above we obtain relative carbon contents as

		%
methane =	94	20.7
ethylene =	336	74.3
ethane =	23	5.0
Total	453	

The total number of carbon atoms is therefore 453 in arbitrary units. From this we can calculate the fraction of the total carbon atom content in each constituent, and thus, from the total carbon atom concentration, the absolute concentration of carbon atoms in each constituent. Division by the number of carbon atoms in the molecule then gives the molar concentration of each constituent thus:

CONSTITUENT	FRACTION OF TOTAL CARBON	CONCENTRATION OF CARBON ($molel^{-1}$)	MOLECULAR CONCENTRATION ($molel^{-1}$)
METHANE	0.207	1.035×10^{-8}	1.035×10^{-8}
ETHYLENE	0.743	3.715 "	1.857×10^{-8}
ETHANE	0.050	0.250 "	0.125×10^{-8}
Total	1.000	Total 5.000×10^{-8}	

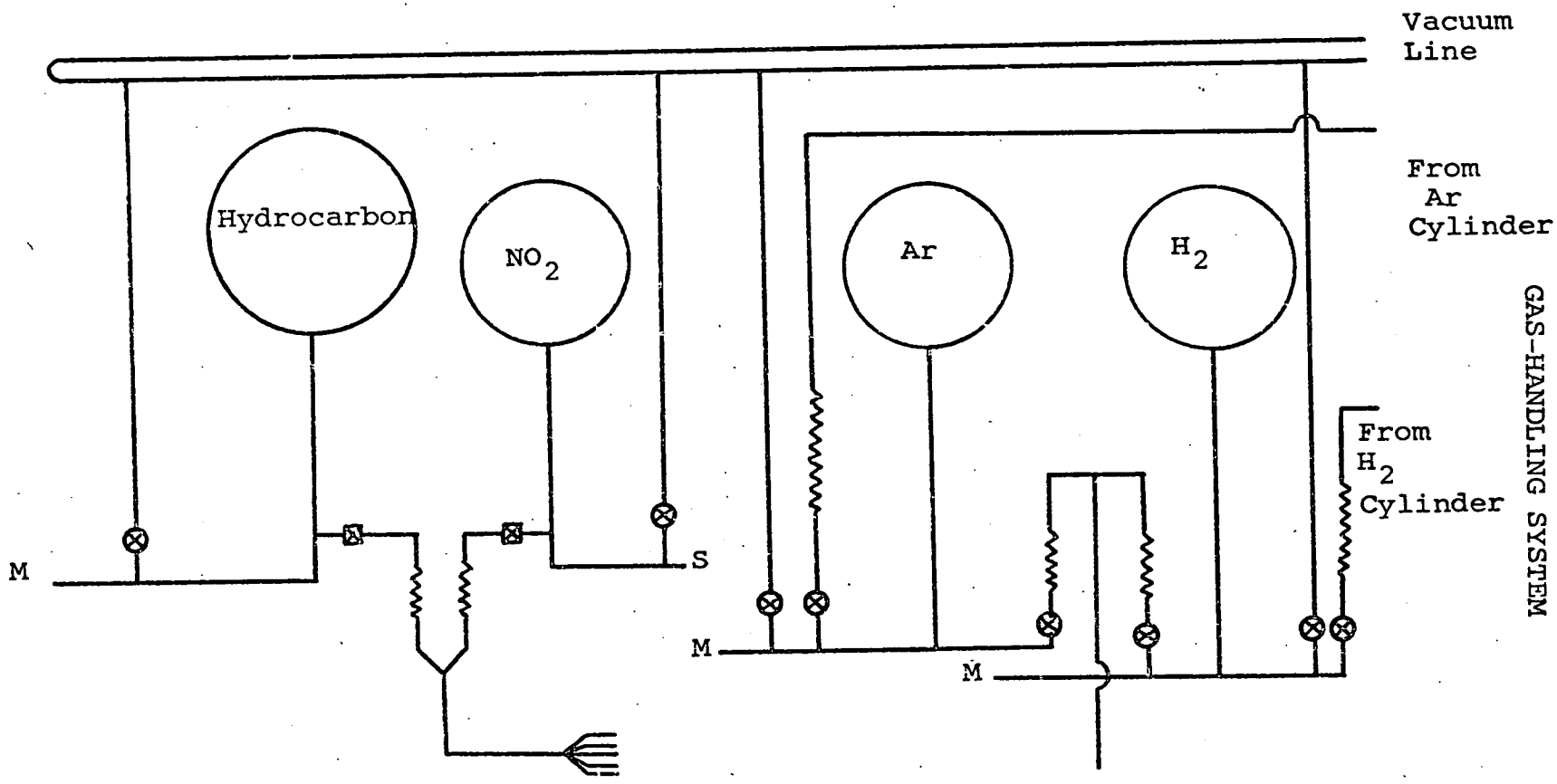

7 mm diameter glass tubing

Glass capillary resistance

Adams Valve Hone Valve

M Mercury Manometer S Spiral Gauge

FIGURE 3.1 GAS-HANDLING SYSTEM

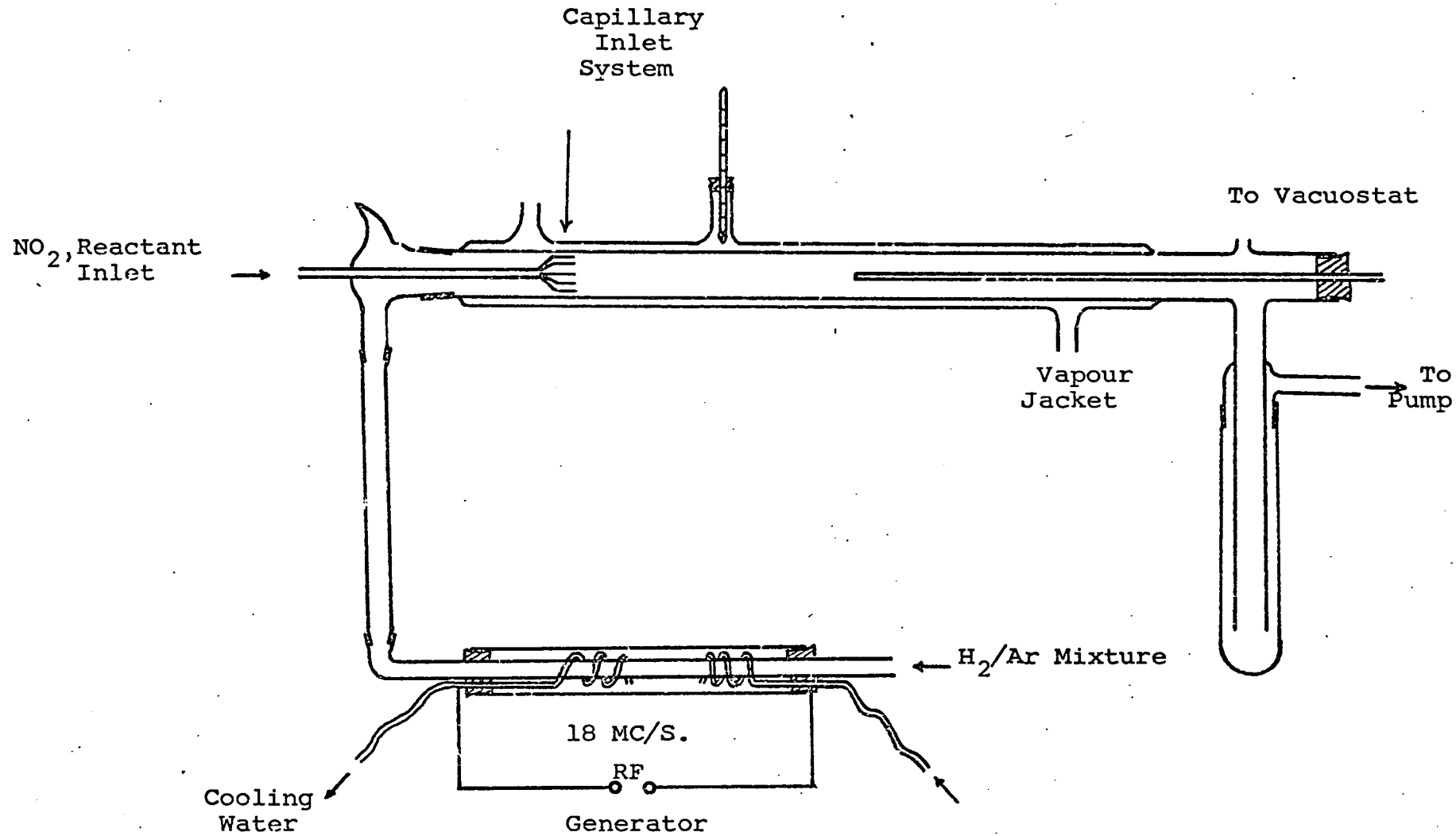

FIGURE 3.2
FLOW SYSTEM

FIGURE 3.3

JET INLET SYSTEM

(actual size)

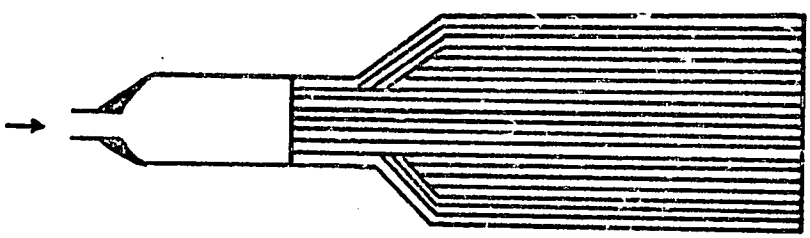

Side View

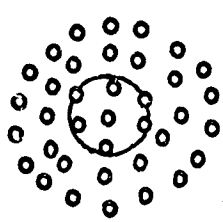

End View

FIGURE 3.4

ARGON FLOWRATE

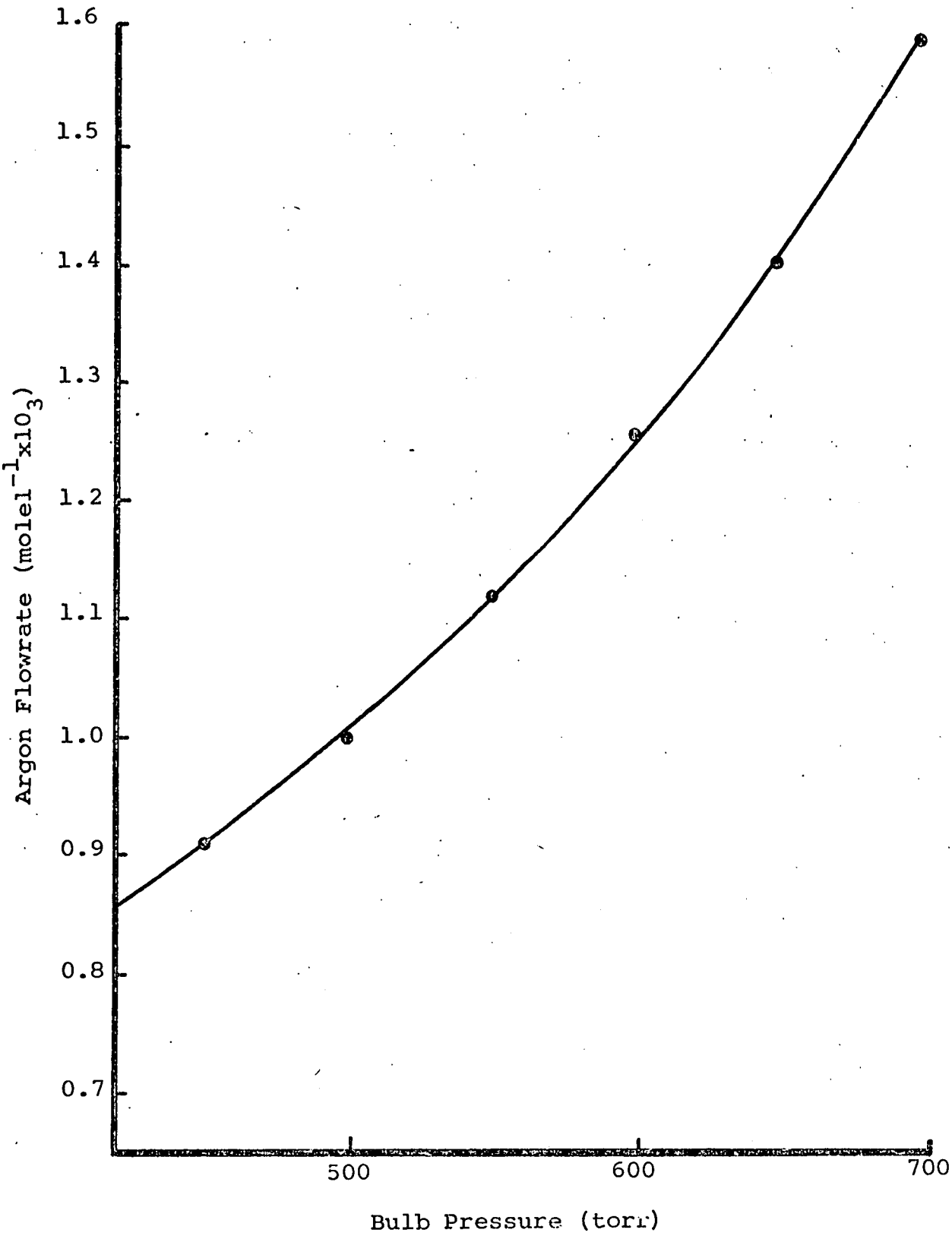

FIGURE 3.5

SAMPLE COLLECTOR AND CHROMATOGRAPHY INJECTOR

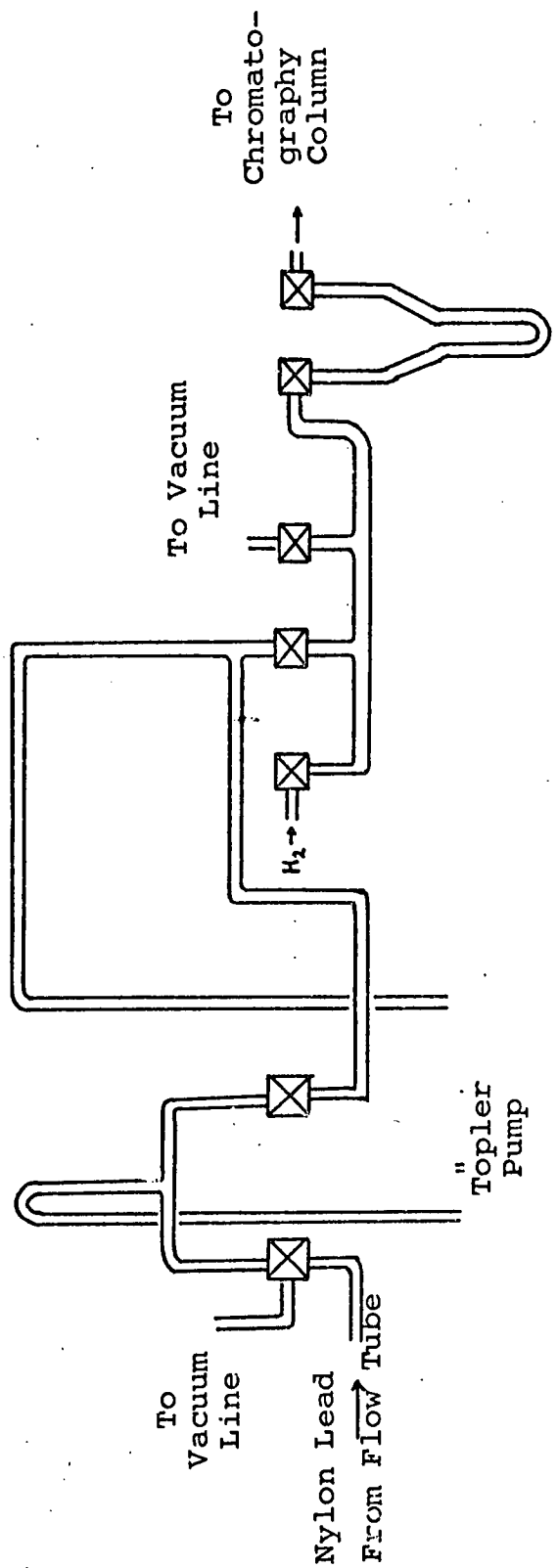

CHAPTER 4

THE REACTION OF H WITH ETHYLENE

4.1 Experimental

Runs for the H + ethylene reaction were carried out using a variety of different initial ethylene and hydrogen atom concentrations. Samples were collected at various distances down the tube by Töpler pumping into a sample tube and were then analysed by gas chromatography using the Porapak column. This gave the relative amounts of methane, ethane and ethylene present. The initial injection rate was measured for each run, and from this the amounts of each constituent present were determined by the type of calculation described on page 65. The reaction was studied over the temperature range 275-373°K and pressure range 0.6 - 3.6 torr. The results of a typical run are given in table 4.1 and figure 4.1.

4.2 Theory and mechanism.

The proposed reaction mechanism is

$$H + C_2H_4 \underset{D}{\overset{k1}{\rightleftharpoons}} C_2H_5^* \xrightarrow{S} C_2H_5 \qquad (1)$$

$$H + C_2H_5 \underset{D}{\rightleftharpoons} C_2H_6^* \xrightarrow{S} C_2H_6 \qquad (2)$$

$$\downarrow D$$

$$2CH_3$$

$$H + CH_3 \underset{D}{\rightleftharpoons} CH_4^* \xrightarrow{S} CH_4 \qquad (3)$$

$$CH_3 + CH_3 \underset{D}{\rightleftharpoons} C_2H_6^* \xrightarrow{S} C_2H_6 \qquad (4)$$

$$\downarrow D$$

$$H + C_2H_5$$

This mechanism is similar to the one proposed by Westenberg and de Hass (WE69) who suggested the mechanism since methane and ethane were (apparently) the only products observable in their system. The product results from their investigation agree with those presented here. Since negligible amounts of C_3 or C_4 products are observable in this reaction under the conditions described, it has not been necessary to include any radical - radical reactions except reaction (4). Radical - molecule reactions also appear to be unimportant in comparison to atom - radical and atom - molecule reactions. This is expected in view of the probable two order of magnitude smaller steric factor and significant activation energies for the first compared to the second and third types of reaction (BEN60), and also the high concentration of H atoms present at all stages.

Each of the four groups of reactions represents the formation of vibrationally excited radicals or molecules (i.e. chemical activation) that may either decompose or be stabilized by collision with a heat bath molecule.

In the second group of reactions, the excited ethane molecules are formed with an average excess energy of 97.5 Kcal $mole^{-1}$ (RAB64). There are two possible channels of decomposition, but the channel for dissociation to methyl radicals is 10 Kcal $mole^{-1}$ lower than that which returns to reactant, and it is therefore likely to be the more important. Rabinovitch and Setser (See Table 1.1) have made calculations for this mode of formation of ethane and predict that stabilization of the excited ethane is unimportant at pressures

less than 10 torr. The result is that reaction group two yields methyl radicals as the major product. This conclusion is in agreement with previous calculations (BAR69), and implies that ethyl rapidly attains a steady - state concentration.

Rabinovitch and Setser have also performed calculations on reaction group (3) in which the excited methane is formed with 102 Kcal $mole^{-1}$ excess energy. Their results indicate that reaction (3) is fully within the low - pressure or third order region.

Reaction group (4) represents the formation of ethane by methyl recombination. The excited ethane molecules are formed with about 87.4 K cal $mole^{-1}$ excess energy (RAB64). The excited ethane from this reaction group can be stabilized more readily than excited ethane from reaction group (2) and should therefore dominate ethane production.

The reaction mechanism thus reduces to

$$H + C_2H_4 \xrightarrow{kal} C_2H_5 \qquad (1)$$

$$H + C_2H_5 \longrightarrow 2CH_3 \qquad (2)$$

$$H + CH_3 + M \longrightarrow CH_4 + M \qquad (3)$$

$$CH_3 + CH_3 \longrightarrow C_2H_6 \qquad (4)$$

Inspection shown that the rate ot depletion of ethylene is given by

$$-\frac{d\ C_2H_4}{dt} = ka_1 \left(C_2H_4\right) \left(H\right)$$

$$\text{i.e.} \quad ka_1 = -\frac{d\,(C_2H_4)/dt}{(C_2H_4)\;(H)} \qquad \text{(Ethylene)}$$

$\frac{d\,(C_2H_4)}{dt}$, (H), (C_2H_4) can all be determined from the product - distance (i.e. time) graphs obtained experimentally and this enables k_{a1}(ethylene) to be calculated.

With the steady state assumption for ethyl radicals the mechanism also predicts

$$-\frac{d\,(H)}{dt} = 2\,ka_1\,(H)\,(C_2H_4) + \frac{d\,(CH_4)}{dt}$$

$$\text{i.e. } ka_1 = -\frac{\frac{d}{dt}\,((H) + (CH_4))}{2\,(H)\,(C_2H_4)} \qquad \text{(Hydrogen)}$$

k_{a1} (H) can be calculated in a similar fashion from the product - time graph. k_{a1}(H) and k_{a1}(ethylene) showed good agreement in all cases. (See below and table 4.2).

In practice product concentration (C) was plotted against distance from the inlet (Z) and the graph immediately yields dC/dZ. Calculation of the total linear flowrates then gives dZ/dt and so,

$$dC/dt = dC/dZ \times dZ/dt$$

Table 4.1, and figure 4.1 show respectively conditions, results and graph obtained for a typical run.

For,

$$H + C_2H_4 \underset{D}{\overset{k1}{\rightleftharpoons}} C_2H_5^{*} \xrightarrow{S} C_2H_5$$

the apparent rate constant is related to k_1 by

$$k_{a1} = \frac{S}{S+D}\,k_1$$

S/D depends on both temperature and pressure so the experimentally determined rate constant has to be corrected to be a meaningful measure of (1) above. The calculations of Rabinovitch and Setser (RAB64) enabled them to predict the variation of S/D with temperature and pressure (table 16 page 63) and this was taken into consideration and the appropriate correction factors made in the results shown in table 4.2. (The data of RAB64 was used to plot S/D against pressure and S/D against temperature and the required correction factor obtained by extrapolation. The graphs are shown in the Appendix).

4.3 Results

A plot of $\log(k_1)$ against $10^3/T$ (figure 4.2) gives the following Arrhenius equation,

$$\log_{10}(k_1) = (10.29 \pm 0.21) - (2960 \pm 320)/4.576T$$

calculation is by the method of least mean squares with the possible error the 95% confidence limits. Units of k_1 are $1.mole^{-1}sec.^{-1}$

Pressure Dependence of the Addition Reaction.

Our results indicate a variation of the experimentally determined rate constant (k_{a1}) with pressure at room temperature. (Table 4.2(2)). Table 4.3 and figure 4.3 show the variation of $\log(k_{a1}/k_1)$ with log(pressure). The limiting high pressure rate constant k_1 was chosen as 1.13×10^8 $1.mole^{-1}sec^{-1}$, which is an average of the estimated high pressure room temperature values. (Table 4.2(1)).

In the discussion the experimental fall-off curve is compared with the theoretical fall-off curve. The former is not fixed in the vertical sense since $\frac{ka1}{k1}$ has been calculated using Rabinovitch and Setser's values of $\frac{S}{D}$. For our data to parallel the theoretical fall-off (see Figure 8.4) $\frac{S}{D}$ has to be increased slightly. This yields a high pressure value for k_1 of 0.96×10^8 l mole^{-1} sec^{-1} (see Table 8.1).

H + Ethylene - Table 4.1.

Typical Run Results - H and Products (run 7)

Reaction temperature - 283°K flowrate (dZ/dt) = 1760 cm sec^{-1}

Flow tube pressure - 1.60 torr.

(1) H atoms.

distance from inlet (Z) cm.	catalytic probe (no reaction) response (mV.)	catalytic probe (reaction) response (mV.)	(H) mole.l^{-1} x10^6
0	7.78	7.78	0.925
2	7.77	5.61	0.668
4	7.77	4.74	0.564
6	7.77	4.26	0.508
8	7.77	3.48	0.414
10	7.76	3.04	0.362
12	7.74	2.50	0.298
14	7.74	2.12	0.253
16	7.74	1.70	0.202
18	7.73	1.53	0.182
20	7.73	1.38	0.164

(2) Products.

distance from inlet (Z) (cm.)	(CH_4) mole.l^{-1}x10^6	(C_2H_4) mole.l^{-1}x10^6	(C_2H_6) mole.l^{-1}x10^6	(H) + (CH_4) mole. l^{-1}x10^6
0	0	0.990	0	0.925
2	0.068	0.960	0.018	0.736
4	0.102	0.920	0.018	0.666
6	0.162	0.881	0.030	0.670
8	0.154	0.862	0.057	0.568
10	0.192	0.842	0.053	0.554
12	0.210	0.820	0.069	0.508
14	0.242	0.763	0.106	0.495
16	0.247	0.752	0.110	0.449
18	0.252	0.718	0.147	0.434
20	0.255	0.735	0.125	0.419

(3) Gradients (from graph)

Distance from inlet (Z) (cm.)	$-d(C_2H_4)/dt \times 10^6$ (mole $l^{-1}s^{-1}$)	$ka_1(C_2H_4) \times 10^{-8}$ (l mole$^{-1}s^{-1}$)	$\frac{d((H)+(CH_4))}{dt} \times 10^6$ (mole $l^{-1}s^{-1}$)	$ka_1(H) \times 10^{-8}$ (l mole$^{-1}s^{-1}$)
4	31.3	0.64	70.5	.68
6	29.6	0.66	61.2	.68
8	22.9	0.66	52.0	.73
10	21.2	0.69	45.3	.73
12	17.6	0.72	35.6	.73
14	13.9	0.72	27.4	.72
16	11.8	0.73	24.1	.74

Mean ka_1 (C_2H_4) = 0.69×10^8 l mole$^{-1}s^{-1}$

Mean ka_1 (H) = 0.72×10^8 l mole$^{-1}s^{-1}$

H + Ethylene - Table 4.2

Run Conditions and Experimental Results.

(1) Constant Pressure (1.60 torr)

Run	Temp.(^{o}K)	$(H)_o x10^6$ (mole.l^{-1})	$(C_2H_4) x10^6$ (mole.l^{-1})	$k_{a1}(H)$	$k_{a1}(C_2H_4)$	S/S+D	k_1
1	273	1.14	0.136	$0.68x10^8$	$0.65x10^8$	0.656	1.01
2	273	1.10	0.190	0.74 "	0.74 "	0.656	1.13
3	287	1.04	0.128	0.68 "	0.67 "	0.583	1.15
4	287	1.01	0.192	0.66 "	0.64 "	0.583	1.11
5	287	0.65	0.256	0.69 "	0.68 "	0.583	1.18
6	288	0.98	0.368	0.65 "	0.70 "	0.583	1.16
7	293	0.92	0.99	0.72 "	0.69 "	0.574	1.18
8	290	1.10	0.246	0.63 "	0.65 "	0.583	1.10
9	314	0.82	0.135	0.73 "	0.67 "	0.530	1.38
10	314	1.22	0.185	0.91 "	0.61 "	0.530	1.72
11	314	0.66	0.215	0.79 "	0.74 "	0.530	1.49
12	371	0.76	0.126	1.04 "	0.93 "	0.432	2.41
13	371	0.79	0.72	1.50 "	1.31 "	0.432	3.24
14	371	0.83	0.79	1.47 "	1.42 "	0.432	3.36
15	371	0.49	0.80	2.26 "	1.79 "	0.432	4.70
16	371	0.59	0.77	1.80 "	1.76 "	0.432	4.11

(2) Constant Temperature (289°K)

Run	Pressure(torr)	(H)x10^6	(C_2H_4)x10^6	k_{al}
17	0.61	1.36	0.39	0.55x10^8 l.mole.$^{-1}$sec.$^{-1}$
18	0.61	1.31	1.20	0.49 " "
19	0.69	1.60	1.65	0.54 " "
20	0.99	1.10	0.84	0.60 " "
21	1.60	1.04	0.13	0.67 " "
22	1.60	1.10	0.25	0.64 " "
23	1.60	0.92	0.99	0.67 " "
24	2.10	0.88	0.69	0.73 " "
25	3.51	1.58	1.30	0.76 " "
26	3.51	0.78	0.22	0.80 " "
27	3.50	0.69	0.42	0.82 " "

H + Ethylene - Table 4.3

Variation of $\log_{10}(k_{al}/k_1)$ with $\log_{10}$(pressure) at 289°K.

$k_1 = 1.13 \times 10^8$ l mole^{-1}sec^{-1}.

Run	$\log_{10}(k_{al}/k_1)$	$\log_{10}$(pressure) (torr)
17	-0.310	-0.222
18	-0.358	-0.222
19	-0.317	-0.162
20	-0.272	-0.004
21	-0.223	0.204
22	-0.243	0.204
23	-0.223	0.204
24	-0.182	0.322
25	-0.167	0.544
26	-0.148	0.544
27	-0.136	0.544

FIGURE 4.1.

H + ETHYLENE RUN 7

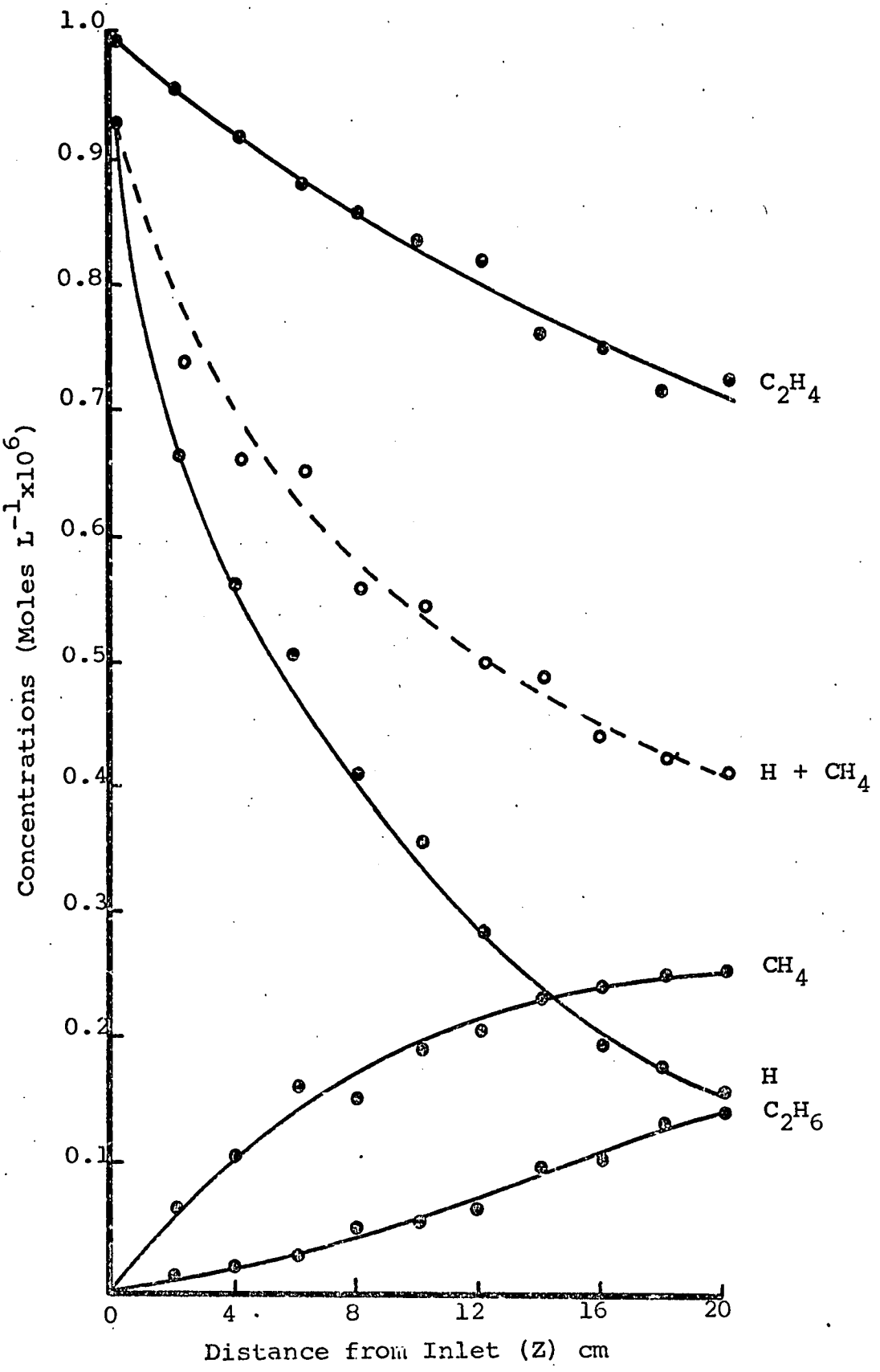

FIGURE 4.2

H + ETHYLENE - ARRHENIUS PLOT OF K_1

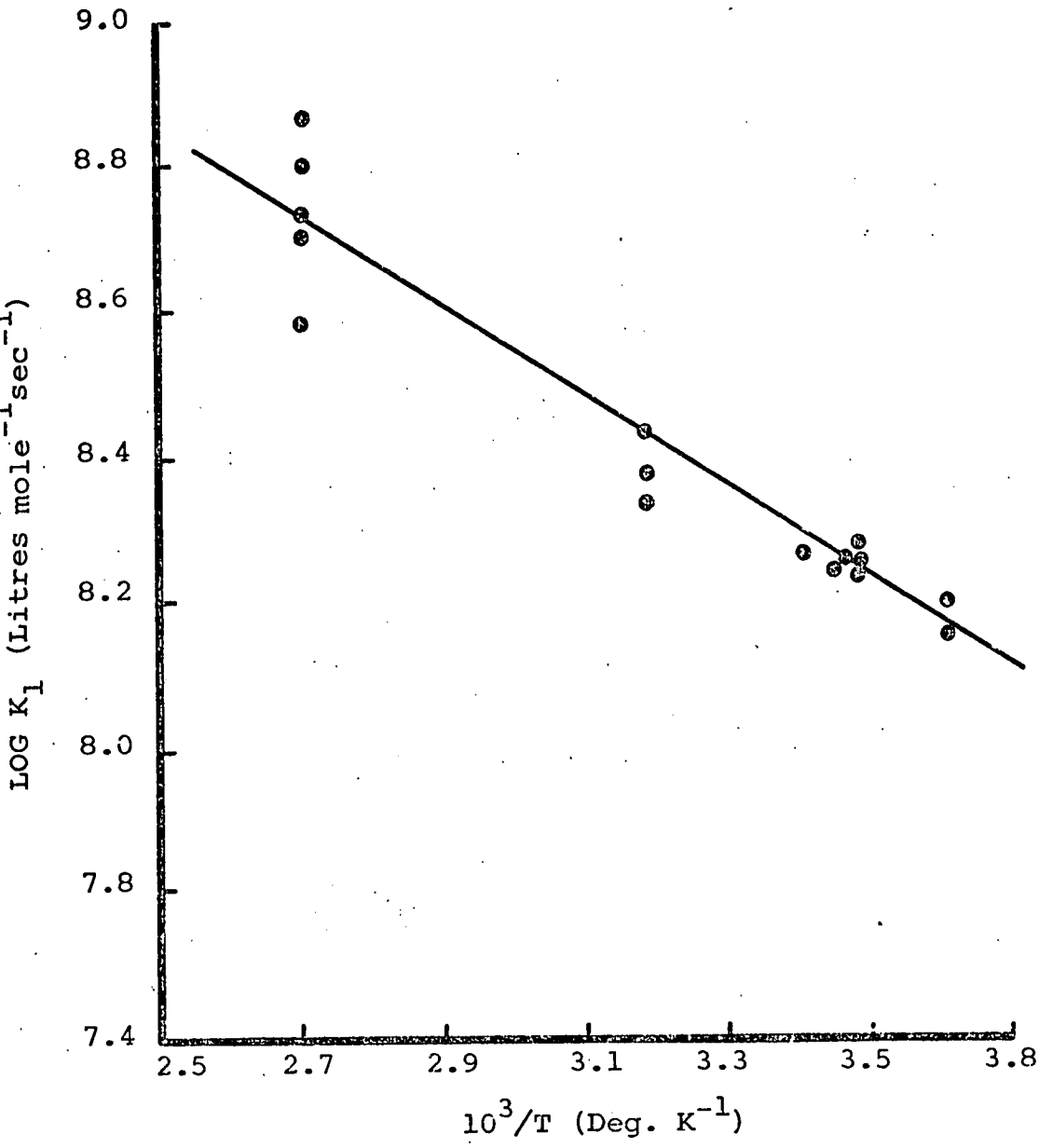

FIGURE 4.3

H + ETHYLENE - $LOG_{10}(ka_1/k_1)$

AGAINST LOG_{10} (PRESSURE)

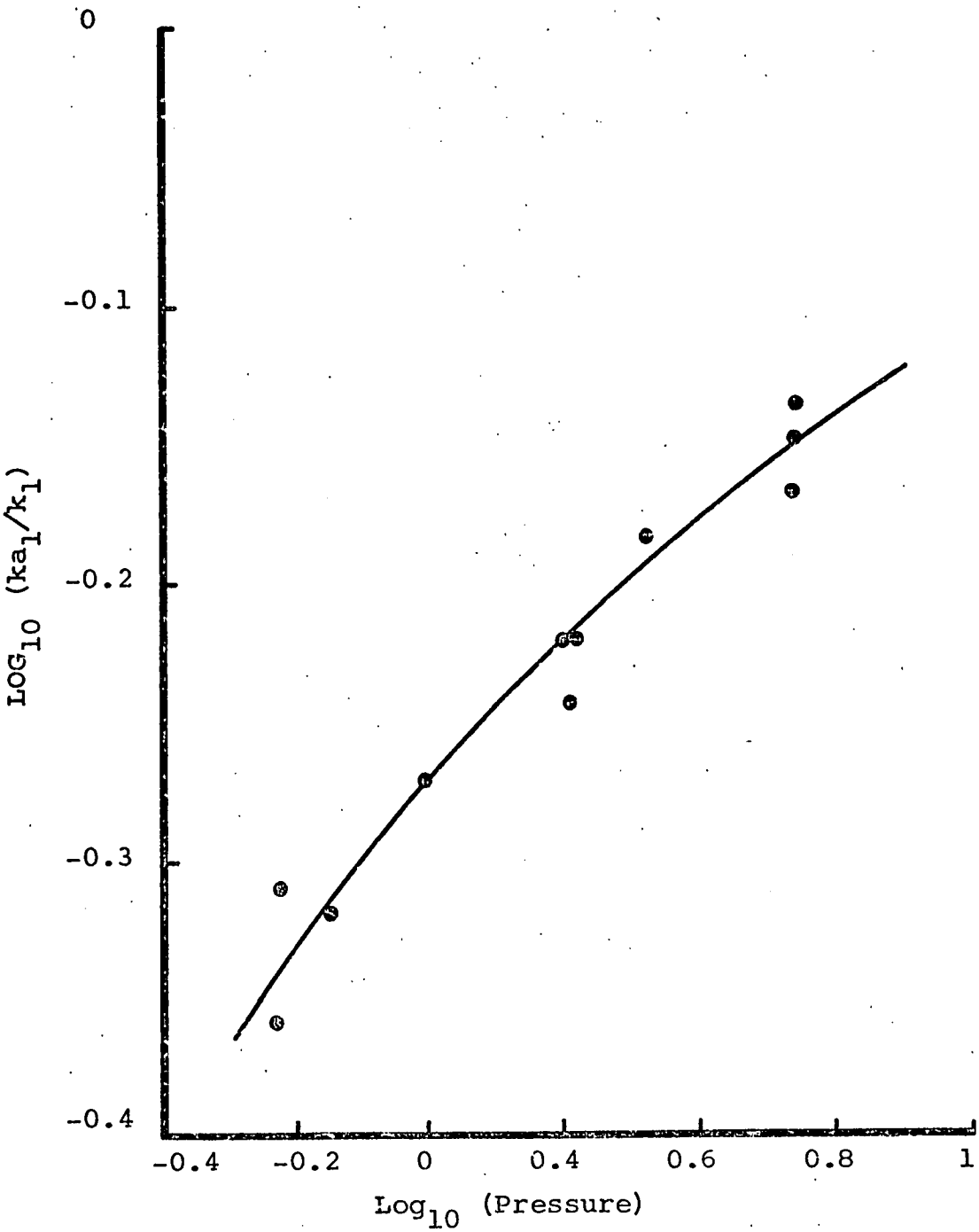

CHAPTER 5

THE REACTION OF H WITH PROPENE

5.1 Experimental.

The H + propene system was investigated in a manner analogous to the H + ethylene study. The temperature range 287 - 371^{o}K was covered together with a pressure spread of 0.6 - 2.2torr. Results of a typical run are shown in table 5.1 and graphical representation of these results shown in figure 5.1.

As can be seen from the graph the products are methane, ethylene, ethane and propane; the propane accounted for 0.2 - 0.3 of the propene lost, while the products of lower carbon number accounted for the remainder. No trace was found of molecules with carbon number greater than 3. This implies that reactions such as,

$$2C_3H_7 = C_6H_{14}$$

$$2C_2H_5 = C_4H_{10}$$

$$C_3H_7 + C_2H_5 = C_5H_{12}$$

$$C_3H_7 + CH_3 = C_4H_{10}$$

can be ignored.

A feature of the reaction is that not all of the H atoms removed appear in the saturated products. This is demonstrated by considering the alkane product concentrations after a reaction time of 5.6 msec. (z = 10 cm). From figure 5.1 the total alkane concentration ($CH_4 + C_2H_6 + C_3H_8$) is 1.83 x10^{7} mole l^{-1}. Since 2 H atoms are removed for every alkane molecule formed this accounts for 3.66x10^{-7}mole l^{-1} removed. The catalytic probe indicates the H decay is 8.1 x10^{-7}mole l^{-1} in the same time. Since heterogeneous wall recombination of H atoms is negligible there must be

some homogeneous reaction occurring, absent for the $H-C_2H_4$ system, which results in the removal of approximately 55% of the atoms. The recycling process $H + C_3H_7 \rightarrow H_2 + C_3H_6$ discovered by Knox and Dalgleish for isobutene is the most likely (KNO69).

5.2 Theory and mechanism.

The initial step is the formation of an activated propyl radical and latest estimates suggest that addition to the terminal carbon atom is preferred so the iso-propyl radical will predominate (FAL63). The propyl radical if stabilised undergoes further H atom addition to yield excited propane which in turn can be stabilised by collision or pyrolise to give CH_3 and C_2H_5 by C-C rupture. The reaction is thus more complicated than the H-ethylene system.

In addition, another means of removing hydrogen atoms must be sought. It has been shown (DAL67) that when H atoms are reacted with isobutene the H atoms are removed predominantly by the following process

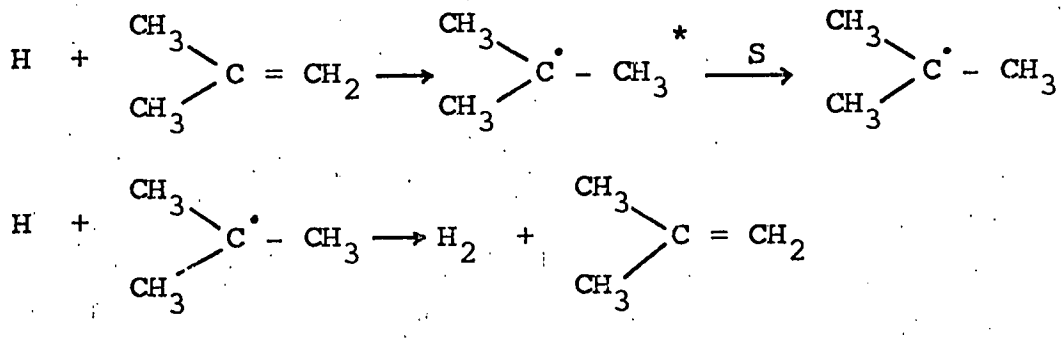

The second step involves abstraction of any one of nine terminal H atoms. It seems reasonable to suggest that the iso-propyl radical with six terminal H atoms available for

abstraction can undergo a similar cycling reaction which results in the catalytic recombination of H atoms and the regeneration of propene

$$H + CH_3-\dot{C}H-CH_3 \longrightarrow H_2 + CH_3-CH=CH_2$$

Our results suggest that more than 50% of the atoms are removed by this cycling reaction.

The complete scheme is,

$$H + C_3H_6 \underset{D}{\overset{k1(iso)}{\rightleftharpoons}} CH_3-\dot{C}HCH_3^{*} \xrightarrow{S} CH_3-\dot{C}HCH_3 \qquad (1)$$

$$H + C_3H_6 \underset{D}{\overset{k1(n)}{\rightleftharpoons}} CH_3CH_2\dot{C}H_2^{*} \xrightarrow{S} CH_3CH_2\dot{C}H_2$$

$$CH_3CH_2\dot{C}H_2^{*} \xrightarrow{D} CH_3 + C_2H_4$$

$$H + \begin{matrix}(n)\\(or)\\(iso)\end{matrix} C_3H_7 \underset{D}{\overset{k_2}{\rightleftharpoons}} C_3H_8^{*} \xrightarrow{S} C_3H_8 \qquad (2)$$

$$C_3H_8^{*} \xrightarrow{D} CH_3 + C_2H_5$$

cycling reaction

$$H + iso\ C_3H_7 \longrightarrow C_3H_6 + H_2 \qquad (3)$$

The reactions of CH_3, C_2H_4, C_2H_5 are then as described for the addition of H to C_2H_4 in chapter 4.

The mechanism is more complex than the ethylene system but certain simplifications are possible if Rabinovitch and Setser's data, regarding the stability of alkyl radicals and alkanes, is adopted. (Table 1.1).

$\underline{isoC_3H_7^*}$

At 1torr and 298°K S/D is given as 65 so that most radicals are stabilised. C-C rupture with H migration to give CH_3 and C_2H_4 is not considered likely (FAL63).

$\underline{nC_3H_7^*}$ (for $nC_3H_7^*$ formed from H + C_3H_6)

S/D = 0.3 where decomposition is splitting of the C-C bond to give CH_3 and C_2H_4 and so most radicals decompose, although the balance is much more even than for iso $C_3H_7^*$. Where decomposition is the reverse of the formation reaction most radicals are stabilised as above.

$\underline{C_3H_8^*}$

Decomposition involves C-C splitting to give CH_3 and C_2H_5. S/D for C_3H_8 formed from $isoC_3H_7$ + H is 0.9 and so decomposition and stabilisation complete nearly equally.

A simplified scheme of reaction is thus.

$$H + C_3H_6 \xrightarrow{k1(iso)} \text{iso } C_3H_7^* \xrightarrow{S} isoC_3H_7 \quad \text{---------(a)}$$

$$H + C_3H_6 \xrightarrow{k1^{(n)}} n\ C_3H_7^* \xrightarrow{S} n\ C_3H_7 \quad \text{---------(b)}$$

$$n\ C_3H_7^* \xrightarrow{D} CH_3 + C_2H_4 \quad \text{---------(c)}$$

$$H + \begin{matrix}(n\ )\\(or\ )\\(iso)\end{matrix} C_3H_7 \xrightarrow{k_2} C_3H_8^* \xrightarrow{S} C_3H_8 \quad \text{----------(d)}$$

$$C_3H_8^* \xrightarrow{D} CH_3 + C_2H_5 \quad \text{-------(e)}$$

$$H + \text{iso } C_3H_7 \xrightarrow{kc} C_3H_6 + H_2 \quad \text{----------(f)}$$

The reaction of CH_3 and C_2H_5 are then as described for the H-C_2H_4 reaction. The amount of ethylene produced was small and never exceeded 20% of unreacted propene and since H atom

addition to the latter is considered to be the faster, consequent H+ethylene reaction was ignored.

The experimental results require interpretation in terms of the above scheme and this leads to information about the following;

(1) the position of H atom addition to propene (whether terminal or non-terminal)

(2) the fall-off with pressure of the rate of formation of propane

(3) the rate constant for the addition of H atoms to propene (k_1)

(1) Position of H atom Addition to Propene.

If it is assumed that the extent of step (b) above is negligible then every n-propyl radical formed will split and form an ethylene molecule and this is the only source of ethylene. For the reaction illustrated, after 5.6 msec 1.26×10^{-7} mole/l C_3H_6 has been removed and 0.29×10^{-7} mole/l C_2H_4 formed which means that of the propene molecules that form products 23% do so by route (c). However only 45% of the propyl radicals initially formed yield products and the other 55% (all iso-propyl) undergo the cycling process already described. Hence only 23% of 45% i.e. 10% of the addition is non-terminal producing n-propyl radicals. This figure represents a lower estimate since step (b), stabilisation of n-propyl radicals, has been ignored.

(2) The Fall-off with Pressure of the rate of Formation of Propane.

The theoretical prediction is that the H atom addition to

propyl radicals is well into the fall-off range at 1.6torr (Table 1.1).

The scheme of reaction above reveals that routes (c), (d) and (e) give stable end products. The extent of route (c) is gauged by the amount of ethylene produced, route (d) by the amount of propane formed and consequently the remainder of propene molecules that react to form products do so by route (e), which involves splitting of an excited propane molecule. Hence S (route (d)) and D (route (e)) can be determined.

For,

$$H + C_3H_7 \xrightarrow{k_2} C_3H_8^* \begin{cases} \xrightarrow{S} C_3H_8 \\ \xrightarrow{D} CH_3 + C_2H_5 \end{cases}$$

the apparent rate constant k_{a2} is related to the high pressure value k_2 by

$$k_{a2}/k_2 = S/S+D$$

Thus a plot of $10g_{10}$ (S/S+D) against $\log_{10}$(pressure) shows the variation of k_2 with pressure.

Table 5.2 contains the calculated values of S/S+D for a pressure range of 0.6 - 2.2 torr and figure 5.2 shows the pressure fall-off graphically.

(3) Rate Constant for the Addition of H Atoms to Propene (k_1)

Evaluation of k_1 is complicated by

(a) the cycling reaction which regenerates propene

(b) several causes of H atom removal which result in the total observed H decay.

Rate of Removal of Propene.

Propene is removed in the formation of propyl radicals and regenerated in the cycling step (f).

Thus,

$$-d(C_3H_6)/dt = k_1(H)(C_3H_6) - k_c(H)(C_3H_7) \quad (1)$$

Rate of Removal of H Atoms.

H atoms are removed in the formation of propyl radicals, the formation of propane, the formation of methane, and in the cycling reaction.

Thus,

$$-d(H)/dt = k_1(H)(C_3H_6) + k_2(H)(C_3H_7) + d(CH_4)/dt + kc(H)(C_3H_7) \quad (2)$$

For the formation of propane,

$$d(C_3H_8)/dt = k_2 x \frac{S}{S+D} (H)(C_3H_7)$$

S/S+D varies with temperature and pressure but for the reaction illustrated it equals 0.5.

Hence $k_2(H)(C_3H_7) = 2\,d(C_3H_8)/dt \quad (3)$

Substitution in (2) for $k_c(H)(C_3H_7)$ (from (1)) and for $k_2(H)(C_3H_7)$ (from (3)) gives,

$$-d(H)/dt = 2k_1(H)(C_3H_6) + 2d(C_3H_8)/dt + d(CH_4)/dt + d(C_3H_6)/dt$$

and so

$$k_1 = \frac{-d/dt\left((H) + 2(C_3H_8) + (CH_4) + (C_3H_6)\right)}{2(H)(C_3H_6)} = \frac{-d(H)p/dt}{2(H)(C_3H_6)}$$

where $d(H)_p/dt$ represents the rate of decay of H atoms due only to formation of propyl radicals.

5.3 Results.

Figure 5.3 shows the variation of $(H)_p$, (H) and (C_3H_6) with time, and from the graph $d(H)_p/dt$ can be determined and so k_1 estimated. The results shown in Table 5.3 give as an average value

$$k_1 = 6.4 \times 10^8 \text{l.mole}^{-1}\text{sec}^{-1}$$

Variation of k_1 with Temperature.

k_1 was calculated in an analogous fashion for each run, over the complete temperature range. S/D for the decomposition of excited propane (steps (d) and (e)) varied with temperature and so this was estimated in each case.

Results are shown in Table 5.4 and an Arrhenius plot (figure 5.4) gives the following Arrhenius equation.

$$\text{Log}_{10}(k_1) = (9.86 \pm 0.20) - (1040 \pm 200)/4.576T$$

(k_1 in $\text{l.mole}^{-1}\text{sec}^{-1}$)

Variation of k_1 with Pressure

There was no apparent variation of k_1 over the pressure range covered in this study.

H + propene - Table 5.1

Typical Run Results - H and Products (run 4)

Reaction temperature = 287°K

Flow tube pressure = 1.60 torr

Linear flowrate (dZ/dt) = 1760 cm/sec

(1) H atoms.

distance from inlet(cm)	probe response(mv) (no reaction)	probe response(mv) (reaction)	(H) $mole.l^{-1} \times 10^{7}$
0.0	9.36	9.36	9.54
0.5	9.36	5.54	5.65
1	9.35	4.8	4.9
1.5	9.35	4.5	4.59
2	9.35	4.2	4.28
3	9.35	3.64	3.71
4	9.34	3.18	3.24
5	9.34	3.18	2.84
6	9.33	2.42	2.47
8	9.30	1.9	1.94
10	9.28	1.53	1.56
12	9.25	1.21	1.23
14	9.20	1.00	1.02
16	9.20	0.80	0.82
18	9.18	0.65	0.66

(2) Products. (concentrations in mole.l^{-1}x10^{7})

distance from inlet (cm)	(CH_4)	(C_2H_4)	(C_2H_6)	(C_3H_6)	(C_3H_8)
0	0	0	0	2.52	0
1	0.680	0.156	0.175	1.910	0.118
2	0.741	0.198	0.268	1.721	0.169
3	0.836	0.236	0.343	1.691	0.276
4	0.850	0.251	0.380	1.600	0.220
5	0.836	0.256	0.420	1.492	0.313
7	0.875	0.267	0.489	1.479	0.323
9	0.878	0.284	0.525	1.271	0.420
11	0.819	0.305	0.590	1.213	0.433
14	0.830	0.308	0.648	1.110	0.496
16	0.853	0.312	0.661	1.057	0.503

H + Propene - Table 5.2

The variation of S/D with pressure for $C_3H^*_8$ $\xrightarrow{S}$ C_3H_8; $\xrightarrow{D}$ $CH_3 + C_2H_5$

Run	Pressure (torr)	$\log_{10}$(pressure) (torr)	S/D	S/S+D	$\log_{10}$(S/S+D)
1	1.60	0.204	0.955	0.488	-0.310
5	1.60	0.204	0.720	0.418	-0.380
15	0.60	-0.222	0.292	0.226	-0.646
16	0.76	-0.120	0.199	0.166	-0.780
17	0.75	-0.125	0.193	0.160	-0.715
18	2.14	0.330	0.850	0.460	-0.338
19	2.15	0.332	1.230	0.550	-0.258
20	2.14	0.330	1.201	0.545	-0.264

H + Propene - Table 5.3

Calculation of k_1 for $H + C_3H_6 \xrightarrow{k_1} C_3H_7^*$

Distance from inlet (cm)	$d(H)_p/dt$ (molel^{-1}sec^{-1})	(H) (molel^{-1})	C_3H_6) (molel^{-1})	k_1 (lmole^{-1}sec^{-1})
4	6.31×10^{-5}	3.20×10^{-7}	1.59×10^{-7}	6.2×10^{8}
6	4.65 "	2.45 "	1.46 "	6.5 "
8	3.37 "	1.95 "	1.35 "	6.4 "
10	2.50 "	1.55 "	1.26 "	6.4 "
12	1.95 "	1.30 "	1.19 "	6.3 "
14	1.56 "	1.05 "	1.11 "	6.7 "

mean value of k_1 = 6.4×10^{8} lmole^{-1}sec^{-1}.

H + Propene - Table 5.4

Run Conditions and Experimental Results.

(1) Constant Pressure (1.60 torr)

Run	$(H) \times 10^7$ molel^{-1}	$(C_3H_6) \times 10^7$ molel^{-1}	Temp.(^oK)	k_1	$\log(k_1)$	$10^3/T$
1	8.75	4.21	287	5.0×10^8	8.701	3.48
2	10.81	0.85	287	6.1 "	8.786	3.48
3	8.75	3.20	287	5.5 "	8.740	3.48
4	9.55	2.52	287	6.4 "	8.806	3.48
5	8.35	2.47	287	5.75 "	8.760	3.48
6	11.85	0.57	287	5.9 "	8.771	3.48
7	6.50	6.15	288	5.9 "	8.771	3.47
8	5.66	7.10	289	5.8 "	8.764	3.46
9	7.50	3.46	338	7.0 "	8.846	2.96
10	4.61	5.20	350	7.4 "	8.860	2.86
11	6.94	4.40	350	8.1 "	8.911	2.86
12	3.74	2.23	371	8.7 "	8.940	2.70
13	4.50	4.01	371	8.3	8.920	2.70
14	4.51	3.72	371	8.4	8.924	2.70

(2) Constant Temperature (287^oK) Pressure (torr)

15	9.00	9.10	0.60	5.2 "	
16	15.00	4.52	0.76	5.9 "	
17	12.80	4.52	0.76	5.8 "	
18	8.85	2.98	2.14	5.1 "	
19	10.20	2.58	2.15	5.5 "	
20	10.20	2.58	2.14	6.2 "	

FIGURE 5.1

H + PROPENE RUN 4

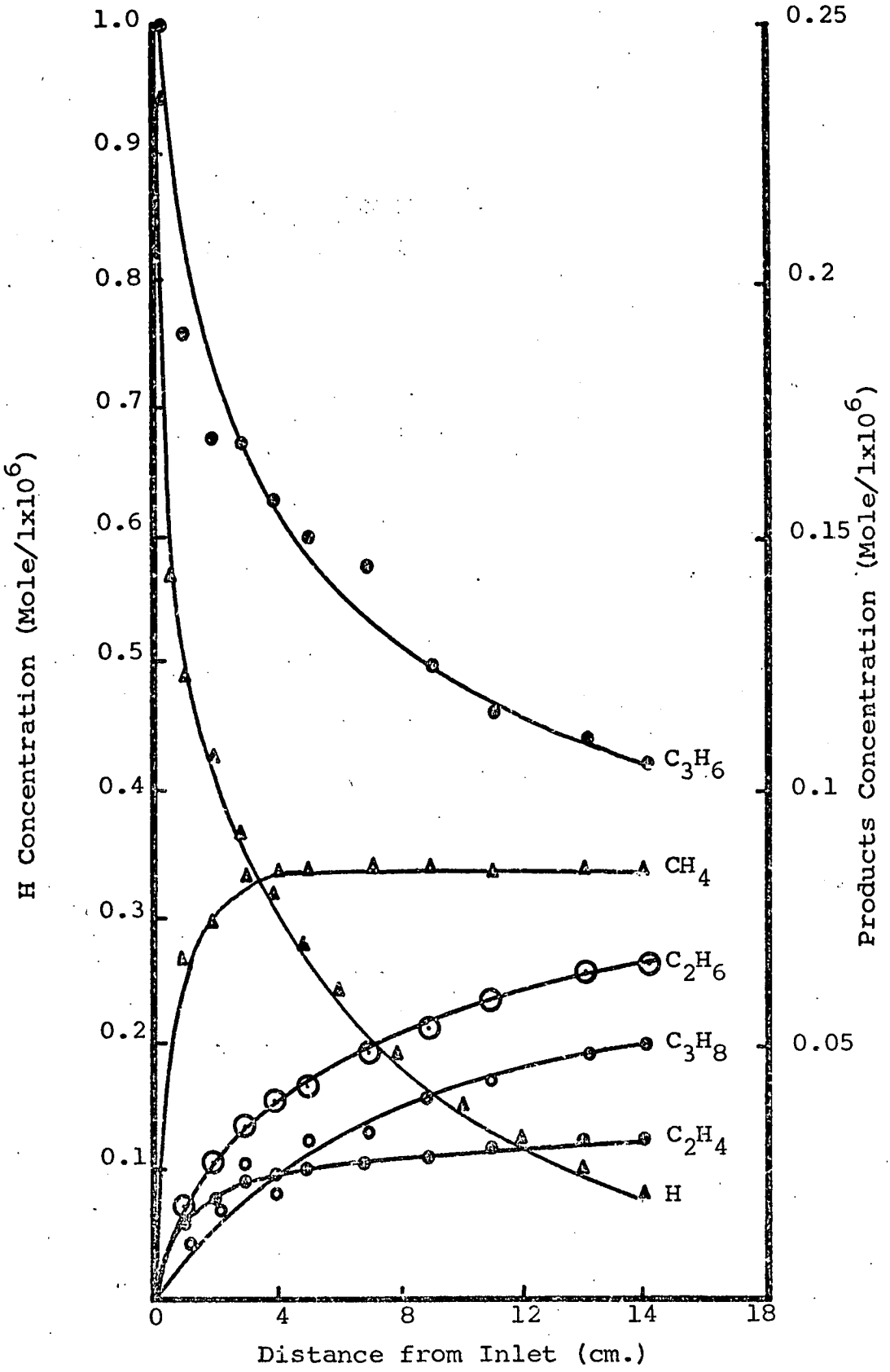

FIGURE 5.2

LOG_{10} ($^{S}/_{S+D}$) AGAINST LOG_{10} (PRESSURE)

FOR H + iso C_3H_7 ⟶ C_3H_8* $\xrightarrow{S}$ C_3H_8

$\xrightarrow{D}$ $CH_3 + C_2H_5$

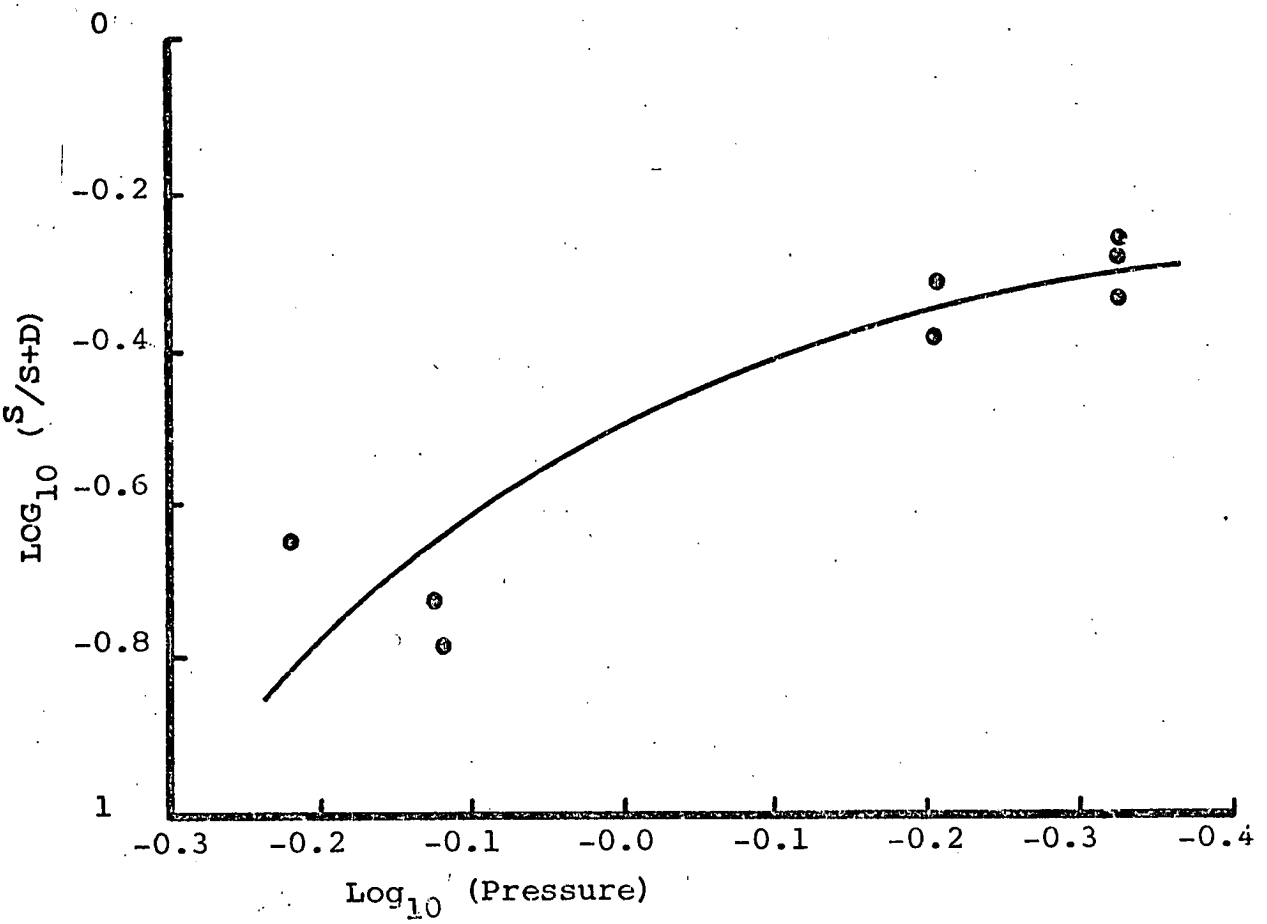

FIGURE 5.3

H + PROPENE RUN 4

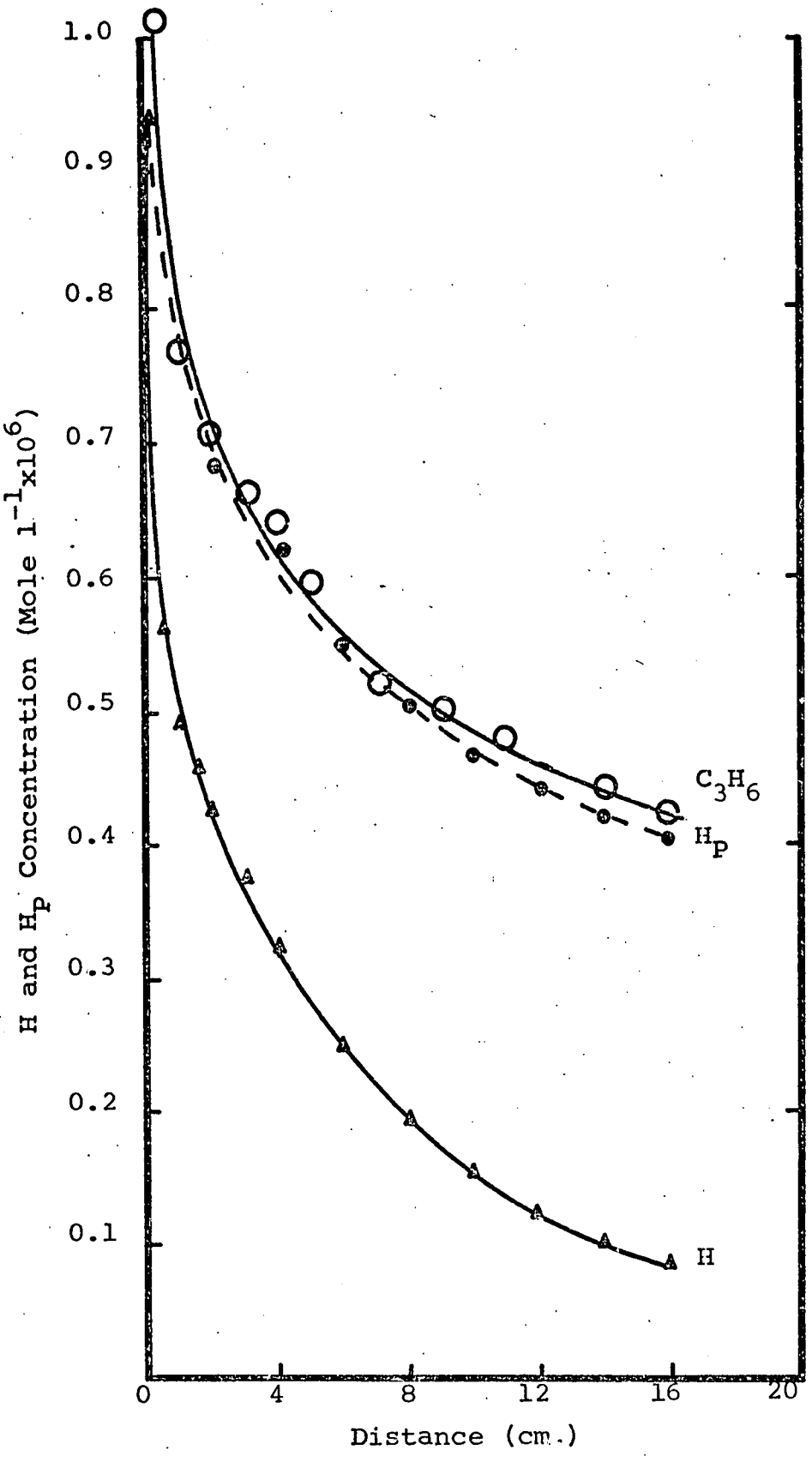

FIGURE 5.4

H + PROPENE - ARRHENIUS PLOT OF k_1

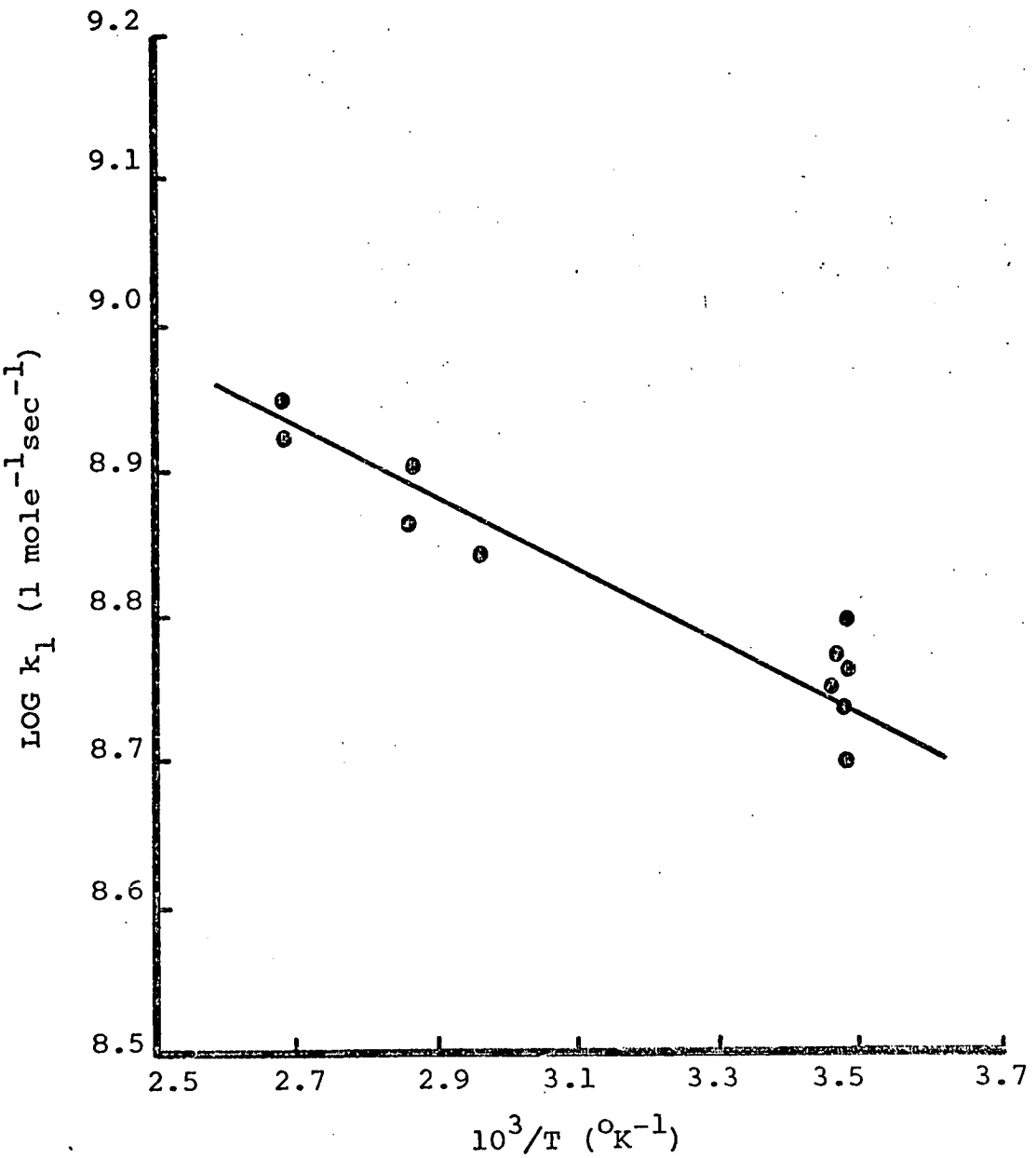

CHAPTER 6

THE REACTION OF H WITH 1-BUTENE

6. The Reaction of Hydrogen Atoms with 1-Butene.

6.1 Experimental.

Products of the reaction were methane, ethane, ethylene, propene, and butane. Significant features of the reaction were the high degree of degradation to methane (70%), the small amount of butane produced (4%) as well as the absence of propane in the products. The reaction differed from the H + propene system in that there was no evidence of a cycling mechanism - all of the hydrogen atoms removed appeared in the alkane products.

Table 6.1 and figure 6.1 show the results of a run at 287°K and 1.60 torr.

6.2 Mechanism.

The initial step in the mechanism is the formation of a vibrationally excited butyl radical which can be sec-butyl, if the addition is to the terminal carbon atom, or n-butyl if the addition is non-terminal. As in the case of the H/propene scheme, formation of the former is the preferred step.

The less stable $n\text{-}C_4H_9^*$ splits to give C_2H_4 and C_2H_5. This is the only source of ethylene and the product analysis shows that 6% of all butene molecules react in this way to yield ethylene. Thus 6% of the addition is non-terminal producing n-butyl radicals.

Sec-butyl radicals can be stabilised by collision or decompose to give CH_3 and propene. Experimental results indicate that 22% of the 1-butene decompose to yield propene

and so the remaining 72% of reacting olefin must lead to stabilized sec-butyl radicals.

Thus for,

$$CH_3 - \dot{C}H - CH_2\ CH_3^* \xrightarrow{S} \text{sec-}C_4H_9 \qquad (72\%)$$

(sec-butyl)

$$\xrightarrow{D} C_3H_6 + CH_3 \qquad (22\%)$$

$$S/D = 3.3$$

The surviving sec-C_4H_9 undergoes further H-addition, leading to the formation of excited n-butane - only 5.5% is stabilized and so the remainding 94.5% decomposes. The excited butane splits symmetrically to give two ethyl radicals which in turn react to give methane and ethane. Unsymmetric splitting would give propyl radicals and some propane would be expected among the products. As mentioned earlier, no trace of propane was found.

So for,

$$C_4H_{10}^* \xrightarrow{S} C_4H_{10} \qquad (5.5.\%)$$

$$\xrightarrow{D} 2C_2H_5 \qquad (94.5\%)$$

$$S/D = 0.06$$

The complete mechanism, accounting for all the products, is shown

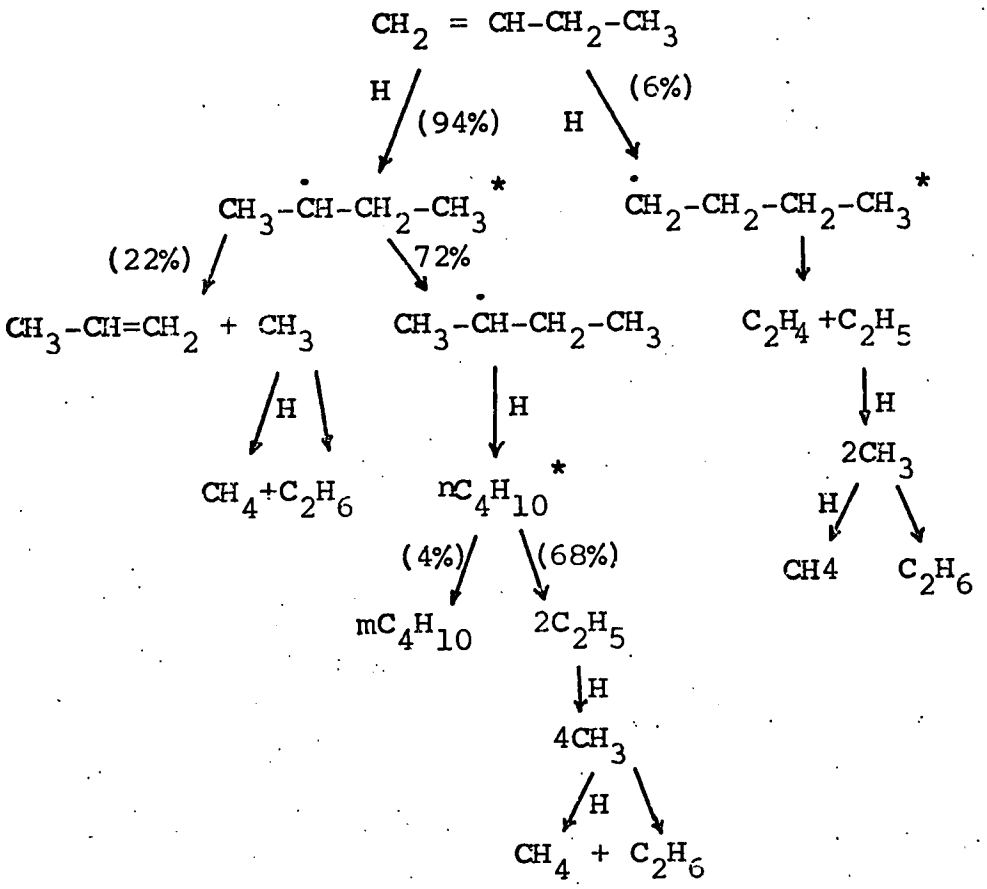

6.3 The Rate of Addition of H Atoms to 1-Butene.

Because of the absence of any complicating cycling reaction the rate constant for the addition reaction can be determined from the rate of removal of 1-butene. So for,

$$H + \text{1-butene} \xrightarrow{k_1} C_4H_9^*$$

$$-d(\text{1-butene})/dt = k_1(H)(\text{1-butene})$$

hence,

$$k_1 = \frac{-d(\text{1-butene})/dt}{(H)(\text{1-butene})}$$

Table 6.2 contains the results for the run illustrated, which gives as an average value,

$$k_1 = 8.4 \times 10^8 \text{ lmole}^{-1}\text{sec}^{-1}$$

The data at room temperature and a study at 371°K suggest an Arrhenius equation of the form

$$\log_{10}(k_1) = 9.80 - 1020/4.576T$$

H + 1 Butene - Table 6.1

Typical Run Results - H and Products (run 1)

Reaction temperature = 287°K

Flow tube pressure = 1.60 torr

Linear flowrate (dz/dt) = 1760 cm/sec

(1) H Atoms.

Distance from inlet(cm)	probe response(mv) (no reaction)	probe response(mv) (reaction)	(H) $mole.l^{-1}x10^7$
0	9.50	9.50	9.60
1	9.50	3.22	3.25
2	9.46	2.13	2.15
3	9.46	1.63	1.65
4	9.46	1.39	1.40
5	9.46	1.14	1.15
6	9.42	0.99	1.00
7	9.42	0.91	0.92
8	9.42	0.79	0.80
9	9.41	0.74	0.75
10	9.40	0.69	0.71
12	9.40	0.64	0.65
14	9.40	0.63	0.64
16	9.37	0.62	0.63
18	9.37	0.62	0.63

(2) Products. (concentrations in mole $l^{-1} \times 10^{7}$)

distance from inlet (cm)	(CH_4)	(C_2H_4)	(C_2H_6)	(C_3H_6)	(C_4H_8)	(C_4H_{10})
0	0	0	0	0	3.62	0
1	1.45	0	0.80	0.11	2.82	0
2	2.12	0.02	1.19	0.36	2.40	0
4	2.44	0.06	1.21	0.29	2.11	0.02
6	2.68	0.10	1.34	0.40	1.92	0.04
8	2.84	0.08	1.57	0.42	1.70	0.08
10	2.94	0.14	1.48	0.40	1.64	0.10
12	3.05	0.14	1.59	0.42	1.57	0.11
14	3.13	0.14	1.60	0.43	1.54	0.10
16	3.20	0.15	1.62	0.44	1.52	0.12

H + 1 Butene - Table 6.2

Calculation of k_1 for $H + C_4H_8 \xrightarrow{k1} C_4H_9^*$

Distance from inlet (cm)	$d(C_4H_8)/dt$ (molel^{-1}sec^{-1})	(H) (molel^{-1})	(C_4H_8) (molel^{-1})	k_1 (1mole^{-1}sec^{-1})
4	2.47×10^{-5}	1.4×10^{-7}	2.1×10^{-7}	8.4×10^{8}
5	1.98 "	1.2 "	1.96 "	8.4 "
6	1.60 "	1.0 "	1.87 "	8.6 "
7	1.36 "	0.9 "	1.80 "	8.4 "
8	1.16 "	0.85 "	1.74 "	8.0 "

mean value of $k_1 = 8.4\times10^{8}$ 1mole^{-1}sec^{-1}

H + 1-Butene - Table 6.3

Run Conditions and Experimental Results.

All results are at a pressure of 1.60 torr.

Run	$(H)\times10^{7}$ (molel^{-1})	$(C_4H_8)\times10^{7}$ (molel^{-1})	k_1	$\log k_1$	temp(^{o}K)
1	9.60	3.62	8.4×10^{8}	8.924	287
2	7.80	3.60	8.6x "	8.935	287
3	2.92	2.76	8.5 "	8.930	287
4	2.80	2.20	12.5 "	9.098	371

FIGURE 6.1

H +1-BUTENE RUN 1

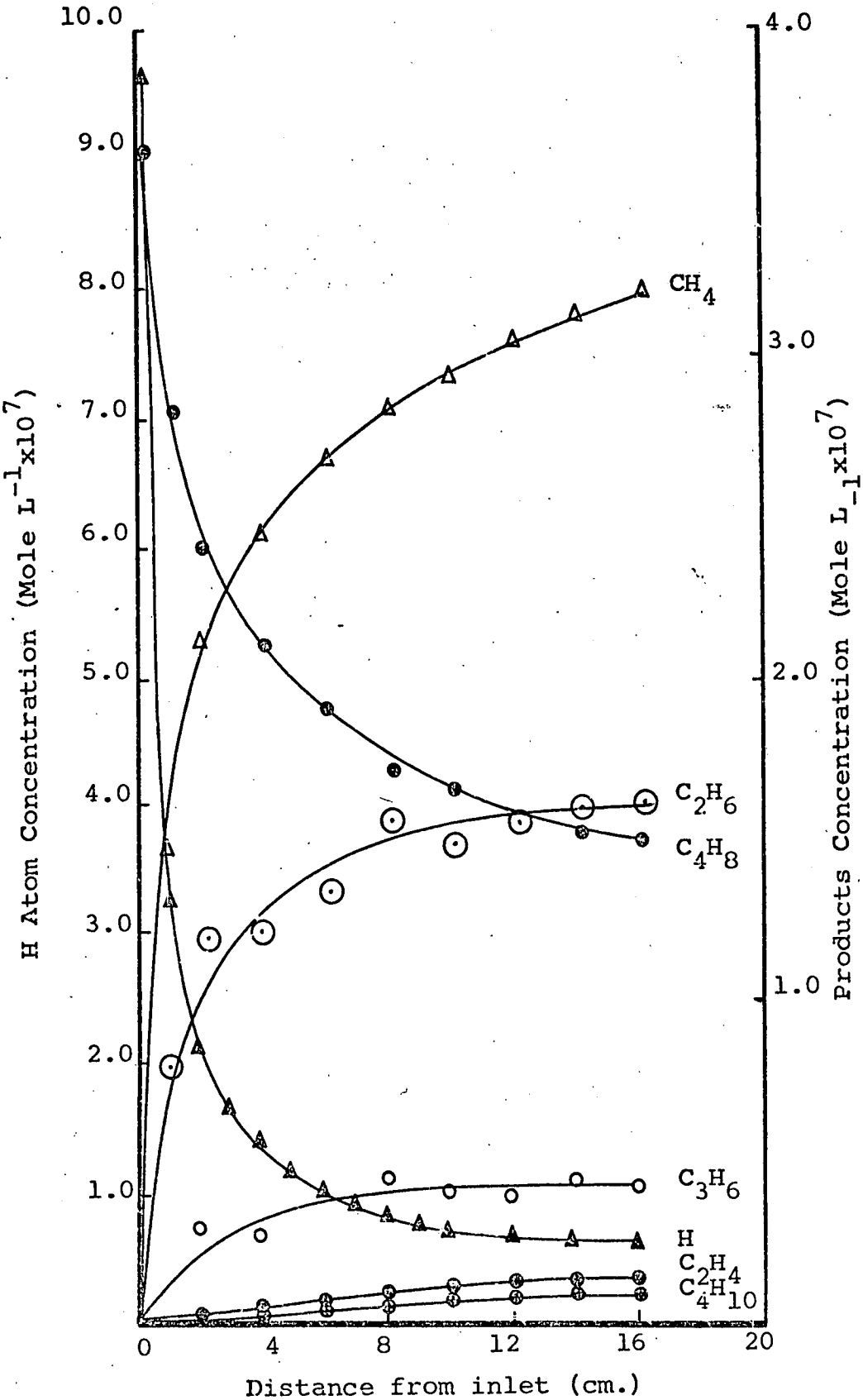

CHAPTER 7

INTERNAL RATE CONSTANTS

7.1 The H Atom/Ethylene System.

Figure 4.1 shows that the data yields on accurate measure of the build up of products CH_4 and C_2H_6 with time during the course of the reaction. $\frac{d(CH_4)}{dt}$ and $\frac{d(C_2H_6)}{dt}$ from these curves can be usefully combined to show the variation of S/D, for

$$CH_3 + CH_3 \underset{D}{\rightleftharpoons} C_2H_6^* \xrightarrow{S} C_2H_6$$

over the pressure range covered in this study.

As mentioned in Chapter 4 (page 77) Rabinovitch and Setser (RAB64) have performed calculations on reaction group (3)

$$H + CH_3 \underset{}{\overset{D}{\rightleftharpoons}} CH_4^* \xrightarrow{S} CH_4 \text{ ----------(3)}$$

and their results indicate that methane formation is fully within the low pressure or third order region, therefore the appropriate rate expression is,

$$\frac{d(CH_4)}{dt} = R(CH_4) = k_3(H)(CH_3)(M) \quad ((M) = \text{Argon Concentration})$$

Various values for k_3 are quoted in the literature ranging from 8.3×10^{12} up to 54×10^{12} $l^2 mole^{-2} sec^{-1}$ at room temperature. (KON70, BAR70). If k_3 is presumed known then

$$(CH_3) = \frac{R(CH_4)}{k3(H)(M)} \qquad (a)$$

Reaction group (4),

$$CH_3 + CH_3 \underset{D}{\overset{k4}{\rightleftharpoons}} C_2H_6^* \xrightarrow{S} C_2H_6$$

represents the formation of ethane by methyl recombination and as already mentioned this reaction dominates ethane production. Rabinovitch and Setser's calculations (Table 1.1) indicate this reaction is well into the fall-off region within our

pressure range (0.6-3.6torr) and so

$$ka_4 = \frac{S}{S+D} \; k_4$$

(ka_4 is the apparent rate constant)

and $$\frac{d(C_2H_6)}{dt} = R(C_2H_6) = ka_4 \; (CH_3)^2 \qquad (b)$$

$$= \frac{S}{S+D} \; k_4(CH_3)^2$$

Hence $$\frac{S}{S+D} = \frac{R(C_2H_6)}{k_4(CH_3)^2}$$

Substitution for (CH_3) from (a) gives

$$S/S+D = \frac{R(C_2H_6) \; k_3^2 \; (H)^2(M)^2}{k_4(R(CH_4))^2}$$

If the high pressure value of k_4 is taken as 3.4×10^{10} $lmole^{-1}sec^{-1}$ (TOB68) and k_3 is taken as $2.7 \times 10^{13} l^2 mole^{-2} sec^{-1}$ (DOD69b) then S/S+D can be estimated since all else can be found from the data. In practice an average was taken of the various values obtained from the initial stages of the reaction. Table 7.1 shows a typical calculation and Table 7.2 shows the variation of S/S+D with pressure. This is illustrated graphically in Figure 7.1.

7.2 The H Atom/Propene System.

A surprising feature of this system (see Figure 5.1) is the rapid increase in the apparent (CH_4) to a maximum value after only 2.5 msec. It seems likely that the experimentally measured CH_4 is in fact both CH_4 and CH_3, the latter being rapidly converted to CH_4 on the probe.

The mechanism for H atom addition to propene suggested in Chapter 5 indicates 10% of the addition is nonterminal

producing excited n-propyl radicals which tend to decompose to CH_3 and C_2H_4 i.e.

$$H + C_3H_6 \longrightarrow nC_3H_7^* \longrightarrow CH_3 + C_2H_4$$

Thus CH_3 radicals are produced at a very early stage in the reaction.

In contrast, for the H/C_2H_4 system, CH_3 results only after excited ethane molecules decompose. i.e.

$$H + C_2H_4 \longrightarrow C_2H_5^* \xrightarrow{S} C_2H_5 + H \longrightarrow 2CH_3$$

and so there is a slower build up of CH_3 which does not affect the CH_4 experimental curve.

The CH_3 radical concentration can be estimated in the H/propene system. From (b) above,

$$(CH_3) = \left(\frac{R(C_2H_6)}{ka_4}\right)^{\frac{1}{2}}$$

$$= \left(\frac{R(C_2H_6)}{\frac{S}{S+D}\,k_4}\right)^{\frac{1}{2}} \quad \text{since } ka_4 = \frac{S}{S+D}\,k_4$$

If S/S+D is taken as 0.35, which is the average of the values at 1.60torr found for the H/ethylene system (see Table 7.2) and k_4 is again taken as 3.4×10^{10} $lmole^{-1}sec^{-1}$, then (CH_3) can be found by measuring the gradient of the C_2H_6 curve. This is shown in Table 7.3.

The correction to $(CH_4)_{observed}$ can now be applied since,

$$(CH_4)_{observed} = (CH_4)_{actual} + (CH_3)$$

This has been done in Figure 7.2, and Table 7.4.

The $C_2H_{6\ actual}$ curves should now be compatible. This can be checked as follows:

$$\frac{d(CH_4)}{dt} = R(CH_4) = k_3(H)(CH_3)(M)$$

Substitution for CH_3 from above gives

$$R(CH_4) = \frac{k_3}{\left(\frac{S}{S+D}\, k_4\right)^{\frac{1}{2}}} \times (R(C_2H_6))^{\frac{1}{2}} \times (H)\,(M)$$

with $k_3 = 2.7\times10^{13}\ l^2 mole^{-2} sec^{-1}$

$k_4 = 3.4\times10^{10}\ l mole^{-1} sec^{-1}$

$(M) = 8.0\times10^{-5}\ mole^{-1}$

and $R(C_2H_6)$ and (H) found from Figure 5.1. Figure 7.3 is the graph of $R(CH_4)_{calc}$ versus time.

Integration gives,

$$(CH_4)_{calc} = \int_o^t R(CH_4)_{calc}\, dt$$

(where t is taken to 6 msec - the end of the reaction)

Table 7.5 shows $(CH_4)_{calc}$ and Figure 7.4 shows a comparison between $(CH_4)_{calc}$ and $(CH_4)_{actual}$. Agreement is good showing the plausibility of the above reasoning.

The process was applied to a different H/propene run and again theory and experiment are compatible.

Our results for the H/propene system are therefore consistent with

(a) $k_3 = 2.7\times10^{13}\ l^2 mole^{-2} sec^{-1}$

(b) $k_4 = 3.4\times10^{10}\ l mole^{-1} sec^{-1}$

(c) $S/S+D = 0.35$ for $CH_3 + CH_3 \longrightarrow C_2H_6^{*} \begin{cases} \xrightarrow{S} C_2H_6 \\ \xrightarrow{D} CH_3 + CH_3 \end{cases}$ (S/D=0.54)

7.3 <u>The H atom/1-Butene System</u>.

The same procedure as for H/propene was followed. i.e. it was assumed that (CH_4) observed = $(CH_4)_{actual} + (CH_3)$

As before,

$$(CH_3) = \left(\frac{R(C_2H_6)}{ka_4}\right)^{\frac{1}{2}}$$

Table 7.6 shows (CH_3) and Figure 7.5 shows (CH_3), $(CH_4)_{obs-}$ $_{erved}$, and $(CH_4)_{actual}$.

Again as before,

$$R(CH_4) = \frac{k_3}{(\frac{S}{S+D}\ k_4)^{\frac{1}{2}}} \times (R(C_2H_6))^{\frac{1}{2}} \times (H)(M)$$

$$\text{with } k_3 = 2.7\text{x}10^{13}\,l^2\text{mole}^{-2}\text{sec}^{-1}$$

$$k_4 = 3.4\text{x}10^{10}\,l\text{mole}^{-1}\text{sec}^{-1}$$

$$(M) = 8.0\text{x}10^{-5}\ \text{mole}l^{-1}$$

Figure 7.6 is a graph of $R(CH_4)$ against time and from this

$$(CH_4)_{calc} = \int_o^t R(CH_4)_{calc}\ dt$$

Table 7.7 shows $(CH_4)_{calc}$ and Figure 7.7 illustrates a comparison between $(CH_4)_{actual}$ and $(CH_4)_{calc}$. This time agreement is not as good. It is necessary to reduce $(CH_4)_{actual}$ and also increase $(CH_4)_{calc}$. This can be achieved by reducing the value of S/S+D to 0.2. Figure 7.8 shows the comparison with this correction applied. This time theory and experiment are in good agreement.

Our results for the H/1-butene system are therefore consistent with

(a) $k_3 = 2.7\text{x}10^{13}\,l^2\text{mole}^{-2}\text{sec}^{-1}$

(b) $k_4 = 3.4\text{x}10^{10}\,l\text{mole}^{-1}\text{sec}^{-1}$

(c) S/S+D = 0.20 for $CH_3 + CH_3 \rightarrow C_2H_6^{*} \xrightarrow{S} C_2H_6$; $C_2H_6^{*} \xrightarrow{D} CH_3 + CH_3$ (S/D=0.25)

H + Ethylene - Table 7.1

Calculation of S/S+D for $CH_3 + CH_3 \longrightarrow C_2H_6^* \xrightarrow{S} C_2H_6$; $C_2H_6^* \xrightarrow{D} CH_3 + CH_3$

Run 7 Reaction temperature = 293°K.

Flowrate = 1760 $cm.sec^{-1}$

Flow tube pressure = 1.60 torr.

Argon concn. ((M)) = $8 \times 10^{-5} mole\,l^{-1}$

$$S/S+D = \frac{R(C_2H_6)\ K_3^2 (H)^2 (M)^2}{K_4\ (R(CH_4))^2}$$

$k_3 = 2.7 \times 10^{13} l^2 mole^{-2} sec^{-1}$

$k_4 = 3.4 \times 10^{10} l mole^{-1} sec^{-1}$

Distance from inlet (cm.)	(H) ($mole\,l^{-1}$)	$(H)^2$	$R(CH_4)$ ($mole\,l^{-1}sec^{-1}$)	$(R(CH_4))^2$	$R(C_2H_6)$ ($mole\,l^{-1}sec^{-1}$)	S/S+D
1	7.8×10^{-7}	6.1×10^{-13}	5.0×10^{-5}	2.5×10^{-9}	8.8×10^{-6}	0.28
2	7.0 "	4.9 "	4.7 "	2.2 "	8.8 "	0.26
3	6.2 "	3.8 "	4.2 "	1.8 "	8.7 "	0.25
4	5.6 "	3.2 "	3.8 "	1.4 "	8.8 "	0.26
5	5.2 "	2.7 "	3.5 "	1.2 "	9.6 "	0.27
6	4.8 "	2.3 "	3.1 "	1.0 "	9.7 "	0.31

mean value of S/S+D = 0.27

H + Ethylene-Table 7.2

The variation of S/S+D with pressure for $C_2H_6^*$ 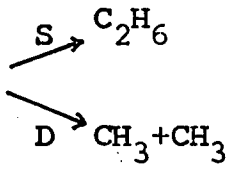

Run	Pressure (torr)	Log_{10}(pressure)	S/S+D	Log_{10}(S/S+D)
7	1.60	0.202	0.272	-0.571
8	1.60	0.202	0.441	-0.352
17	0.61	-0.222	0.081	-1.091
18	0.61	-0.222	0.077	-1.114
20	0.99	-0.004	0.135	-0.872
22	1.60	0.202	0.491	-0.309
25	3.51	0.544	0.881	-0.055
26	3.51	0.544	0.522	-0.284

H + Propene - Table 7.3

$$(CH_3) = \left(\frac{R(C_2H_6)}{S/S+D\ k_4}\right)^{\frac{1}{2}}$$

$S/S+D = 0.35$

$k_4 = 3.4 \times 10^{10} \text{lmole}^{-1}\text{sec}^{-1}$

Distance from inlet (cm)	$R(C_2H_6)$ (molel^{-1}sec^{-1})	$(R(C_2H_6))^{\frac{1}{2}}$	(CH_3) (molel^{-1})
0.5	24×10^{-6}	0.49×10^{-2}	0.45×10^{-7}
1.0	18.6 "	0.43 "	0.39 "
1.5	13.7 "	0.37 "	0.34 "
2.0	11.6 "	0.34 "	0.31 "
2.5	9.4 "	0.31 "	0.28 "
3.0	6.9 "	0.26 "	0.24 "
3.5	5.75 "	0.24 "	0.22 "
4.0	4.76 "	0.22 "	0.20 "
5.0	3.88 "	0.20 "	0.18 "
6.0	3.84 "	0.19 "	0.17 "
7.0	3.05 "	0.17 "	0.16 "
8.0	2.70 "	0.16 "	0.15 "
9.0	2.34 "	0.15 "	0.14 "
10.0	2.00 "	0.14 "	0.13 "

H + Propene - Table 7.4

$$(CH_4)_{actual} = (CH_4)_{observed} - (CH_3)$$

Distance from inlet (cm)	$(CH_4)_{observed}$ (molel^{-1}x10^7)	(CH_3) (molel^{-1}x10^7)	$(CH_4)_{actual}$ (molel^{-1}x10^7)
0.5	0.51	0.45	0.06
1.0	0.67	0.39	0.28
1.5	0.72	0.34	0.38
2.0	0.76	0.31	0.45
2.5	0.78	0.28	0.50
3.0	0.80	0.24	0.56
3.5	0.82	0.22	0.60
4.0	0.83	0.20	0.63
5.0	0.84	0.18	0.66
6.0	0.85	0.17	0.68
7.0	0.85	0.16	0.69
8.0	0.86	0.15	0.71
9.0	0.86	0.14	0.72
10.0	0.86	0.13	0.73

Table 7.5

$$\underline{\text{H + Propene}} \quad - \quad (CH_4)_{calc} = \int_0^t R(CH_4)_{calc}\, dt$$

Time (msec)	Distance from inlet (cm)	$(CH_4)_{calc}$ ($molel^{-1} x10^7$)
0.5	0.85	0.250
1.0	1.70	0.425
1.5	2.55	0.530
2.0	3.40	0.605
2.5	4.25	0.645
3.0	5.10	0.670
3.5	5.95	0.690
4.0	6.80	0.700
4.5	7.65	0.715
5.0	8.50	0.720
5.5	9.35	0.725
6.0	10.20	0.730

Table 7.6

H + 1-Butene: $(CH_3) = \left(\frac{R(C_2H_6)^{\frac{1}{2}}}{\frac{S}{S+D}\ k_4}\right)$ $S/S+D = 0.35$ $k_4 = 3.4 \times 10^{10}\ l\,mole^{-1}\,sec^{-1}$

Distance from inlet (cm)	$R(C_2H_6)$ $(mole\,l^{-1}\,sec^{-1})$	$(R(C_2H_6))^{\frac{1}{2}}$	(CH_3) $(mole\,l^{-1})$
1	9.6×10^{-5}	9.8×10^{-3}	8.4×10^{-8}
2	3.8×10^{-5}	6.2 "	5.3 "
3	2.3×10^{-5}	4.8 "	4.2 "
4	1.58×10^{-5}	4.0 "	3.4 "
5	0.97×10^{-5}	3.1 "	2.6 "
6	0.76×10^{-5}	2.7 "	2.3 "
7	0.58×10^{-5}	2.4 "	2.0 "
8	0.44×10^{-5}	2.1 "	1.8 "
10	0.119×10^{-5}	1.09 "	1.0 "
12	0.079×10^{-5}	0.88 "	0.81 "
14	0.032×10^{-5}	0.57 "	0.52 "
16	0.020×10^{-5}	0.45 "	0.41 "
18	0.019×10^{-5}	0.44 "	0.40 "

Table 7.7

$$H + \text{1-Butene} - (CH_4)_{calc} = \int_0^t R(CH_4)_{calc}\, dt$$

Time (msec)	Distance from inlet (cm)	$(CH_4)_{calc}$ ($molel^{-1} x10^7$)
0.5	0.85	0.26
1.0	1.70	0.74
1.5	2.55	1.06
2.0	3.40	1.30
2.5	4.25	1.48
3.0	5.10	1.63
3.5	5.95	1.75
4.0	6.80	1.84
4.5	7.65	1.91
5.0	8.50	1.97
5.5	9.35	2.04
6.0	10.20	2.08

FIGURE 7.1

H + ETHYLENE

$LOG_{10}(^{S}/_{S+D})$ AGAINST LOG_{10}(PRESSURE)

FOR $CH_3 + CH_3 \longrightarrow C_2H_6^* \xrightarrow{S} C_2H_6$

$\qquad\qquad\qquad\qquad\qquad\qquad\qquad\qquad\qquad\qquad\qquad\quad \xrightarrow{D} CH_3 + CH_3$

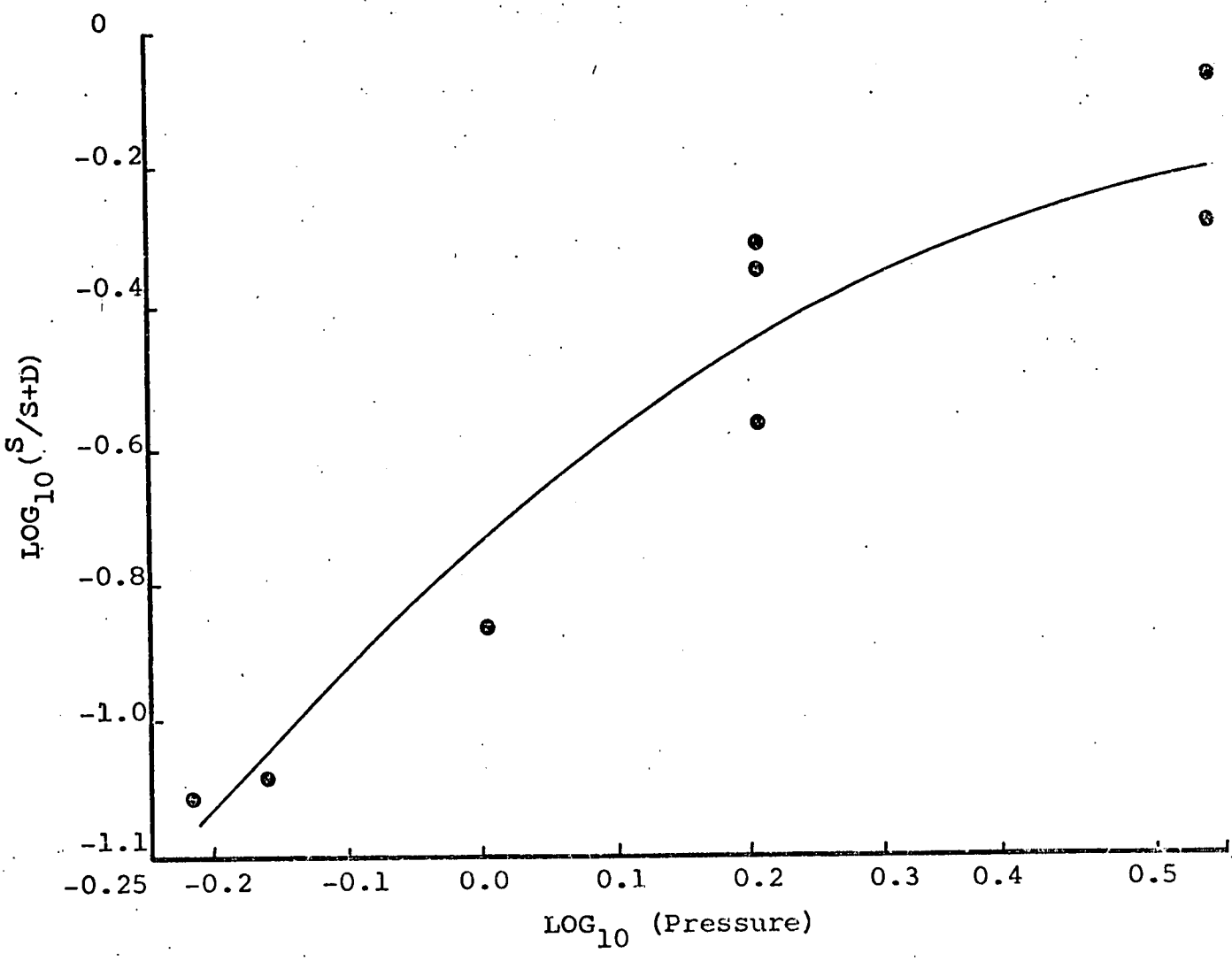

FIGURE 7.2

H + PROPYLENE

$(CH_4)_{Observed}$, $(CH_4)_{actual}$, (CH_3), C_2H_6

$$(CH_4)_{Observed} = (CH_4)_{actual} + (CH_3)$$

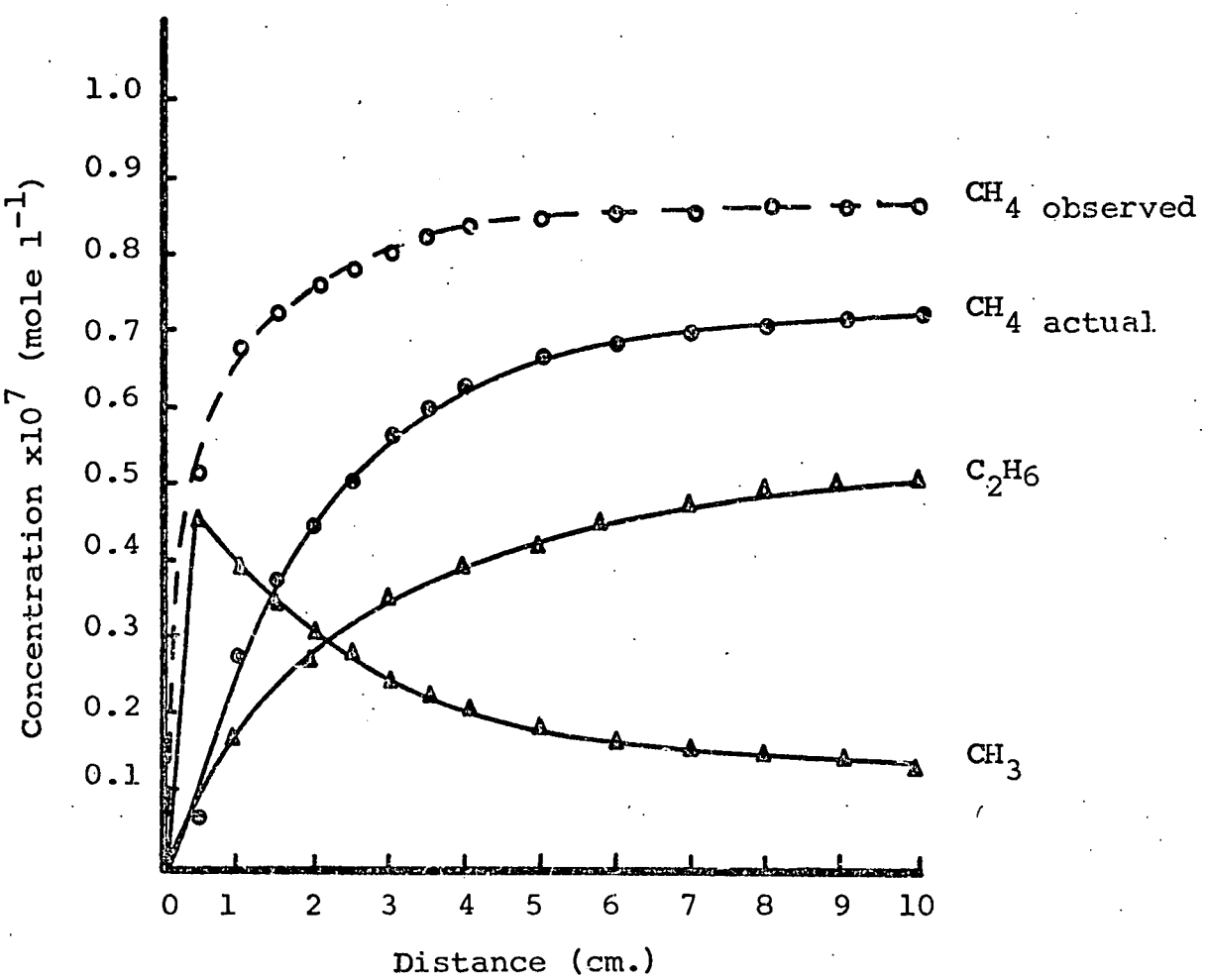

FIGURE 7.3

H + PROPENE

$\frac{d(CH_4)}{dt} = R(CH_4)$ AGAINST TIME

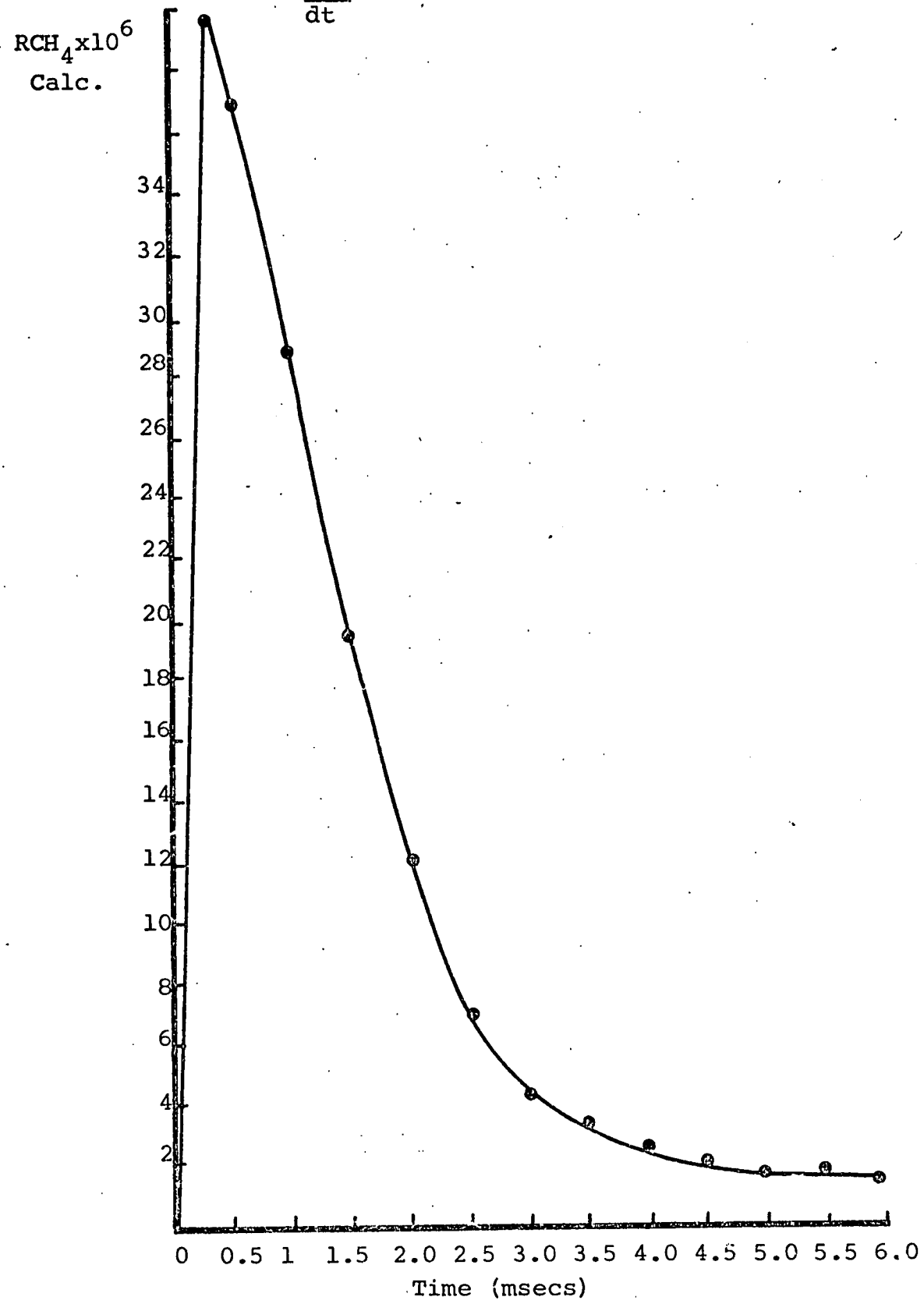

FIGURE 7.4

H + PROPENE

$(CH_4)_{Actual}$ and $(CH_4)_{Calc.}$ Compared

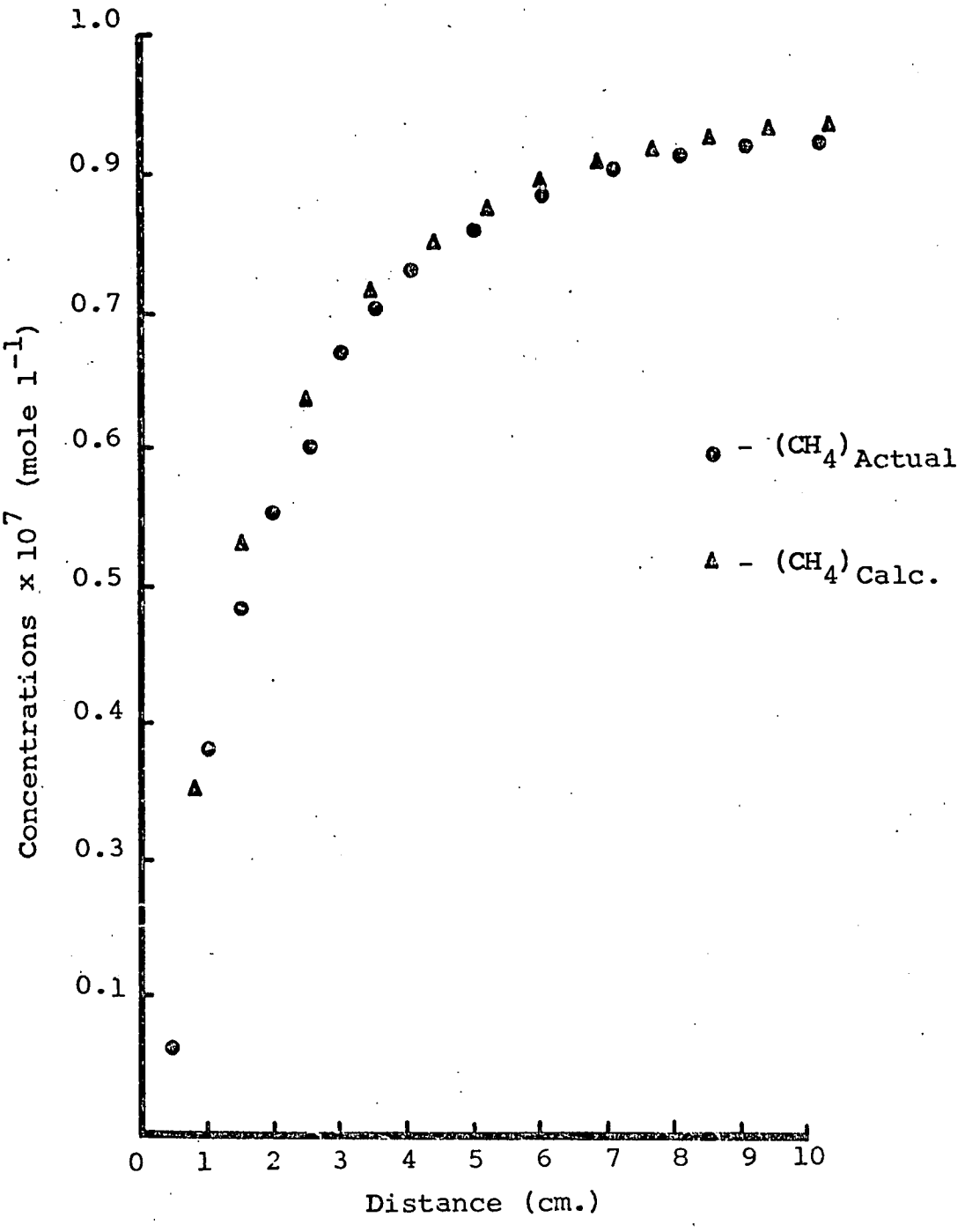

FIGURE 7.5

H + 1-BUTENE

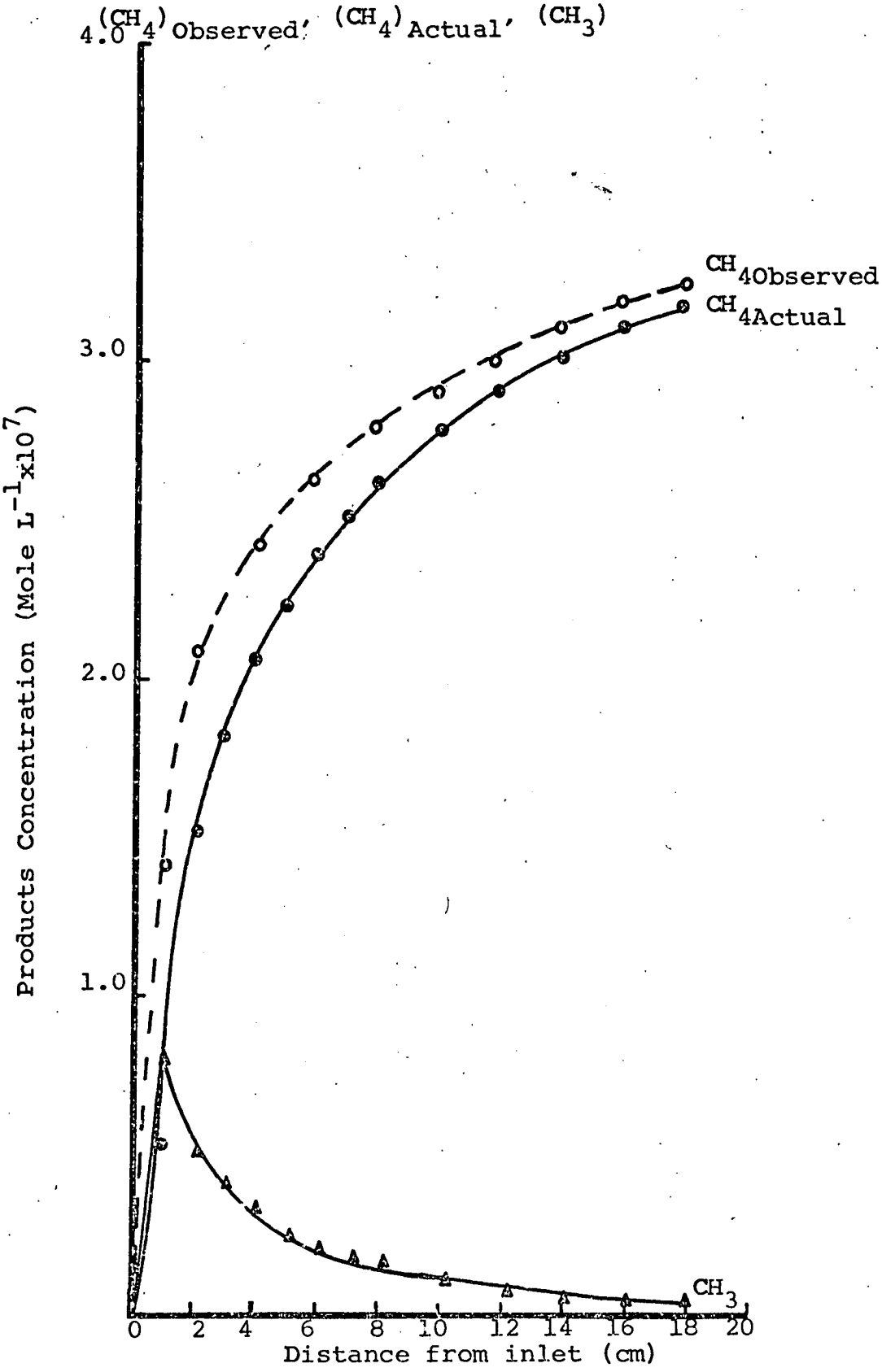

FIGURE 7.6

H + 1-BUTENE

R (CH_4) Against Time

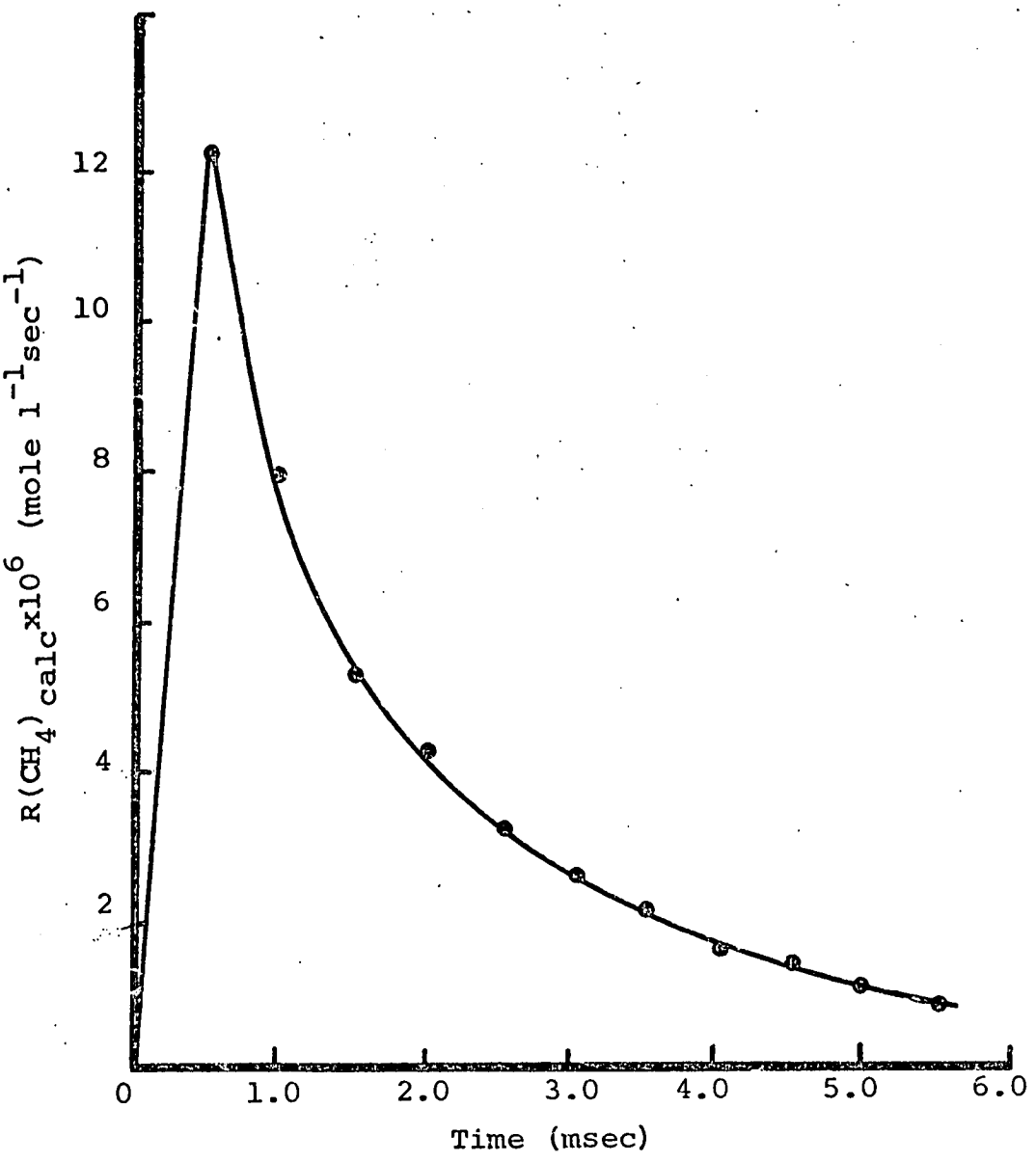

FIGURE 7.7

H + 1-BUTENE - $(CH_4)_{Actual}$ and $(CH_4)_{Compared}$

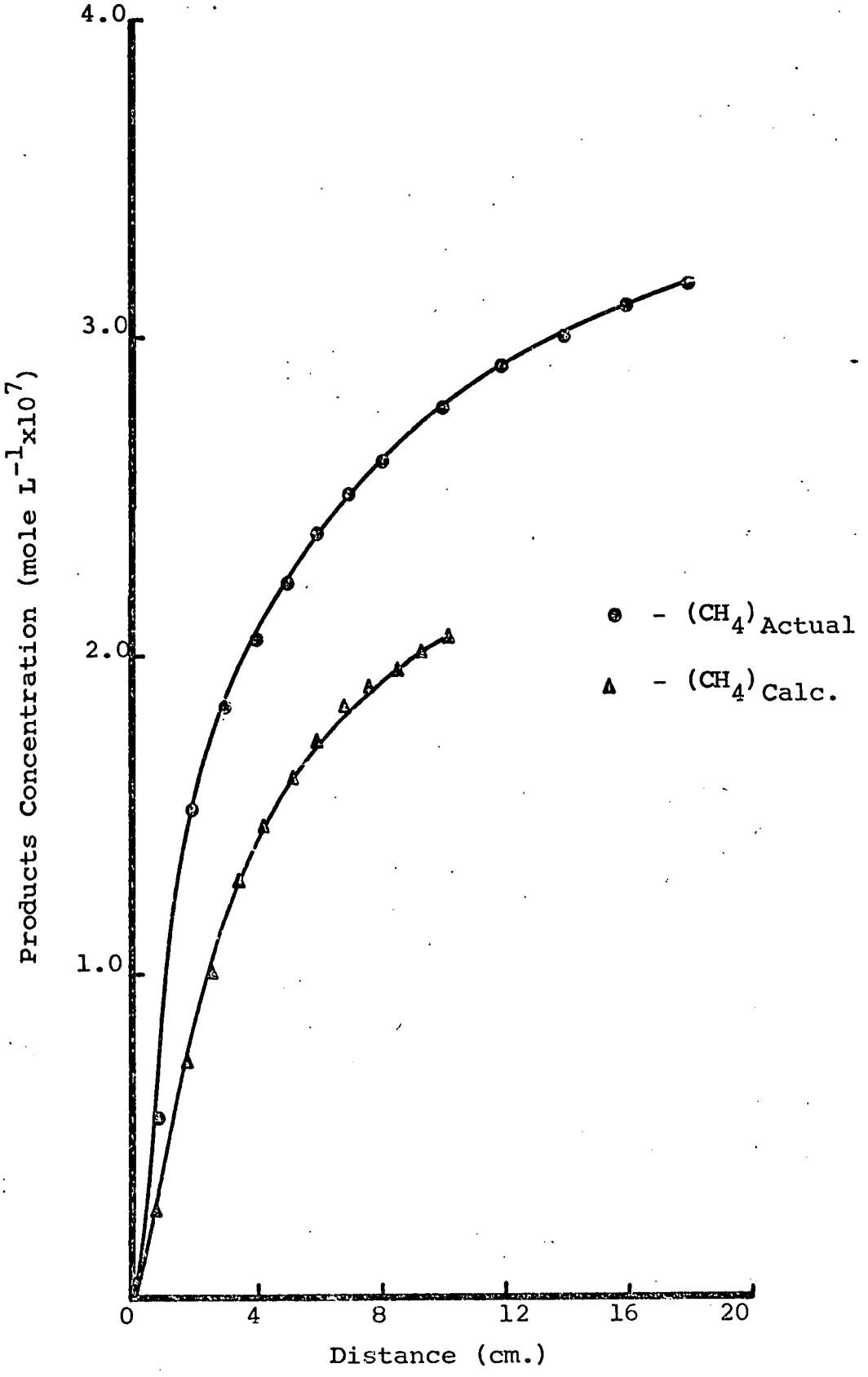

FIGURE 7.8

H + 1-BUTENE $(CH_4)_{Actual}$ and $(CH_4)_{Calc}$ with $S/S+D = 0.20$

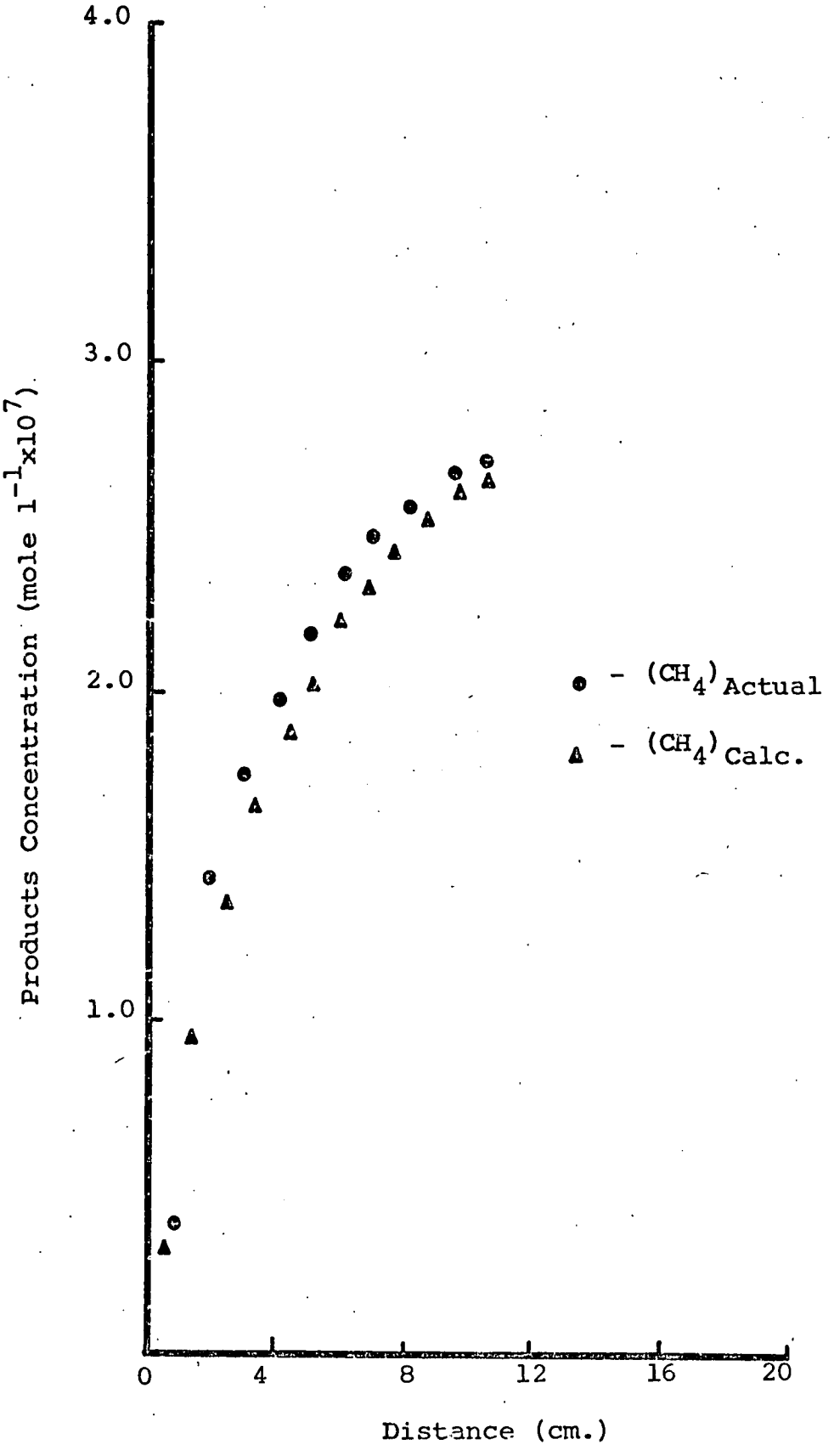

CHAPTER 8

DISCUSSION AND SUMMARY

8.1 Comparison of Rate Constants with those of other Workers.

The rate constants for the reaction of H with ethylene and propene found in this work compared with other workers as shown in figures 8.1 and 8.2. Although the reactions have been studied extensively there is surprisingly little agreement between the various laboratories. This is particularly true of the ethylene reaction although a comparison of the results shown in table 1.3 shows that the apparent discrepancies which have existed for this reaction may be due to a rather strong pressure effect on the reaction rate. Few reports have been made of the hydrogen/1-butene system but the value of the addition rate constant determined in this study (8.6×10^8 l.mole^{-1}s^{-1}) does compare favourably with the value of 8.3×10^8 l.mole^{-1}s^{-1} obtained by Daby, Niki and Weinstock (DAB71) working at a similar pressure (2torr). A more pertinent correlation is a comparison of the results with the theoretical predictions of Rabinovitch and Setser (RAB64).

8.2 Hydrogen Atom Addition to Ethylene.

The pressure dependence of the addition rate constant has now been well established by several independent studies. Michael and Weston (MIC66), using a flow system with Lyman α detection of H atoms have shown a pressure dependence over the range 0.5 - 5 torr. Barker, Keil, Michael and Osborne (BAR69) established a pressure fall-off with three independent experimental techniques. Thus using a conventional discharge flow system with Lyman α photometric

detection of H atoms, a time resolved Lyman α photometric system, and a discharge flow system coupled to a 'time of flight' mass spectrometer they established the pressure dependence of the rate constant over the range 1 - 5 torr. The mass spectrometric technique developed by Dodonov et al enabled them to study the H/C_2H_4 reaction between 2 and 25 torr. These results, together with the Rabinovitch and Setser (RAB64) calculated pressure dependence, are compared with the fall-off established in this study in figure 8.3.

Because the different studies differ in their estimation of k_1^{∞} the limiting high pressure rate constant it has been necessary to plot $\log(k_{al}/k_1^{\infty})$ against pressure, where k_{al} is the experimental addition rate constant at that pressure. This was also necessary for comparison with the theoretical fall-off since Rabinovitch and Setser calculated S/D for,

$$H + C_2H_4 \underset{D}{\rightleftharpoons} C_2H_5^* \xrightarrow{S} C_2H_5$$

which gives $k_{al}/k_1^{\infty} = S/S+D$

Figure 8.3 illustrates that the three mentioned experimental studies show a steeper fall-off with pressure than the theoretical curve. Also Michael and Weston's results are in good agreement with those of Dodonov et al, both indicating the fall-off at a higher pressure than predicted.

Our experimental points were derived using Rabinovitch and Setser's data for S/S+D which then enabled k_1^{∞} to be calculated. An alternative approach is to adjust our points

so that the pressure fall-off of k_{al}/k_1^{∞} exactly parallels that of Rabinovitch and Setser's theoretical S/S+D values. This has been done in Figure 8.4. k_1^{∞} is required to be decreased slightly so that the new estimate of k_1^{∞} is 0.96×10^8 $lmole^{-1}sec^{-1}$ at room temperature (see Table 8.1).

The results from this study indicate the fall-off to be at a slightly lower pressure than theory predicts. This could be due to some systematic error in our results of which we are unaware or some defect in the molecular model used by Rabinovitch and Setser to calculate their results.

8.3. Hydrogen Atom Addition to Propene.

An interesting feature of the mechanism which has evolved from this study is the catalytic recombination of H atoms by propene. The analogous reaction in the H-isobutene system was first observed by Knox and Dalgleish (KNO69) who found that the H atom decay could be substantially accounted for in terms of the catalytic recombination of H atoms by isobutene. Later work by Daby, Niki and Weinstock (DAB71) has confirmed the reasonableness of their overall mechanism. The H atoms are removed predominantly by the following process:

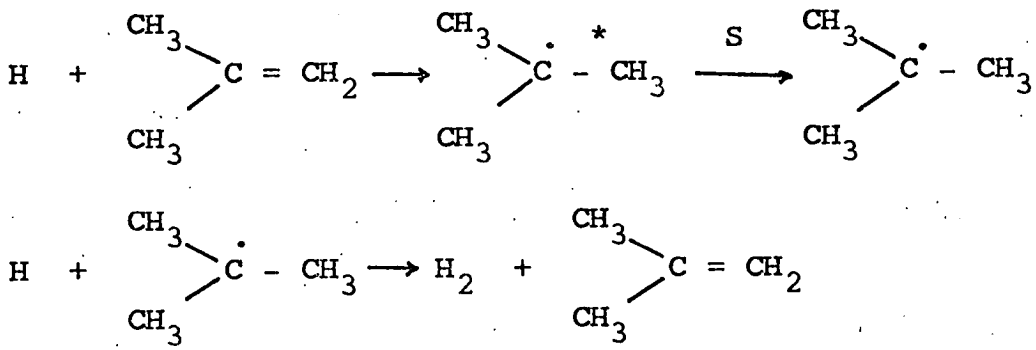

The second step involves abstraction of any one of the nine terminal hydrogen atoms. Our results suggest a similar cycling mechanism, namely

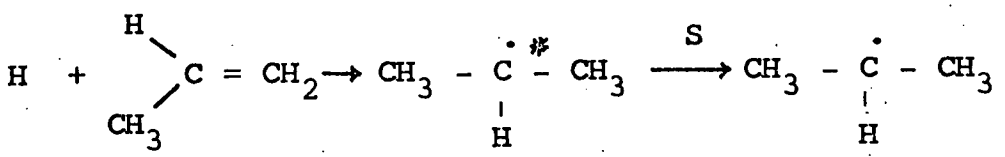

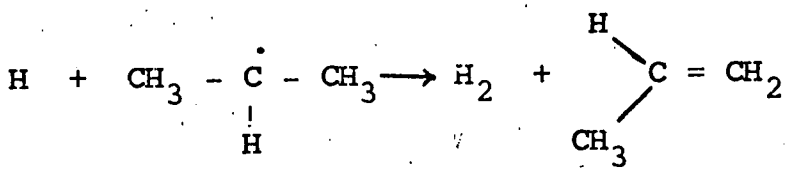

However with only six hydrogen atoms available for abstraction the contribution to the H atom decay is less significant - our results indicate that some 50% of the hydrogen atoms are removed by this cycling mechanism. It is surprising that of the several investigations reported on the H/propene system only Lexton, Marshall and Purnell (LEX71) have suggested the existence of the above mechanism.

No pressure dependence was observed for the addition rate constant in this study although experiments were confined to a rather small pressure range (0.6-3.6 torr). This is in keeping with Kurylo, Peterson and Braun (KUR71) who recorded only a 40% change in rate constant over the range 5--500 torr.

Our results at room temperature have shown that approximately 10% of the hydrogen atoms add on to the non-terminal olefinic position. Since the Arrhenius A factors for both terminal and non-terminal attack should be approximately equal this 9:1 ratio can be translated into a maximum activation energy difference of 1.3 kcal. $mole^{-1}$ between the two positions

of addition. Other reports suggest non-terminal addition is less favourable. Yang (YAN62) has calculated activation energies of 1.5 (terminal) and 3.1 (non-terminal) kcal. $mole^{-1}$ which means a 6% production of n-propyl radicals, while other estimates suggest only 0%-6% of the addition is non-terminal producing n-propyl radicals. (FAL63, MOO48, BOD59, BRA56 LEX71).

8.4 Inefficient Collisional Deactivation.

Consideration has been given to the possibility of breakdown of the strong collision assumption. Certainly in chemically activated systems energized species may have high excess energies and the strong collision assumption is more likely to break down. The experiments of Michael and Weston and Dodonov et al on the H/C_2H_4 system (see Figure 8.3) were carried out using helium diluent and if this is an inefficient collisional deactivator the effect would be to shift the fall-off curve to higher pressures. If

$$P_{eff} = \lambda\ P_{total}$$

where, P_{eff} = effective pressure

λ = collisional efficiency

P_{total} = total measured pressure

Then a value of λ of the order of 0.1 is necessary to make experiment agree with theory for the lower pressures. This is somewhat less than the collisional efficiency of 0.26 (CUR64) which has been suggested. However there is no obvious explanation for the results of Barker and co-workers who also

used helium diluent (see Figure 8.3).

Rabinovitch and Setser have predicted that the H atom addition to iso-propyl radicals is also well into the fall-off range at 1.60 torr (Table 1.1). Figure 8.5 illustrates that the experimental results suggest a fall-off at a slightly higher pressure than theory predicts - an indication that argon is an inefficient collisional deactivator.

Using, $P_{eff} = \lambda P_{total}$ as before

λ is of the order 0.5.

Similarly Figure 8.6 shows the comparison between theory and experiment for

$$CH_3 + CH_3 \longrightarrow C_2H_6^* \xrightarrow{S} C_2H_6$$
$$\qquad\qquad\qquad\qquad\qquad\quad \xrightarrow{D} CH_3 + CH_3$$

Again the indication is that the collisional efficiency of argon is somewhat less than 1 - this time of the order 0.1 at the lower pressures.

Hence the collisional efficiency of argon seems to lie between 0.1 and 0.5. This is in general agreement with Volpe and Johnston (VOL56) who estimated λ to be 0.21 and Kohlmaier and Rabinovitch (KOH63) with a λ value of 0.38.

8.5 Summary

This study has shown that the rate constants for the addition of hydrogen atoms to olefins can be expressed as Arrhenius equations of the forms:

Ethylene $\log k_1 = (10.29 \pm 0.21) - (2960 \pm 320)/4.576T$

Propene $\log k_1 = (9.86 \pm 0.20) - (1040 \pm 200)/4.576T$;

1-Butene $\log k_1 = 9.80 - 1020/4.576T$

Our experiments have yielded values of S/D for the following reactions at room temperature and at a pressure of 1.6 torr. Rabinovitch and Setser's theoretical predictions (RAB64) are also shown.

	Our value	R and S value
$H + C_2H_4 \longrightarrow C_2H_5^* \xrightarrow{S} C_2H_5$; $\xrightarrow{D} H+C_2H_4$	2.1	1.4
$CH_3 + CH_3 \longrightarrow C_2H_6^* \xrightarrow{S} C_2H_6$; $\xrightarrow{D} CH_3+CH_3$	0.25-0.54	1.51
$H + \text{iso } C_3H_7 \longrightarrow C_3H_8^* \xrightarrow{S} C_3H_8$; $\xrightarrow{D} CH_3+C_2H_5$	0.88	1.10

The diluent in our experiments was argon while the S/D values predicted by Rabinovitch and Setser are a function of pure ethylene pressure. Our results indicate the collisional efficiency of argon lies between 0.1 and 0.5.

When hydrogen atoms add onto propene 10% of the addition is non-terminal producing n-propyl radicals.

An unusual feature of the hydrogen atom addition to

propene is a cycling mechanism which removes some 50% of the hydrogen atoms via,

$$H + C_3H_7 \longrightarrow H_2 + C_3H_6$$

H + Ethylene - Table 8.1

Values of k_{al}/k_1^{∞} adjusted to fit the theoretical curve (Figure 8.6)

Run	Pressure (torr)	log k_{al}/k_1^{∞}	k_{al}/k_1^{∞}	k_{al} ($lmole^{-1}sec^{-1}$)	k_1^{∞} ($lmole^{-1}sec^{-1}$)
27	3.5	-.06	0.87	0.82×10^8	0.95×10^8
24	2.1	-.12	0.76	0.73 "	0.96 "
23	1.6	-.16	0.69	0.67 "	0.97 "
20	0.99	-.20	0.63 "	0.60 "	0.95 "
18	0.61	-.29	0.51	0.49 "	0.96 "

mean value of $k_1^{\infty} = 0.96 \times 10^8$ $lmole^{-1}sec^{-1}$

FIGURE 8.1

H + ETHYLENE - COMPARISON OF RESULTS

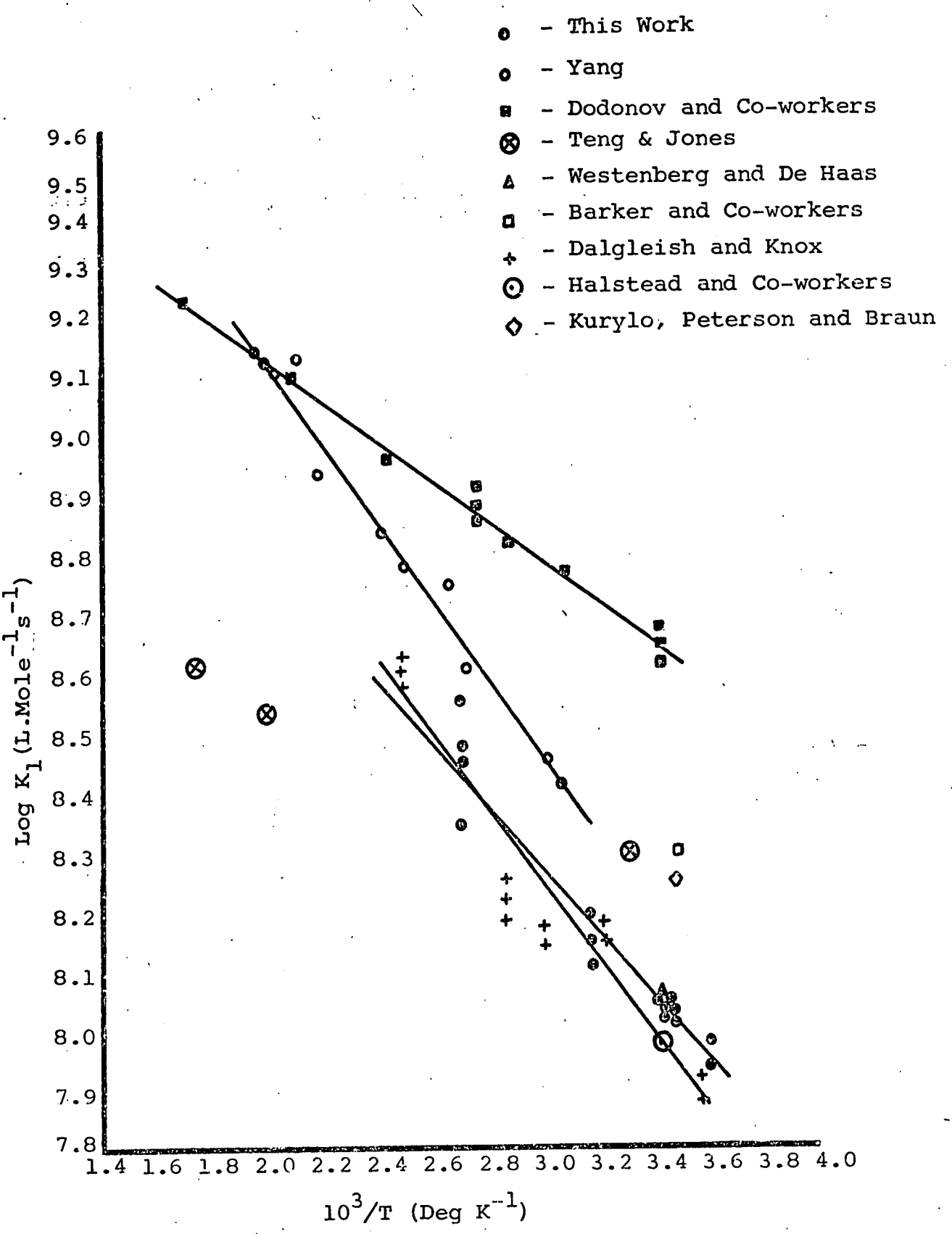

FIGURE 8.2

H + PROPENE - COMPARISON OF RESULTS

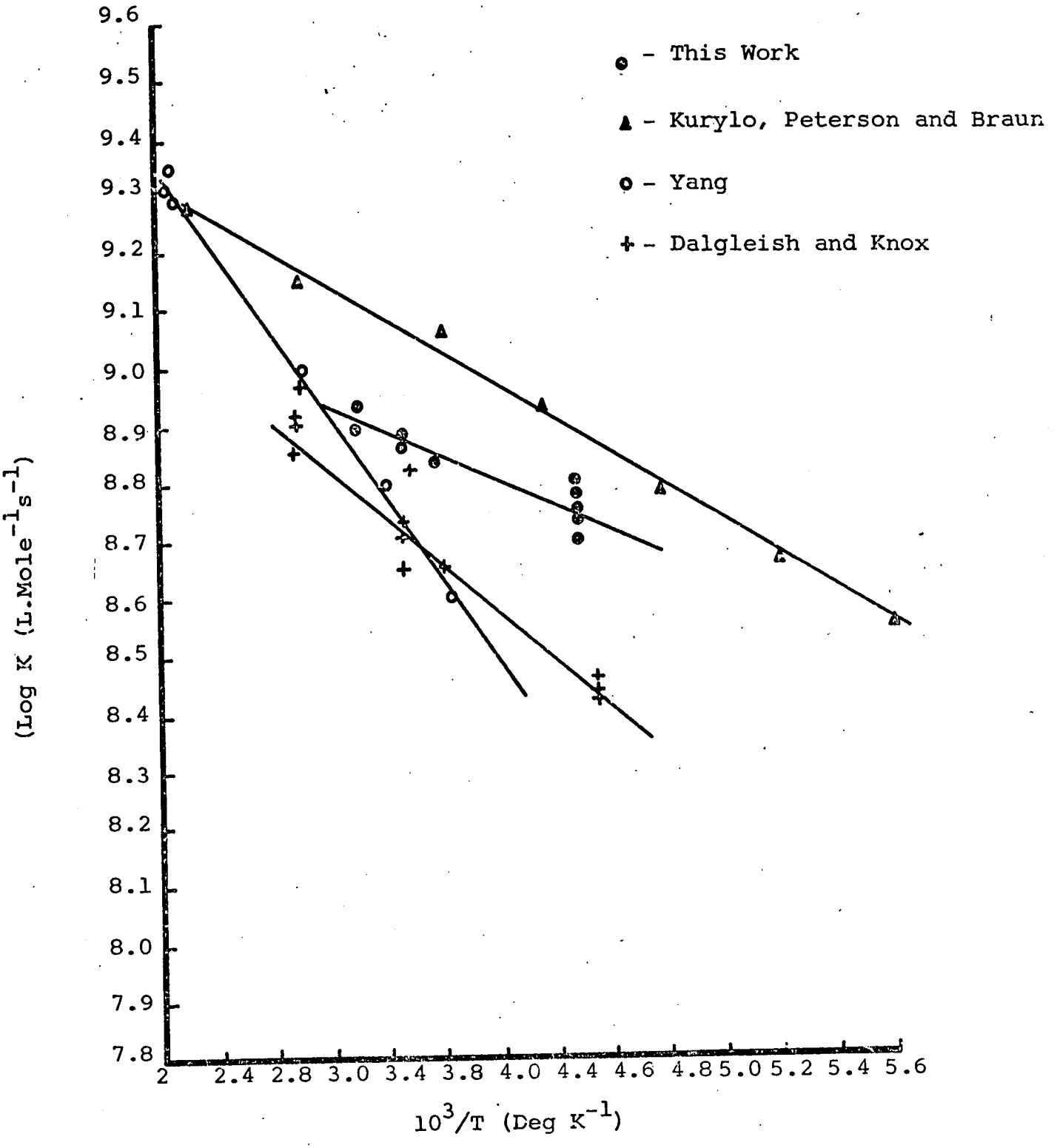

FIGURE 8.3

H + ETHYLENE - PRESSURE DEPENDENCE OF k_{al}

COMPARISON OF RESULTS

$$H + C_2H_4 \xrightarrow{k_1} C_2H_5^* \begin{matrix} \xrightarrow{S} C_2H_5 \\ \xrightarrow{D} H+C_2H_4 \end{matrix}$$

⊗ - Michael and Weston

o - Barker, Keil, Michael and Osborne

▲ - Dodonov and Co-workers

Solid Line - The R.S. Calculated Fall off Curve

● - This Work

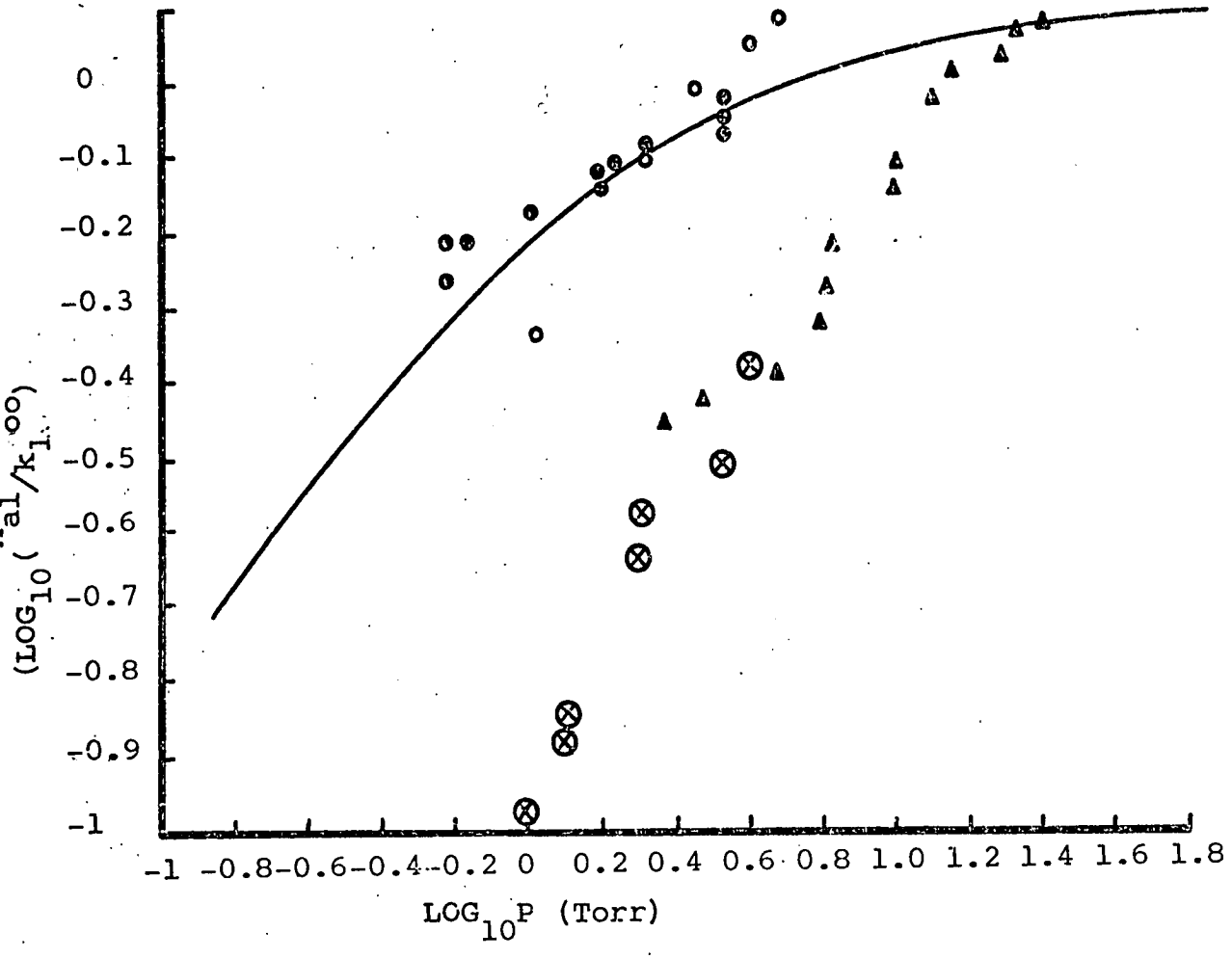

FIGURE 8.4

$LOG_{10}(^{S}/_{S+D})$ against LOG_{10}(Pressure) For,

$$H + C_2H_4 \longrightarrow C_2H_5^{*} \begin{cases} \xrightarrow{S} C_2H_5 \\ \xrightarrow{D} H+C_2H_4 \end{cases}$$

● - Experimental Points

Solid Line - Rabinovitch and Setser's Predicted Fall-off

⊙ - Experimental Points Adjusted so that the Experimental Fall-off is Parallel to the Theoretical Fall-off

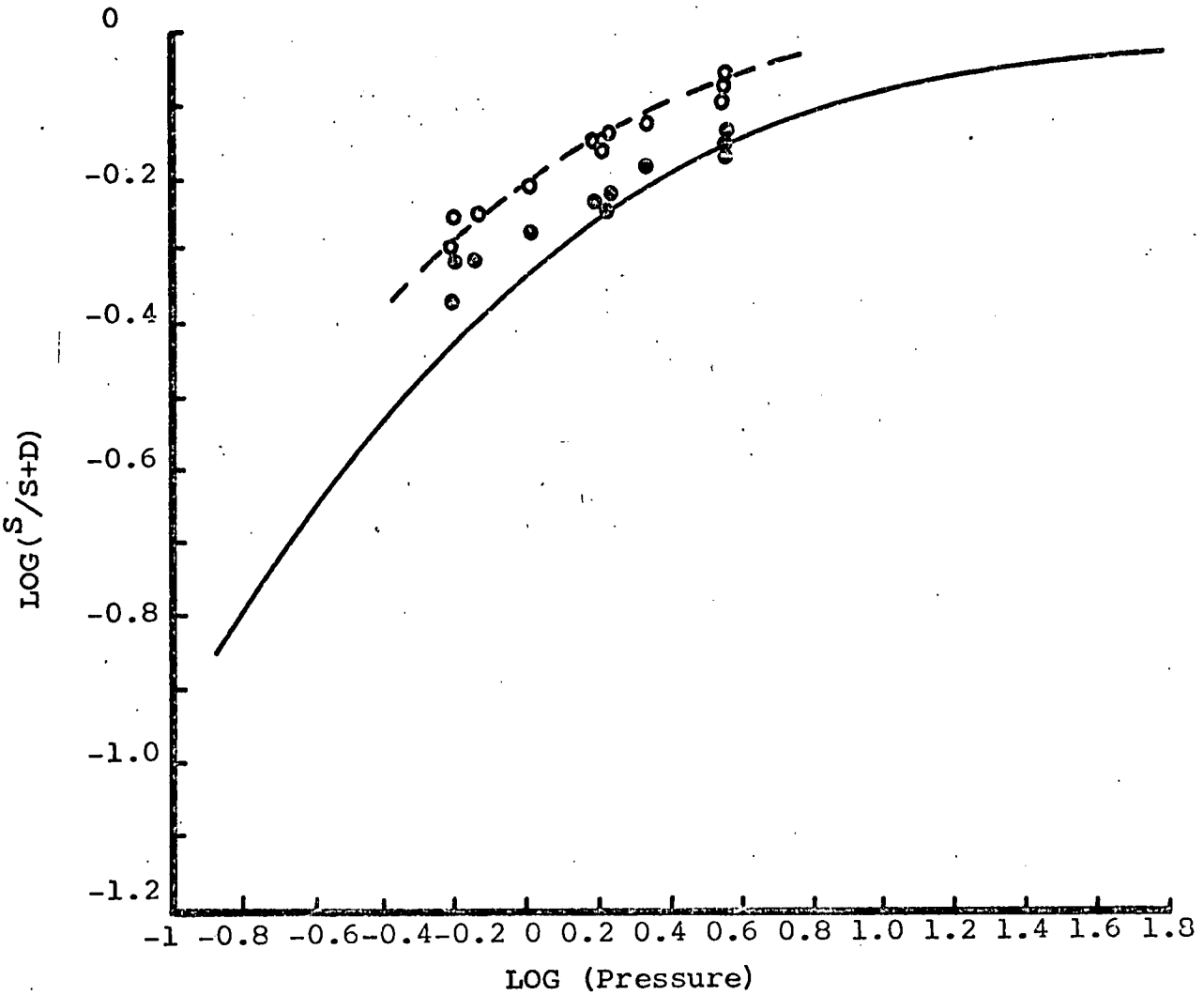

FIGURE 8.5

$LOG_{10}(^{S}/S+D)$ against LOG_{10}(Pressure)

$$H + {}^{iso}C_3H_7 \longrightarrow C_3H_8^{*} \begin{cases} \xrightarrow{S} C_3H_8 \\ \xrightarrow{D} CH_3+C_2H_5 \end{cases}$$

(Comparison with the Theoretical Predictions of Rabinovitch and Setser).

● - Experimental Points

Solid Line - The R & S calculated fall-off Curve

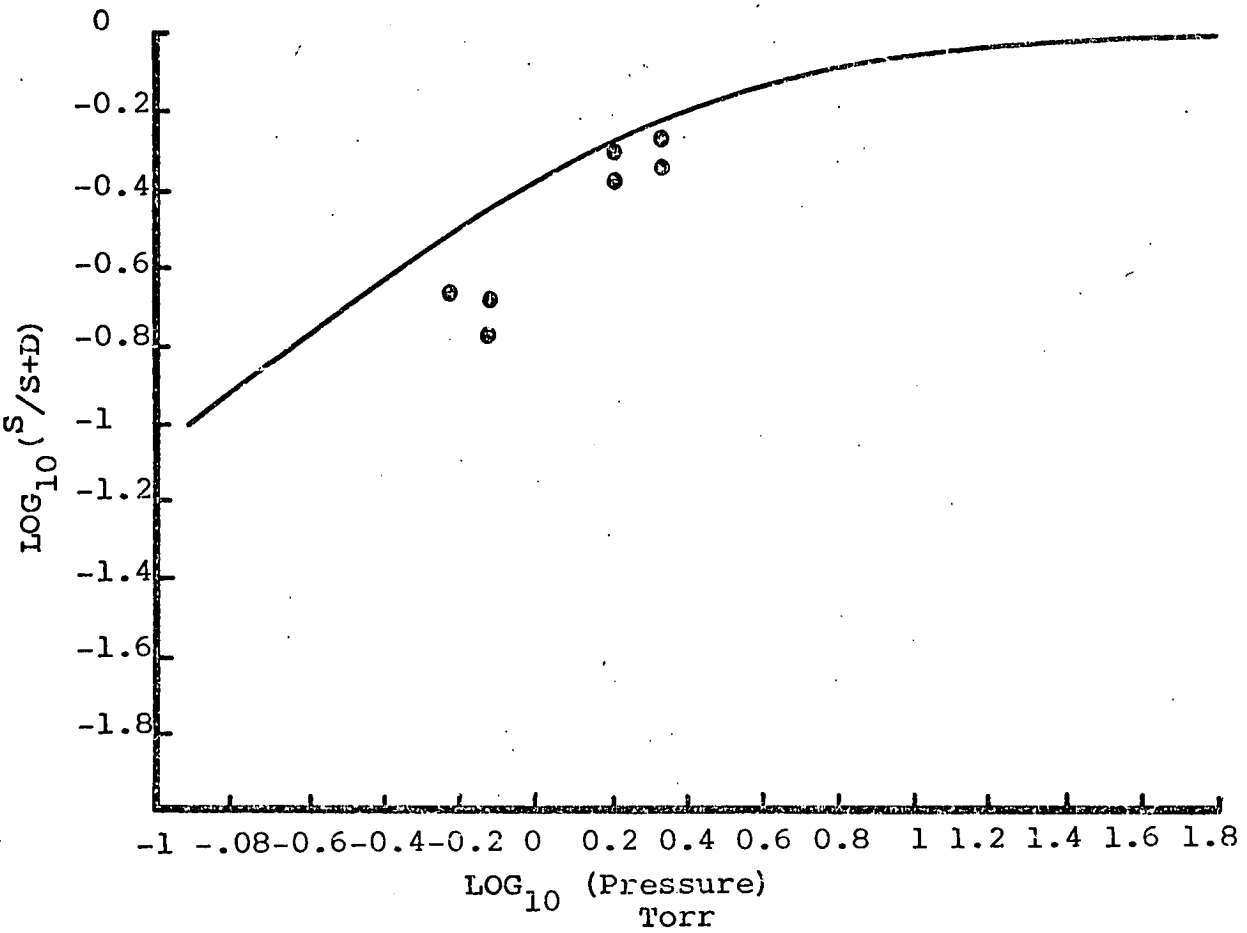

FIGURE 8.6

$LOG_{10}(^{S}/S+D)$ against LOG_{10}(Pressure)

FOR $CH_3 + CH_3 \longrightarrow C_2H_6^*$ $\xrightarrow{S}$ C_2H_6; $\xrightarrow{D}$ CH_3+CH_3

(Comparison with the Theoretical Predictions of Rabinovitch and Setser)

● - Experimental Points

Solid Line - The R and S Calculated Fall-off Curve

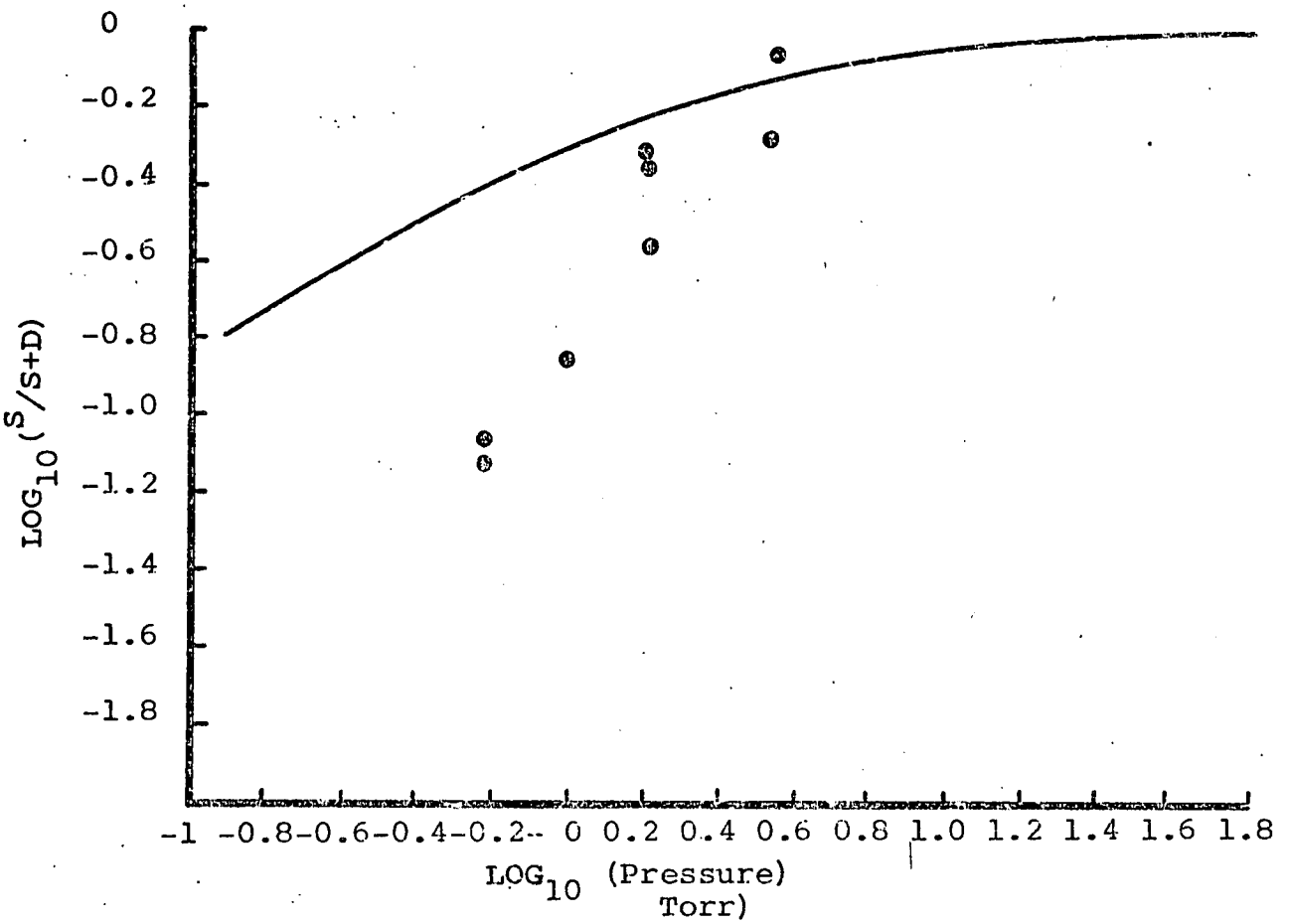

APPENDICES

APPENDIX 1.

Calculation of NO_2 Flowrates from the NO_2-N_2O_4 Equilibrium.

Since NO_2 in the gas phase coexists with N_2O_4 in an equilibrium mixture, the flowrate of NO_2 cannot be calculated in the simple manner described in chapter 3 , since the measurement of the number of moles leaving the storage globe will not account for the N_2O_4 leaving. At low pressures, the N_2O_4 dissociates completely, so the number of moles leaving the globe will give an underestimation of the true NO_2 flowrate in the flow system. Factors to account for this can be calculated from the known data on the NO_2 - N_2O_4 equilibrium, as investigated by Verhoek and Daniels (VER31).

Assuming we start with a moles of N_2O_4, and allow this to come to equilibrium, the amount of NO_2 produced will be 2x moles, and the remaining N_2O_4 will be (a-x) moles. If the total pressure is P, then

$$p_{N_2O_4} = p(a-x)/(a+x) \quad \text{and} \quad p_{NO_2} = 2px/(a+x).$$

The equilibrium constant, K, is given by

$$K = (p_{NO2})^2/(p_{N2O4})$$

$$= 4x^2p/(a^2-x^2)$$

which gives $x/a = (K/(4p+K))^{\frac{1}{2}}$.

Thus the amounts of NO_2 and N_2O_4 present at any time can be found from the knowledge of the value of the equilibrium constant (in pressure units) at the required pressure p.

If, at a given pressure, it is known that the mixture contains y moles of N_2O_4 and x moles of NO_2, the 'average mole' present is composed of fractions

$x/(x+y)$ of NO_2 and $y/(x+y)$ of N_2O_4,

but when this enters the flow system, the N_2O_4 dissociates to NO_2 and the total moles now become $x+2y$ instead of $x+y$. The fractional change in the number of moles leaving the globe is therefore $(x+2y)/(x+y)$. This is calculated giving the factor c. To obtain the true flowrate of NO_2, the number of moles leaving the globe in a given time is found from the pressure drop, and this is then multiplied by the factor c to give the flowrate of NO_2.

The proportions of NO_2 and N_2O_4, and the factor c, are shown in the following table, as functions of pressure.

Pressure (torr.)	(N_2O_4) (mole/l.x10^3)	(NO_2) (mole/l.x10^3)	
119	2.58	3.82	1.403
161	3.90	4.76	1.450
220	5.99	5.82	1.507
249	7.35	6.38	1.535
278	8.28	6.68	1.553
300	9.06	7.06	1.562
320	9.93	7.30	1.576
349	11.12	7.64	1.593
368	11.88	7.92	1.600
399	13.15	8.34	1.612
414	13.78	8.48	1.619
457	15.55	9.02	1.632

To enable the value of c to be found at any pressure, these results were plotted, and then a smooth curve was drawn through them, as in Figure A.1.

FIGURE A.1

CORRECTION FACTORS FOR NO_2 FLOWRATES.

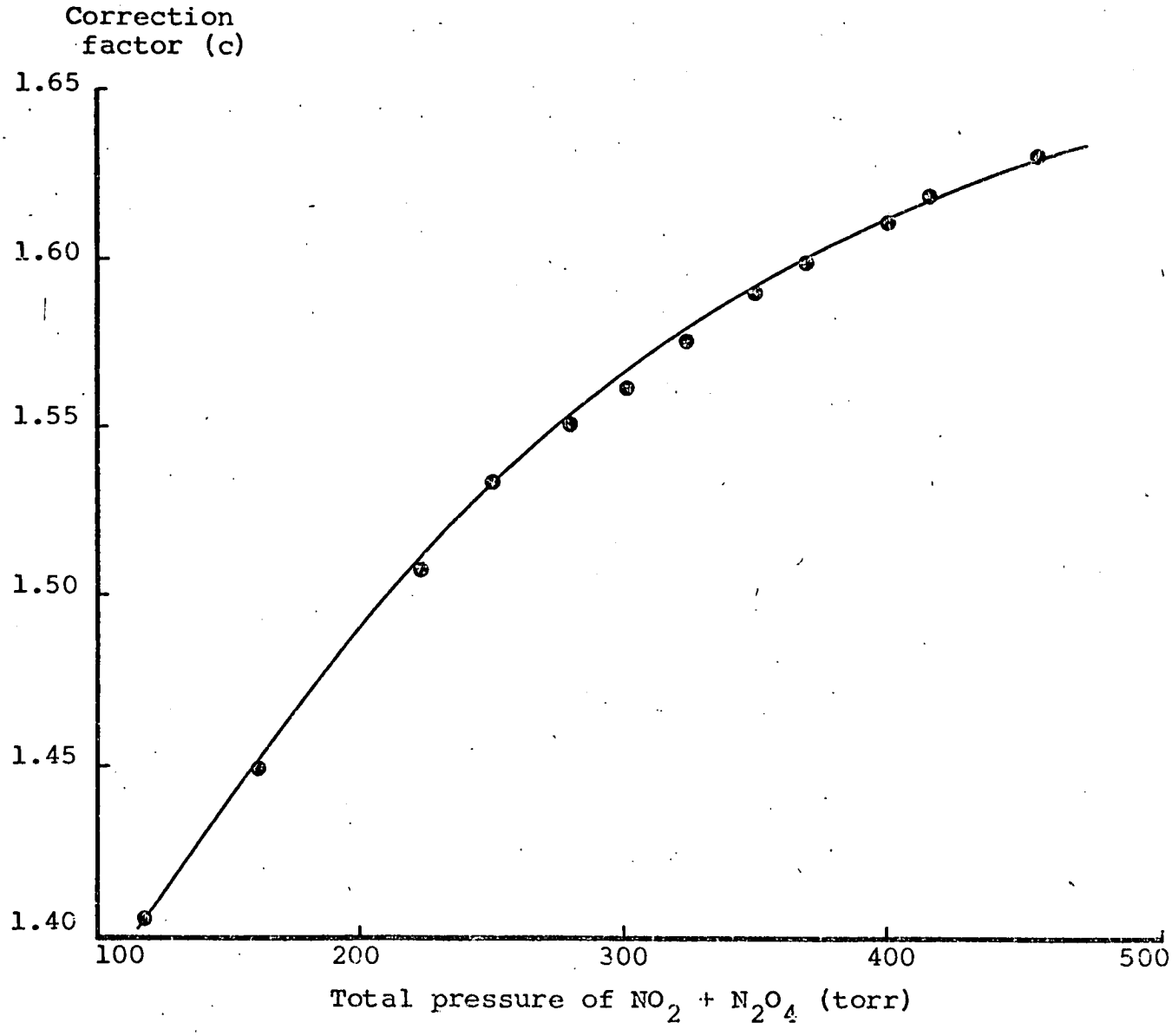

APPENDIX 2.

S/D values for $H + C_2H_4 \underset{D}{\rightleftharpoons} C_2H_5^* \xrightarrow{S} C_2H_5$ at various temperatures and pressures using the data of Rabinovitch and Setser (RAB64).

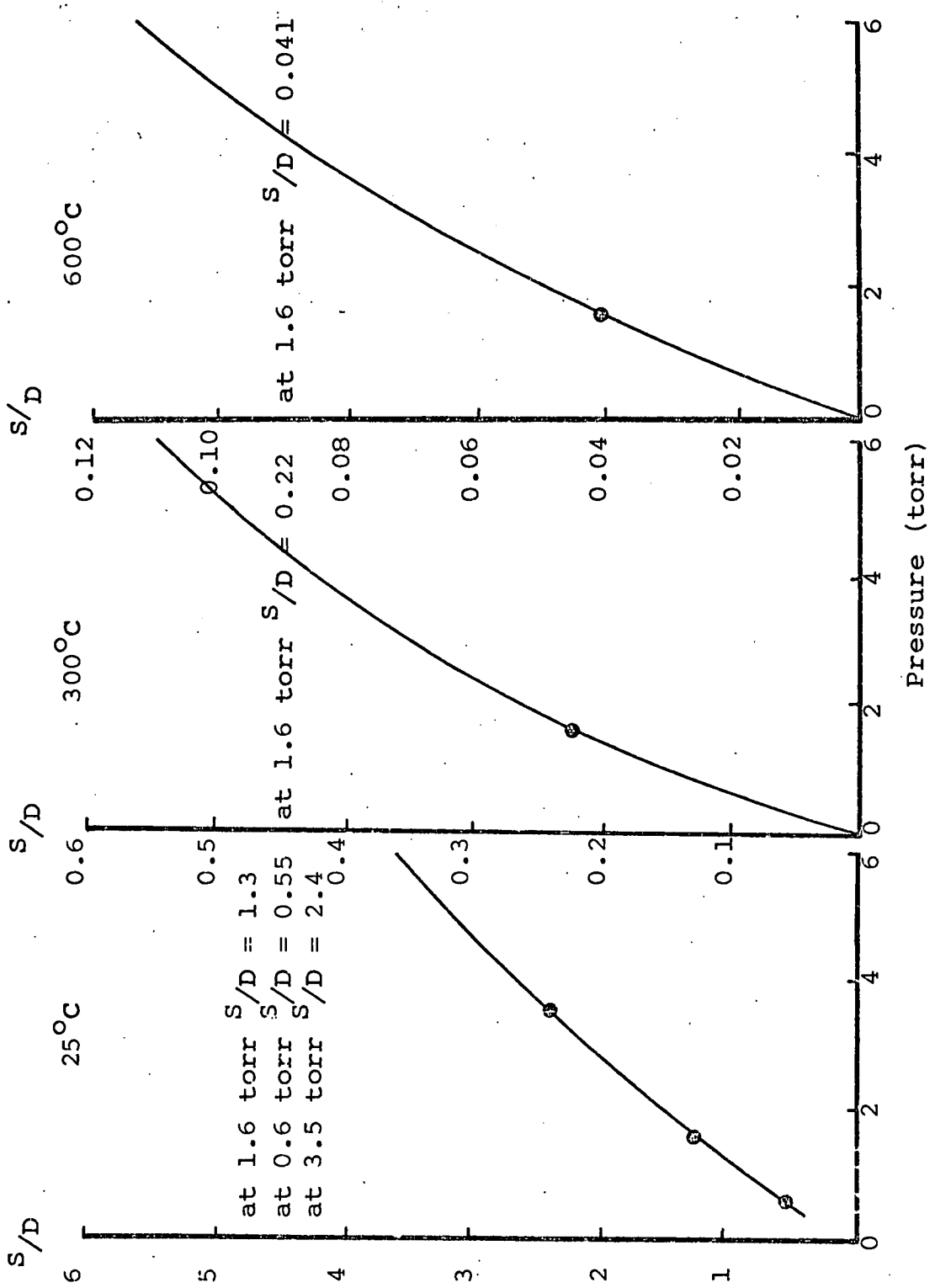

S/D AGAINST TEMPERATURE (at 1.6 torr)

for $H + C_2H_4 \longrightarrow C_2H_5^* \xrightarrow{S} C_2H_5$; $\xrightarrow{D} H+C_2H_4$

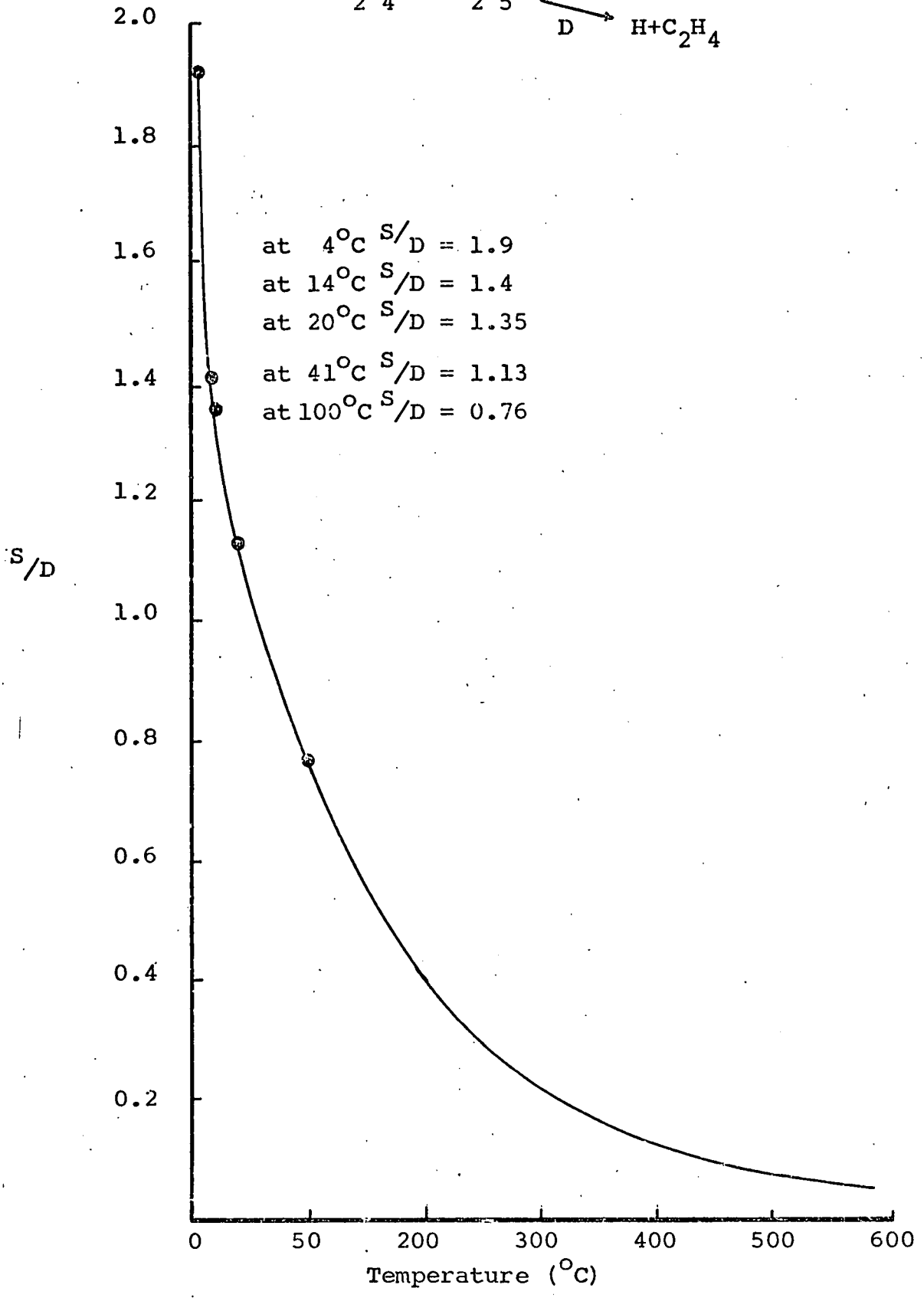

REFERENCES

ALL53 -	P.E.M. Allen, H.N. Melville and J.C. Robb	Proc.Roy.Soc. A218,311 (1953)
ARR65 -	C.A. Arrington, W. Brennen, G.P. Glass, J.V. Michael and H. Niki	J.Chem.Phys. 43,525, (1965)
BAR62 -	C.A. Barth, A.F. Hilderbrandt and M. Papatoff	Disc.Far.Soc. 33,162, (1962)
BAR69 -	J.R. Barker, and J.V. Michael	J.Chem.Phys. 51,850 (1969)
BAR70 -	J.R. Barker, D.G. Keil, J.V. Michael and D.T. Osborne	J.Chem.Phys. 52,2079, (1970)
BEN60 -	S.W. Benson	The Foundation of Chemical Kinetics P280 (McGraw-Hill Book Company New York (1960)
BER52 -	R. Beringer and E.B. Rawson	Phys.Rev. 87,228, (1952)
BRA56 -	J.N. Bradley, H.W. Melville and J.C. Robb	Prdc.Roy.Soc. A236,339 (1956)
BRA67 -	W. Braun and M. Lenzi	Disc.Far.Soc. 44,252, (1967)
BOD59 -	P.J. Body and J.C. Robb	Proc.Roy.Soc. A249,518 (1959)
CLY62 -	M.A.A. Clynne and B.S. Thrush	Trans.Far.Soc. 33,139. (1962)
CLY63 -	" "	Proc.Roy.Soc. A275,544, (1963)
COW71 -	J.A. Cowfer, D.G. Keil, J.V. Michael and C. Yeh	J.Phys.Chem. 10,1584, (1971)
CUR64 -	J.H. Current and B.S. Rabinovitch	J.Chem.Phys. 40,2742, (1964)

CVE69 -	R.J. Cvetanovic and L.C. Doyle	J.Chem.Phys. 50,4705 (1969)
DAB71 -	E.E. Daby, H. Niki and B. Weinstock	J.Phys.Chem. 75,1601, (1971)
DAL67 -	D.G. Dalgleish	Ph.D. Thesis Univ. of Edinburgh
DEL62 -	F.P. Delgreco and F. Kaufman	Disc.Far.Soc. 33,128, (1962)
DOD66 -	A.F. Dodonov et al	Kinet.& Catal. 1,22, (1966)
DOD69a-	A.F. Dodonov et al	" " 10,22, (1969)
DOD69b-	"	" " 10,477, (1969)
EYR70 -	K. Eyre, N. Hikida, P. Dorfmann	J.Chem.Phys. 53,1281, (1970)
FAL63 -	W.E. Falconer, B.S. Rabinovitch and R.J. Cvetanovic	J.Chem.Phys. 39,40, (1963)
FEN58 -	C.P. Fenimore and G.W. Jones	J.Phys.Chem. 62,693, (1958)
FON53 -	J. Foner and R. Hudson	J.Chem.Phys. 21,1374, (1953)
FOX59 -	J.W. Fox, A.C.H. Smith and E.J. Smith	Proc.Phys.Soc. 73,533 (1959)
GAR58 -	Garvin, Green and Lipworth	Phys.Rev. 111,534 (1958)
GRE59 -	Greaves and Linnett	Trans.Far.Soc. 55,1338 (1959)
HAL60 -	K. Halbach	Phys.Rev. 119,1230, (1960)

HAL70 -	M.P. Halstead, D.A. Leathard, R.M. Marshall and J.H. Purnell	Proc.Roy.Soc.Ser. A,316 575, (1970)
HIN27 -	C.N. Hinshelwood	Proc.Roy.Soc.(a),113, 230, (1927)
HOR69 -	B. Horne	Ph.D. Thesis, Univ. of Edinburgh
HEN61 -	K.R. Jennings & R.J. Cvetanovic	J.Chem.Phys. 35,1233, (1961)
KAS28 -	L.S. Kassel	J.Phys.Chem. 32,225 (1928)
KAS28 -	"	" " " 32,1065, (1928)
KAS32 -	"	Kinetics of Homogeneous Gas Reactions, Chemical Catalog Co., New York, 1932
KAU61 -	Kaufman	Prog.React.Kinet. 1 3 (1961)
KOH63 -	Kohlmaier and B.S. Rabinovitch	J.Chem.Phys. 38,1692 & 1709 (1963)
KON61 -	V.N. Kondratiev & V.V. Voevodsky	Prog.React.Kin. 1,55, (1961)
KON70 -	" " "	Handbook of Rate Constants for Gas Phase Reactions - U.S.S.R. Academy of Sciences Moscow
KNO69 -	J.H. Knox and D.G. Dalgleish	Int.J.Chem.Kinet. 1,69, (1969)
KRO59 -	S. Krongelb and M.W.P. Strandberg	J.Chem.Phys. 31,1196 (1959)
KUR70 -	M.J. Kurylo, N.C. Peterson and W. Braun	J.Chem.Phys. 53,1281 (1970)

KUR71 -	M.J. Kurylo, N.C. Peterson and W. Braun	J.Chem.Phys. 54,4662, (1971)
LEX71 -	Lexton, R.M. Marshall, J.H. Purnell	Proc.Roy.Soc. A324,433, (1971)
LER53 -	D.J. LeRoy and M.R. Berlie	Disc.Far.Soc. 14,50, (1953)
LIN22 -	F.A Lindemann	Trans.Far.Soc. 17,598, (1922)
LIN56 -	J.W. Linnett and D.G.H. Marsden	Proc.Roy.Soc. A234,489, (1956)
MAR51 -	R.A. Marcus and O.K. Rice	J.Phys.&Colloid,Chem. 55,894, (1951)
MAR52 -	R.A. Marcus	J.Chem.Phys. 20,352 & 359, (1952)
MAR66 -	R. Martin and M.A.D. Fluendy	Rev.Sci.Inst. 36, (1966)
MEL64 -	H.W. Melville and B.G. Gowenlock	Exp.Methods in Gas Kinetics (MacMillan London 64)
MEL49 -	" " J.C. Robb	Proc.Roy.Soc. A194,445,466, 479,494, (1949)
MIC66 -	J.V. Michael and R.E. Weston	J.Chem.Phys. 45,3632,(1966)
MOO48 -	W.J. Moore	" " " 16,916 (1948)
OGR61 -	J. Ogryzlo	Can.J.Chem. 39,2556,(1961)
PHI62 -	Philips and Schiff	J.Chem.Phys. 37, 1233, (1962)
PRI53 -	Pritchard, Sowden and Trotman-Dickenson	Proc.Roy.Soc. A217,567, (1953)
POO37 -	H.G. Poole	Proc.Roy.Soc.A163,404, (1937)
RAB61 -	B.S. Rabinovitch, D.W. Setser and F.W. Sneider	Can.J.Chem. 39,2609,(1961)

RAB64 -	B.S. Rabinovitch and D.W. Setser	Advances in Photochemistry Vol. 3 1-82 (1964)
RIC27 -	F.O. Rice	J.Amer.Chem.Soc. 49,1617, (1927)
RIC28 -	"	" " " " 50, 617, (1928)
ROD33 -	Rodebush and Klinglehoffer	" " "" " 55, 130, (1933)
SCH62 -	F.W. Sneider and B.S. Rabinovitch	J.Amer.Chem.Soc. 84,4215, (1962)
SCH62 -	W.R. Schulz and D.J. LeRoy	Can.J.Chem. 40,2413, (1962)
SET62 -	D. Setser and B.S. Rabinovitch	" " " 40,1425, (1962)
SHA59 -	T.M. Shaw	J.Chem.Phys. 31,1142, (1959)
SLA59 -	N.B. Slater	Theory of Unimolecular Reaction (Methuen London (1959)
STE31 -	W. Steiner and F.W. Wicke	Z. Physik.Chem.Bodenstein Festb. 817, (1931)
STE62 -	J.C. Sternberg	Gas Chromatography 231, (1962) (Academic Press)
TEN72 -	Teng and Jones	Far.Trans. 1,1273, (1972)
TOB68 -	S. Toby and H. Shaw	J.Phys,Chem. 72,2337, (1968)
TOL48 -	E.L. Tollefson and D.J. LeRoy	J.Chem.Phys. 16,1057, (1948)
VER31 -	F.H. Verhoek and F. Daniels	J.Amer.Chem.Soc. 53,1250, (1931)
VOL56 -	Volpe and Johnston	" " " " 78,3909, (1956)

WES64 -	A.A. Westernberg and N.J. DeHaas	J.Chem.Phys. 40,3087, (1964)
WES69 -	" " "	" " " 50,707, (1969)
WHI63 -	G.Z. Whitton and B.S. Rabinovitch	" " " 38,2466, (1963)
WIE62 -	G.M. Wieder and R.A. Marcus	" " " 37,1835, (1962)
WOO22 -	R.W. Wood	Proc.Roy.Soc. A97,455, (1922)
WOO61 -	B.J. Wood and H. Wise	J.Phys.Chem. 65,1976, (1961)
WRE29 -	E. Wrede	Z.Physik. 54, 53, (1929)
YAN62 -	K. Yank	J.Amer.Chem.Soc. 84,719, (1962)